Pharmacological reprogramming of macrophages through aptamiRs

Dissertation

zur

Erlangung des Doktorgrades (Dr. rer. nat.)

der

Mathematisch-Naturwissenschaftlichen Fakultät

der

Rheinischen Friedrich-Wilhelms-Universität Bonn

vorgelegt von

Usman Akhtar

aus

Lahore, Pakistan

Bonn 2019

Angefertigt mit Genehmigung der Mathematisch-Naturwissenschaftlichen Fakultät
der Rheinischen Friedrich-Wilhelms-Universität Bonn

1. Gutachter: Prof. Dr. Günter Mayer
2. Gutachter: Prof. Dr. Gerd Bendas
Tag der Promotion: 19.02.2020
Erscheinungsjahr: 2020

INDEX

1 Abstract

Nucleic acid-based molecules have certain advantages over conventional drugs or protein-based target approaches. Chemically synthetized nucleic acids-based molecules are known as aptamers. They are selected from a combinatorial oligonucleotide library in a unique way called “SELEX” (systematic evolution of ligands by exponential enrichment). These are single-stranded oligonucleotides with specific three-dimensional configuration. They can be bound to their specific target with high affinity and specificity. Recently, aptamers targeting mammalian cells have emerged as potential candidates for use as delivery vehicles. Numerous therapeutic agents including miRNA, siRNA, peptides, proteins, nanoparticles, and chemotherapeutics can be delivered into the cells via cell-targeting aptamers.

Macrophages and dendritic cells (DCs) play a vital role in the immune response. These cells are involved in physiological and pathological processes in the body. DCs are considered to be one of the most potent “professional” antigen presenting cells (APCs) and have the properties to present endogenous or foreign antigens on their surfaces for the activation of T cells. Therefore, DC-based vaccines designed for activation and proliferation of T cells have significant immunotherapy-related importance. On the other side, macrophages play a key role in different diseases including chronic inflammation. miRNA 125a-5p is highly upregulated in chronic inflammatory macrophages and may have an impact on the polarization of macrophages or on the condition of the disease.

In the current study, it was explored that an aptamer targeting immune cells could be used as a delivery vehicle. Herein, Next generation sequencing (NGS) data of murine bone marrow-derived DCs cell-SELEX was used to identify a promising aptamer targeting macrophages and DCs. DC 12 aptamer has been identified and characterized as a promising and suitable delivery vehicle. It has been shown that DC 12 aptamer is non-immunogenic and internalizes into the cells.

The study found that DC 12 aptamer guided uptake of antagomir 125a-5p may end up in the endosomal compartment of macrophages, thereby limiting its inhibitory effect. However, DC 12 has the potential to deliver OT-I peptide into the desired processing compartment of BM-DCs for the targeted activation of CD8 T cells. In summary, aptamers have the potential to replace other carrier molecules, but further investigation will be needed as regards the delivery of the cargo into the cell cytoplasm.

2 Zusammenfassung

Moleküle auf Nukleinsäurebasis haben gewisse Vorteile gegenüber konventionellen Medikamenten oder protein-basierenden Zielansätzen. Chemisch synthetisierte, auf Nukleinsäuren basierende Moleküle werden als Aptamere bezeichnet. Die Selektion von Aptameren aus einer kombinatorischen Oligonukleotid Bibliothek wird als SELEX (systematicevolutionofligandsbyexponentialenrichment) genannt. Aptamere sind einzelsträngigeOligonukleotide mit einer spezifischen drei-dimensionalen Struktur, welche in der Lage sind ihr Zielmolekül mit hoher Affinität und Spezifität zu binden. Kürzlich haben sich Aptamere, die an Säugetierzellen binden, als potenzielle Liefermoleküle erwiesen. Zahlreiche therapeutische Wirkstoffe wie miRNA, siRNA, Peptide, Proteine, Nanopartikel und Chemotherapeutika können über zellspezifische Aptamere in die Zellen transportiert werden.

Makrophagen und Dendritische Zellen (DCs) spielen eine zentrale Rolle in der Immunabwehr. Diese Zellen sind in physiologischen und pathologischen Prozessen involviert. DCs werden als eine der wirksamsten „professionellen“ antigenpräsentierenden Zellen (APCs) angesehen, die die Eigenschaft besitzen endogene und fremde Antigene auf der Zelloberfläche zu präsentieren um T-Zellen zu aktivieren. Daher sind Impfstoffe basierend auf dendritische Zellen, die zur Aktivierung und Proliferation von T-Zellen beitragen, von immunotherapeutischer Relevanz. Andererseits spielen Makrophagen eine Schlüsselrolle in verschieden Krankheiten wie zum Beispiel chronischen Entzündungen. Die Expression von miRNA 125a-5p ist in chronisch entzündlichen Makrophagen stark überexprimiert, welche eventuell einen Einfluss auf die Polarisierung der Makrophagen oder die Ausprägung der Krankheit haben kann.

In der nachfolgenden Studie wurde untersucht, ob einAptamer, das an Immunzellen bindet, als Liefermolekülgenutzt werden könnte. Dabei wurden Daten des„nextgenerationsequencing“ (NGS) von der aus murinem Knochenmark gewonnenen DCs Zell-SELEX verwendet, um Aptamere zu finden, die an

Makrophagen und DCs binden. Das Aptamer DC 12 wurde identifiziert und als vielversprechendes und geeignetes Liefermolekül charakterisiert. Es konnte gezeigt werden, dass DC 12 nicht immunogen ist und von den Zellen internalisiert wird.

In der Studie konnte außerdem gezeigt werden, dass die von DC 12 gesteuerte Aufnahme von Antagomir 125a-5p im endosomalen Kompartment der Makrophagen enden könnte und somit den inhibitorischen Effekt limitiert. Allerdings hat DC 12 das Potential OT-I Peptide in die entsprechenden Kompartimente von BM-DCs für die gezielte Aktivierung von CD8 T-Zellen zu transportieren. Zusammenfassend haben Aptamere das Potential andere Transportmoleküle zu ersetzen, jedoch sind weitere Studien nötig in Bezug auf die Lieferung des Frachtmoleküls in das Zytoplasma der Zelle.

3 Introduction

3.1 Aptamers

Nucleic acid-based molecules, known as aptamers, are ssDNA or RNA that have well defined three-dimensional configurations[1] **(Figure 3.1.1)**. They exhibit a high specificity and affinity for their targets including small molecules, extracellular proteins, enzymes, peptides, and even for the whole cell. These properties are based on several types of interactions such as complementarity shape, van der Waals forces, base stacking, hydrogen bonding, hydrophobic, and electrostatic interactions[2].

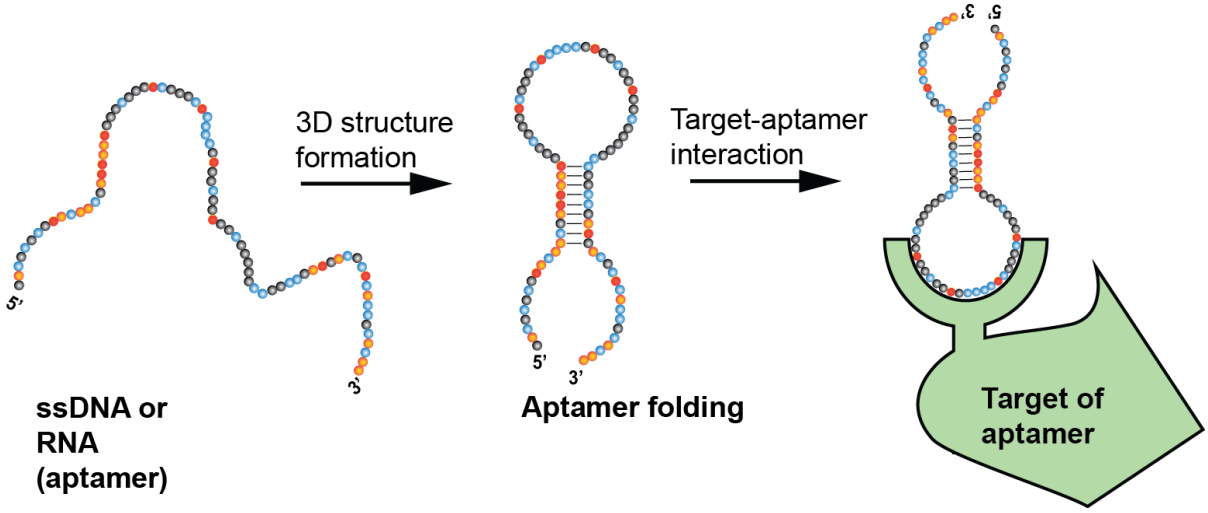

Figure 3.1.1: Schematic illustration of the ssDNA or RNA aptamer binding to the target depending on the three-dimensional configuration of the aptamer. ssDNA or RNA aptamer folds into a 3D structure, upon which it interacts with the target (e.g., small molecules, peptides, and cells etc)[3].

3.1.1 Selection method of aptamers

Aptamers are selected from the ssDNA or RNA library followed by a process known as SELEX[4]. This selection method was introduced by three independent groups; Szostak & Ellington, Gold & Tuerk, and Robertson & Joyce groups in the 1990's[5-7]. The selection procedure starts with the incubation of the starting library of 10^{14} to 10^{15} random sequences with the target of interest. The random sequence is flanked by constant primer binding sites on both sides of the sequence to allow PCR

(polymerase chain reaction) amplification. After incubation, the target-bound sequences are isolated from the unattached or weakly bound sequences. The isolation process is either facilitated by immobilizing of the respective target on the matrix or by the unattached and weekly bound sequences are separated by flow cytometry, electrophoresis or centrifugation[8-10]. The target bound sequences are amplified by PCR after decoupling from the target of interest. Single-stranded sequences are generated from amplified PCR products that are further used for the next rounds of SELEX. In general, 8-10 cycles of SELEX are needed to find the most promising candidate sequence, which binds with high affinity and specificity[11,12]. The promising candidate sequences are sequenced and synthesized using solid phase synthesis for further characterization.

3.1.2 Selection method for cell-targeting aptamers

In order to identify the whole cells-targeting aptamers, both prokaryotic and eukaryotic cells can be used without the preliminary knowledge of the putative target molecule on the cell surface[13]. Morris *et al*.[14] described the cell-based SELEX methodology (cell-SELEX) for the first time, using a complex mixture of human red blood cell membrane targets. The main advantage of the cell-SELEX is that the target proteins are naturally folded and native state to the cell surface[15]. Aptamers have been selected against different types of cancer cells[16] and also against live pathogens such as viruses[17] and bacteria[18]. Cell-SELEX based selection usually involves both positive and negative selection **(Figure 3.1.2)**. The positive selection is used to identify the aptamers that are specific to target the positive cells while negative selection is used to eliminate nonspecific sequences that bind negative cells. The target of interest can be expressed naturally, as in various diseases, or overexpressed on the surface of the cells. Negative cells must be unrelated to positive cells in terms of target expression in order to remove non-specific sequences from the library[19]. Cell-SELEX can generate a variety of aptamers that can differentiate between different cancer cells or between cancer cells and normal cells[13].

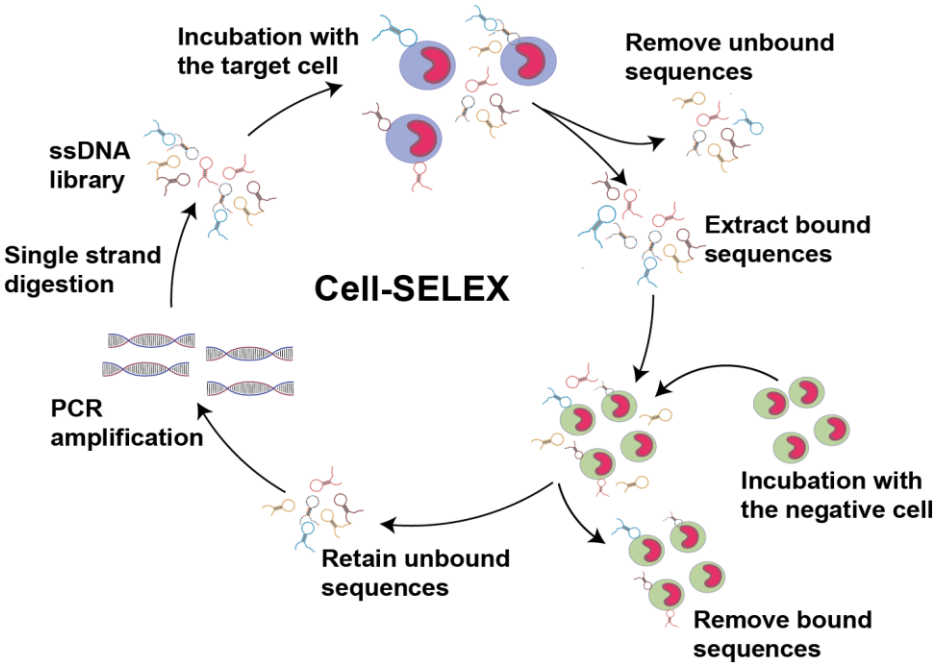

Figure 3.1.2: Schematic illustration of the cell-SELEX process
Cell-SELEX is performed to obtain cell-targeting aptamers for different applications. In general, the oligonucleotide library of 10^{14} to 10^{15} random sequences is incubated with the cells (1), the sequences bound to the target are dissociated from the unbound sequences (2), dissociation of target-bound sequences from the target (3), incubation with the negative cells (4), unbound sequences are retained (5), amplified (6), single strand digestion of PCR product (7), and used in the next selection cycle (8).

3.1.3 Cell-targeting aptamers

Cell-targeting aptamers have certain advantages over other targeting molecules such as antibodies as they are small in size and easy to synthesize[20]. Aptamers are chemically synthesized due to which they are also termed as “chemical antibodies” and their functional properties are also similar to antibodies. For example, epithelial cell adhesion molecule (EpCAM) aptamer has been shown to be more promising agent for targeting cancer cells and molecular imaging compared to the EpCAM antibody[21].

After the selection procedure, aptamers can be chemically modified to overcome their limitations such as short half-life and nuclease degradation. Polyethylene glycol (PEG) and the introduction of chemical modifications e.g., 2′-fluoropyrimidines, 2′-O-methyl ribose purines, and 2′-amino pyrimidines alters the overall pharmacokinetic profile and minimize the attack from the nucleases, respectively[22,23].

Another of the most promising features of cell-targeting aptamers is their ability to internalize into the respective cells after binding[24]. These aptamers can be used as a delivery vehicle for delivery of cargo molecules such as proteins, nucleic acids, nanoparticles, and drugs[25-29] **(Figure 3.1.3)**.

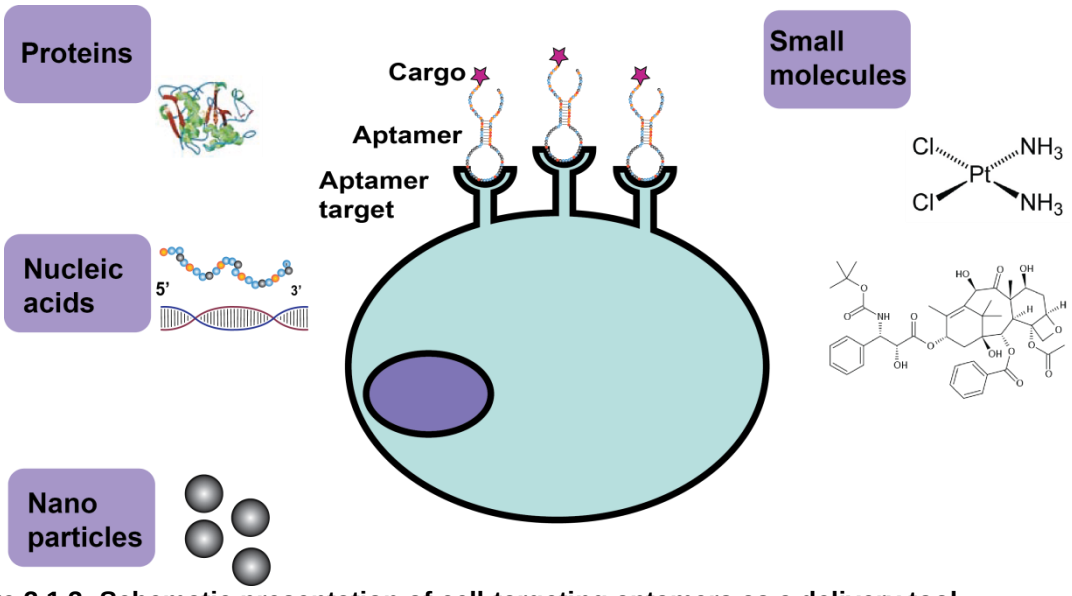

Figure 3.1.3: Schematic presentation of cell-targeting aptamers as a delivery tool
Different cargo molecules can be coupled to the cell-targeting aptamers for delivery into the cells (modified from Mayer *et al.*[30]).

Furthermore, a few cell-targeting aptamers used for the delivery of cargo molecules (nucleic acids) e.g., miRNA, anti-miRNA, and siRNA are listed below **(Table 3-1)**.

Table 3-1 Cell-targeting aptamers delivered cargo nucleic acids

Aptamer	Type	Targeted cell/model	Cargo nucleic acid
GL21.T[31]	RNA	A549	miRNA212
GL21.T[32]	RNA	A549	let-7g miRNA
A 10[33]	RNA	Prostate cancer tumor model	siRNA
A10.32[34]	RNA	LNCaP	miRNA 15a, miRNA-16-1
AptNCL[35]	DNA	CL1-5	siRNA
EpAPT[36]	RNA	WERI-Rb1 and MCF7 cell lines	siRNA
AS1411[28]	DNA	MCF-7	Anti-miRNA 21
MUC1[37]	DNA	Xenograft tumor models	miRNA-29b
TRA[38]	RNA	HUVEC	miRNA-126
HER2, HER3[39]	RNA	HER2+ Breast cancer	siRNA
DNA aptamer[40]	DNA	T-cells	siRNA

3.1.4 Aptamers targeting immune cells as a delivery vehicle

As described above, the cell-targeting aptamers have a number of advantages. They have the ability to recognize target proteins in their native states and according to the expression level of the target on the cell surface[15,19]. Until then, the different molecules involved in the immune system have been targeted by aptamers and are capable of altering the immune reaction. The important role of aptamers can be explored as a new pharmacological agent in the diagnostic and therapeutic tool for immune diseases[41].

The main challenges in immune modulation or therapy can be addressed by aptamers. The three main challenges are; to increase tumor immunogenicity, inhibit immunosuppressive mechanisms, and activate immune receptors[42]. Therefore, aptamers targeting immune cells (monocytes, DCs, and macrophages) could be suitable for modulating the immune response in different diseases. Immune cell-targeting aptamers could be used as an agonist or antagonist to specific receptors, identification of biomarkers for immune specific disorders or as a delivery vehicle. In this study, an aptamer targeting immune cells was characterized and used as a delivery vehicle.

Berezhnoy *et al*.[43] have shown that aptamer conjugated with siRNA has the ability to target CD8+ T cells and induce vaccine-mediated memory and antitumor effect. The aptamer was designed to target 4-1BB, the major costimulatory receptor on the surface of activated T cells[44]. Song *et al.*[45] described that CD4 aptamer has the potential to deliver siRNA by targeting CD4+ human T cells. Thus, an aptamer targeting immune cells could be a promising tool to be used as delivery of cargo molecules for immune disorders.

3.2 The mononuclear phagocyte system (MPS)

The mononuclear phagocyte system is a well-defined group of cells comprising of DCs, monocytes, and macrophages, whereas, monocytes are the major type of MPS in the blood. Macrophages and DCs have the same functional properties and the latter are potent professional APCs[46-48].

The origin of macrophages, DCs, and monocytes originate from two types of progenitors in the bone marrow; the common DC progenitor (CDP) and monocyte & DC progenitor (MDP). MDP can give rise to monocytes and DCs, but CDP is specific to DCs only[49,50].

3.2.1 Monocytes

Members of the mononuclear phagocyte system, monocytes, play a significant role in immune defense, homeostasis, and inflammation. These are bone-marrow derived leukocytes that are released and circulated in spleen and blood. They have the characteristic property of sensing "danger signals" through pattern recognition receptors[51]. These cells have the ability for phagocytosis, antigens presentation, secretion of chemokines, proliferation, and initiate adaptive immunity[51,52]. Monocytes are also considered as progenitor pool because of their ability to differentiate between macrophages and DCs[51,52].

3.2.1.1 Monocytes subsets

During circulation in the blood, monocytes are considered to be a flexible and dynamic cell population consisting of different subsets. They differ in their phenotype, morphology, size, and transcriptional profiles depending to their location in the blood[53]. In humans, CD14 and CD16 surface marker expression and in mice LY6C, CCR2, and CX_3CR1 markers could be used to distinguish between different subset populations[54] **(Figure 3.2.1)**. $CD14^+$ and $CD16^-$ monocytes are considered as classical monocytes which make up to ~85% of the circulating pool whereas 15%

consists of intermediate monocytes ($CD14^{+}CD16^{+}$) and nonclassical monocytes ($CD14^{lo}CD16^{+}$) in humans[53,55] **(Figure 3.2.1)**. Likewise, in the mice, two discrete monocyte subsets have been described, classical monocytes ($LY6C^{hi}CCR2^{+}CX_3CR1^{int}$) and non-classical monocytes ($LY6C^{lo}CCR2^{-}CX_3CR1^{hi}$)[53,56] **(Figure 3.2.1)**.

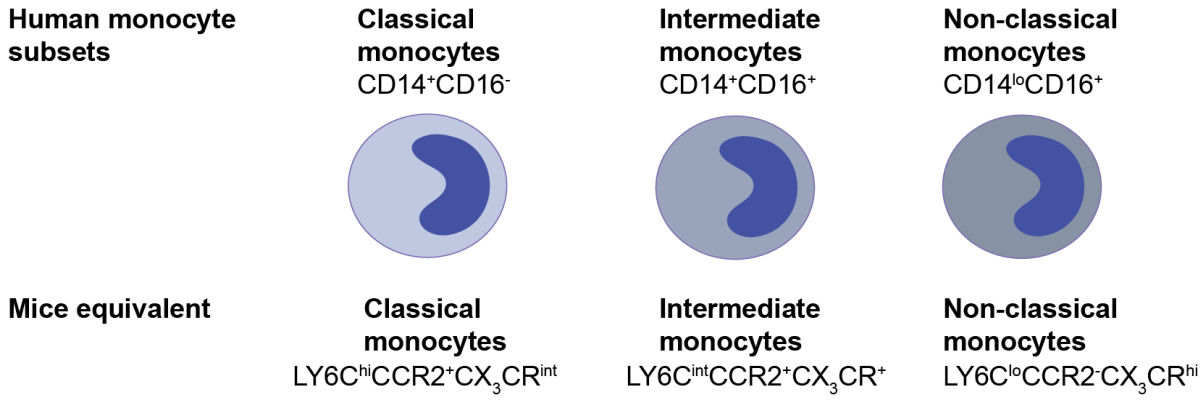

Figure 3.2.1: Human monocytes are classified into three subsets depending on the expression level of CD14 and CD16: classical ($CD14^{+}CD16^{-}$), intermediate ($CD14^{+}CD16^{+}$), and non-classical ($CD14^{lo}CD16^{+}$) monocytes. Mice equivalent subsets have different expression levels of LY6C, CCR2, and CX_3CR: classical ($LY6C^{hi}CCR2^{+}CX3CR^{int}$), intermediate ($LY6C^{int}CCR2^{+}CX3CR^{+}$), and non-classical ($LY6C^{lo}CCR2^{-}CX3CR^{hi}$) monocytes[53-56].

“Classical monocytes” have upregulated chemokine receptor CCR2 **(Figure 3.2.1)** and may be recruited at the site of infection or injury and differentiated into inflammatory macrophages, in mice[56,57]. They are known as inflammatory mediators and are the most abundant subset population recognized in atherosclerotic plaques[58].

“Non-classical monocytes” are also known as patrolling monocytes because they continuously patrol the luminal side of the vascular endothelium and clean the debris[59,60].

“Intermediate monocytes” are generally have inflammatory characteristics, but have high expression of CX_3CR1 adhesion-related receptors. These monocytes are different from the other subsets and do not participate in patrolling of vascular endothelium[61,62].

Monocytes are considered to be the main component of the mononuclear phagocyte system. They are also known as the natural reservoir of macrophages and DCs. The

majority of macrophages have been found in tissues, including vital organs. DCs are well known and most efficient APCs of the mononuclear phagocyte system[63].

3.2.2 Dendritic cells

These cells were described by Steinman and Cohn[64], regard to the establishment of the connection between innate and adaptive immunity[65,66]. They are the most efficient and powerful APCs with distinctive properties to activate naïve T-cells[67]. In the innate immune system, DCs usually recognize pathogen-associated molecular patterns (PAMPs), damage-associated molecular patterns (DAMPs), and release protective cytokines[66,68]. In the acquired immune system, they mostly act as APCs by antigen uptake, processing, and presenting of harmful molecules and antigens. Thus, play an important role in the initiation of adaptive immunity[66].

3.2.2.1 Dendritic cells subsets

DCs are divided mainly into two subsets, plasmacytoid DCs (pDCs) and conventional/classical DCs (cDCs)[66,69]. The pDCs have a different life cycle than the cDCs but the origin of both subsets are similar. pDCs are mainly reside in the blood and lymphoid tissues. They enter the lymph nodes through blood circulation. They have low expression levels of major histocompatibility class II (MHC II), costimulatory molecules, and integrin CD11c in the steady state[70]. These cells are the major effector cells in the innate immune response after viral infection due to their powerful capability to release type I interferons (IFN). In the immature state, these cells could be involved in tolerance (immune suppression)[71].

All DCs other than pDCs are considered to be cDCs. cDCs are a small subset of tissue hematopoietic cells that reside in the lymphoid and non-lymphoid tissues. These cells have a powerful ability to recognize tissue damage, trap or engulf environmental, and cell-associated antigens, process and present these engulfed antigens to activate T lymphocytes. Thus, the cDCs have the property to induce immunity to any exogenous antigens and to impose tolerance to endogenous

antigens[70]. Bacterial molecules are also sensed by cDCs, which results in the release of certain cytokines, including proinflammatory cytokines (TNF-α and interleukin-6) and interleukin-12p70 (IL-12p70) for the activation of T cell subsets (Th1 and Th17). These cells are therefore able to recruit cytotoxic T cells (CTLs)[66,69].

3.2.2.2 Recognition, capture, processing, and presentation of the antigens

PAMPs are recognized by immature DCs, including microbial lipids, nucleic acids, intermediates of viral proteins, and carbohydrates through pattern recognition receptors (PRRs). Different PRRs could be involved in the pathogen recognition processes, such as Toll-like receptor (TLR), RIG-I-like helicases, C-type lectin receptors (CLRs), active protein kinase (PKR), and nucleotide-binding oligomerization domain (NOD-like) receptors[66,71].

Once PAMPs are recognized, DCs can capture or engulf the antigen through different mechanisms such as endocytosis, macropinocytosis, and receptor-mediated phagocytosis[58,72,73]. Particles and microbes are taken up by the DCs through phagocytosis. Macropinocytosis refers to the process by which extracellular fluid and solutes are taken after the formation of large pinocytic vesicles. DCs express different types of receptors that facilitate the process of endocytosis, such as C-type lectin receptors like the macrophage mannose receptor, epithelial cell receptor 205 kDa (DEC-205), and Fc receptors[65]. Once the antigen is captured, it is delivered to the antigen processing compartments[71].

DCs process proteins and degraded them into antigenic peptides that are loaded on the major histocompatibility complex (MHC), either MHC class I (MHC I) or class II (MHC II) molecules[69,72]. Whereas, the process of the lipids molecules is different and they are loaded onto non-classical MHC molecules[72].

DCs present antigens after processing in three different ways:

1. *MHC I to CD8 T cells:* Intracellular antigens (endogenous peptides) are loaded to the cell surface of MHC class I molecules and are recognized by the CD8 T cells. For example, if a cell is infected with a virus, viral peptides are processed and presented by DCs. It allows the immune system to detect and activate CD8 T cells to kill the infected cells[69,74].

2. *MHC II to CD4 T cells:* The exogenous peptides are loaded on MHC class II and activate CD4 T cells. They are derived from the proteins that are endocytosed and then degraded by acid-dependent proteases in the endosomes[69,74].

3. *Cross-presentation:* An important feature of DCs is cross-presentation, mainly of specific subsets of DCs including CD8 DCs and migratory CD13 DCs[75]. It consists of presenting exogenous antigens on MHC class I molecules and has been involved in the stimulation of CD8 T cells[69,74,75].

3.2.2.3 DCs as a therapeutic target

The distinctive family of professional APCs known as DCs is able to induce and regulate immune responses when they come into contact with the antigens[7676,77]. Since the 1990s, different protocols for *in vitro* culture of the human and mouse DCs have been studied which have helped to understand the biology of DCs[78]. DCs play a very important role in linking the innate and adaptive immune response. These features have made them an appropriate therapeutic target for immunotherapy. Various attempts have been made and are currently under study to develop DC-based vaccines. These vaccines can be considered as preventive or therapeutic vaccines for the treatment of cancer. The main purpose of the preventive vaccines is to prevent immune memory diseases, while the therapeutic vaccines target existing cancer cells by inducing an immune response[79,80].

These vaccines generally contain DCs loaded with the tumor antigens, for initiation and regulation of an immune responses in cancer patients. These DC-based vaccines are also used in the development of different immunotherapies against autoimmune disorders, infectious diseases, and cancer (all of these which requires T cell-mediated immunity)[81]. Generally, DC-based vaccines are primarily classified into two categories: *ex vivo* antigen-loaded DC-based vaccines and *in vivo,* DC-targeted vaccines[81,82].

Ex vivo DCs are generated from the BM-progenitor cells, loaded with an antigen, activated in the presence of granulocyte-macrophage-colony-stimulating factor (GM-CSF), interleukin (IL)-4 and IL-13. These cells are then re-injected into the patient[83,84]. Whereas, *in vivo* targeted vaccines refer to direct targeting of natural DC subsets at different sites, stimulate and activate DCs *in vivo*. It has several advantages over the *ex vivo* DC generation. *In vivo* targeting is less expensive, less laborious, easier to standardize, and scale up than the *ex vivo* DC generation [84].

The first DC-based vaccine approved by the Food and Drug Administration (FDA), Sipuleucel-T,[85] is a successful example of an *ex vivo* antigen-loaded DC-based vaccine for the treatment of prostate cancer. Patient's own peripheral blood mononuclear cells (PBMC) including APCs are obtained and in the presence of a recombination fusion protein (PA2024) consisting of prostatic acid phosphate (PAP) and GM-CSF become activated *ex vivo*. The cells are then re-injected to the patient. Activated APCs are considered to induce an immune response to PAP[86,87]. However, the *ex vivo* antigen-loaded DC-based vaccine has certain limitation and inconveniences. High cost of production and time-consuming preparation are the most important which lead to the study of different alternative methods, but with similar strategies[88].

In vivo activation of DCs and antigen loading is an interesting strategy. It provides a physiological environment, targeting of all the DCs subsets present in the physiological system and it may be able to overcome all the limitations of *ex vivo* DC

vaccines[88]. For *in vivo* activation, different carrier molecules are used to deliver antigens specifically to DCs. The carrier molecules currently used are monoclonal antibodies[89], nanoparticles[90], liposomes[91], viruses[92], receptor ligands[93], synthetic long peptides[94], and toxins[95].

These all carriers have certain limitations such as immunostimulatory effects of viruses and toxins[96,97], time-consuming preparation, generation of monoclonal antibodies[98,99], stability problems with liposomal preparations[96], shelf-life of proteins or antibodies[96], and lack of specificity of nanoparticles and liposomes[100].

Aptamers have recently been used as an emerging class of carrier molecules for targeted activation of T-cells[101].

3.2.3 Macrophages

Macrophages have a significant role in the innate immune response and, through biologically active molecules, in the adaptive immune response. They have a significant impact on different human diseases such as infection, allergy, inflammation, and cancer[102-104]. These cells are located in different organs of the body including vital organs such as the liver and brain. They have a specific role in maintaining physiological homeostasis in each organ[105,106].

These cells have distinct plasticity and the ability to change their phenotype according to the microenvironment of the tissue[107]. They release certain types of cytokines to regulate the functioning of other immune cells[108]. During the development and throughout the life span of an individual, macrophages perform phagocytic clearance of dying or dead cells and protect the host from different types of microbial pathogens[109,110].

Over the last few decades, two major phenotypes of macrophages have been studied and recognized according to the concept of T helper type 1-T helper type 2

(Th1-Th2) polarization[111]. Mosmann *et al.*[112] have studied that individual clones of helper T cells could be distinguished as two classes according to the specific cytokines released during antigenic stimulation. Interferon-gamma (IFN-ɤ) and IL-2 are primarily secreted by Th1 cells, while IL-4,-5,-6,-10 and-13 are secreted by Th2 cells[113]. Therefore, the phenotype of macrophages depends primarily on the type of cytokines that the macrophages are exposed to **(Figure 3.2.2)**. Cytokines secreted by Th1 cells e.g., IFN-ɤ and certain bacterial moieties such as lipopolysaccharide (LPS) have the potential to polarize the phenotype of macrophages towards M1 (classically activated macrophages) **(Figure 3.2.2)**. Whereas, Th2 cell cytokine IL-4 polarizes macrophages towards M2 (alternatively activated macrophages)[111] **(Figure 3.2.2)**. In 2014, the spectrum model of macrophages was proposed using nine different types of activation stimuli[114]. The characterization of each phenotype identifies a unique macrophage phenotype that is linked to chronic inflammation stimuli. The cytokines that polarize macrophages towards TPP macrophage phenotype, are tumor necrosis factor, prostaglandin E2, and TLR2-ligand (Pam3CSK4)[114] **(Figure 3.2.2)**.

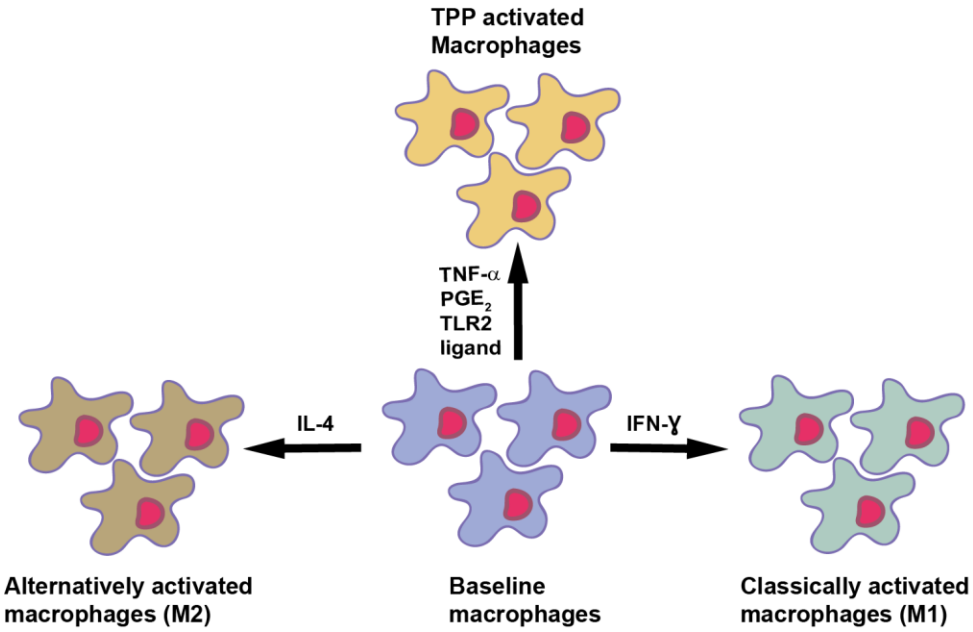

Figure 3.2.2: Schematic illustration of the macrophage activation program. Baseline macrophages can be differentiated into classically activated macrophages (M1), alternatively activated macrophages (M2), and TPP activated macrophages (modified from Xue *et al.*[114]).

3.2.3.1 Classically activated macrophages (M1 or IFN-ɤ)

Th1 cells secrete IFN-ɤ, which has the potential to drive macrophages polarization towards classically activated macrophages (M1 or IFN-ɤ) **(Figure 3.2.2)**. Classically activated macrophages are considered to have improved microbicidal, tumoricidal effects, and secretion of high pro-inflammatory cytokines properties[115,116]. These cells secrete pro-inflammatory cytokines, reactive oxygen, and nitrogen intermediates. They also express MHC II higher/more abundant and are capable of presenting antigens. M1 cells have improved the ability to kill invading viruses, bacteria or certain type of pathogens[117]. LPS, as the main component of Gram-negative bacteria also polarizes the resting macrophages towards M1 or IFN-ɤ phenotype. LPS targets cell surface receptor CD14 on macrophages[118]. The high concentration of LPS can induce CD14 independent polarization[119,120]. In the inflammatory diseases, the production of pro-inflammatory cytokines by classically activated macrophages leads to inflammatory response and causes tissue injury[121].

3.2.3.2 Alternatively activated macrophages (M2 or IL-4)

In contrast to classically activated macrophages, alternatively activated macrophages secrete anti-inflammatory cytokines to resolve inflammation. They produce a particular type of extracellular matrix (ECM) for tissue repair and regeneration[122,123]. Likewise, Th2 polarization, M2 or IL-4 macrophage polarization state can be driven by exposure of different cytokine types including, IL-4,-13 and -10[116,123] **(Figure 3.2.2)**.

3.2.3.3 TPP activated macrophages (TNF, PGE_2, and TLR2 Ligand)

Xue *et al.*[114] used and characterized a new stimulation condition TPP for macrophages activation. TPP stimulation condition is closely related to the chronic granulomatous inflammation such as granulomatous listeriosis or tuberculosis. TPP activated macrophages associated with chronic inflammatory diseases can be driven

by exposure to TNF, PGE_2, and TLR2 ligand (TPP stimulants) **(Figure 3.2.2)**. In 2014, nine different activation programs[114], M1 and M2 polarization model were extended to the spectrum model of macrophages activation. The M1 and M2 polarization models were very helpful in the immune studies related only to acute infections, allergy, asthma, and obesity[124]. The observations, which were obtained from different studies on macrophages related to chronic inflammation, chronic infection and even cancer significantly, illustrate a more diverse spectrum of activation depending on the changes in the environment[114].

TPP activated macrophages have phenotypic and functional differences from IFN-ɤ and IL-4 activated macrophages. Signal transducer and activator of transcription 4 (STAT4), transcription factor and upregulation of CD14 and CD25 surface markers were only identified in the TPP activated macrophages, which makes it distinct from the other phenotypes[114]. At-posttranscriptional level, miRNA 125a-5p is highly upregulated and certain miRNAs are downregulated in the TPP macrophages[114] **(Figure 3.2.3)**.

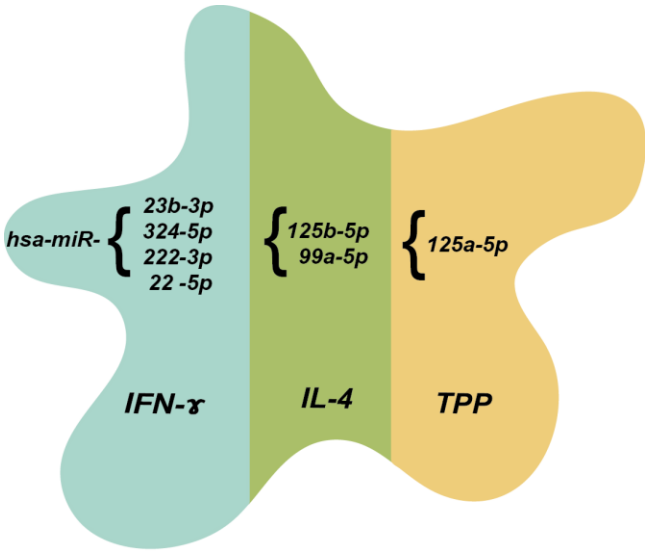

Figure 3.2.3: Overview of miRNA expression level in different macrophage phenotypes
Five different miRNAs have the same expression level in IFN-ɤ stimulated macrophages. Two miRNAs are highly upregulated in IL-4 stimulated macrophages. One miRNA is highly upregulated in TPP stimulated macrophages. (miRNA expression level was taken from Xue *et al.*[114]).

3.2.3.4 Macrophages as a therapeutic target

It has been well accepted that macrophages play an important role in various physiological and pathological conditions. They are involved at different levels starting from developmental stages to homeostatic functions of the tissues and also play a pivotal role in different human diseases[125]. During chronic inflammatory diseases, macrophages are the key player cells of the body[126,127]. In the last few decades, macrophages have been well studied for their biology, their activation programs, and their role in various diseases[107,110,114,117,127]. But still, it seems difficult to target macrophages in a more precise manner.

Schultze[128] described in his review (2016), that there is not even a single treatment available on the market specifically for macrophages. However, different pre-clinical and clinical efforts are currently under investigation to targeting macrophages[128-132]. Previously, the major areas of interest in targeting macrophages include depletion of macrophages, reprogramming or re-education of macrophages, and inhibiting the recruitment of macrophage[125].

"Macrophage depletion" refers to the direct killing of macrophages. They are targeted by macrophage-specific cell surface receptors such as colony stimulating factor 1 receptor (CSF1R) using anti-CSF1R antibodies or by the use molecules such as bisphosphonates and trabectedin. These molecules have the property to exert a specific toxic effect against macrophages[125,133,134]. This targeting strategy may have certain limitations such as inflammatory diseases. If the inflammation is limited to a certain part of the body and the macrophages are even depleted from all health tissues, it will have a pronounced undesired effect on the physiology and homeostatical role of macrophages in all tissues of the body[128,135]. Macrophage depletion is unfavorable in clinical use due to an increased risk of infection when the patient is already immune-compromised by side-effects of chemotherapy[136].

"Macrophages re-education" or *"reprogramming"* refers to the properties of macrophages to differentiate between different phenotypes according to the micro-

environmental signals. Therefore, these cells are considered to have a great plasticity[103,137]. This strategy is used in the field of anticancer therapy, to re-educate the pro-tumor M2-like macrophages to M1-like macrophages with the antitumor properties[138,139] **(Table 3-2)**. Song *et al.*[140] have successfully used this strategy with bioconjugated manganese dioxide nanoparticles to enhance the chemotherapy response with anti-tumor properties[140].

"Inhibition of macrophage recruitment" into the tumor cells is another approach to targeting the macrophages[141] **(Table 3-2)**. The inhibition of chemokine (CCL2) or its receptor (CCR2) that regulates the migration of monocytes and macrophages significantly affects the overall growth of hepatocellular[142] and renal cell carcinomas[143]. Surprisingly, breast cancer metastasis is accelerated following cessation of CCL2 inhibition by promoting the angiogenesis[144] indicating the significance of CCL2 role in regulating metastasis[136]. Another chemokine (CXCL12) regulates the chemotaxis of macrophages through endothelial barriers to the tumor milieu. The stromal cells secrete this chemokine to stimulate the movement of cancer cells by upregulation of their CXCR4 receptors[145]. The pharmacological inhibition pathway of CXCL12/CXCR4 provides a promising approach to altering macrophage recruitment and combat metastasis[145]. In the mouse model, treatment with CXCR4 antagonist showed a significant reduction in tumor growth as well as in combating metastasis of breast cancer[146].

Table 3-2 Different target strategies for tumor-associated macrophages (TAMs) are listed (adapted from Panni *et al.*[141])

Target or Drug	Mechanism of action
CCL2-CCR2 axis	Prevents monocyte recruitment
CSF1-CSF1R axis	Inhibits/reprograms TAMs
CXCL12-CXCR4 axis	Prevents recruitment of macrophages
DNA repair mechanisms (trabectedin)	Targets TAMs
Clodronate and zoledronic acid	Induces macrophage apoptosis
Anti-CpG and IL-10 Ab	Prevents antitumor to protumor macrophage polarization
CD40 agonist	Restores tumor immunity
Sibilin	Suppresses NF-κB and STAT3 phosphorylation, blocks angiogenesis

Ab: Antibody; CSF1R: CSF1 receptor; TAM: Tumor-associated macrophage

During the last few decades, several studies have described that the activation and biological response of macrophages is regulated by miRNAs[147]. These tiny molecular rheostats play a significant role in the innate immune system and macrophage biology. They act as a rheostat because of their role as fine-tuning of cellular response rather than switching on/off[148]. The expression levels of different miRNAs are significantly altered by the exposure of TLR ligands to THP-1 monocytes and primary mouse macrophages. These miRNAs have a significant effect on macrophage activation biology[149,150] and on different phenotypes of macrophages as presented in **Figure 3.2.3**. Therefore, miRNAs might be considered to be cell-specific and tissue-specific in different diseases. Thus, targeting strategies at the epigenetic and transcriptional level such as miRNAs may have the potential for therapeutic options in the future[128].

3.3 microRNAs (miRNAs)

In the early 1990s, approximately 22 and 61 nucleotides long lin-4 transcripts were identified in *Caenorhabditis elegans* (*C.elegans*)[151,152]. These sequences were complementary to the 3' untranslated region (UTR) of lin-14 messenger RNA (mRNA). Therefore, Wightman *et al.*[151] proposed that lin-4 regulates the translation of lin-14 via an antisense RNA-RNA interaction. Thus, a new non-coding RNA regulatory mechanism was discovered, but no single non-coding RNA regulatory mechanism was studied in any species until 2000. In 2000, Reinhart *et al.*[153] reported that lethal-7 (let-7) encodes a non-coding 21-nucleotide long RNA sequence, that complementary to the 3' UTR regions of the lin-14, lin-28, lin-41, lin-42, and daf-12 genes. It was an indication that the expressions of these genes were controlled by let-7[153]. Since then, these small non-coding RNAs, now known as microRNAs (miRNAs), have been identified in eukaryotes, that are involved in the regulation of different developmental and cellular processes[154]. Interestingly, 60% of protein-coding genes in the human genome are regulated by miRNAs[155]. These tiny RNAs are of significant importance for normal development and play a pivotal role in different biological processes[156]. An abnormal expression level of miRNA is most

likely associated with different human diseases[157] including diabetes, cardiovascular disease, kidney disease, and cancer[158].

3.3.1 Biogenesis of miRNAs

Biogenesis of miRNAs occurs in multiple steps through canonical or non-canonical pathways[159] **(Figure 3.3.1)**. Genes for miRNAs are generally transcribed from the RNA polymerase II promoters. In the canonical pathway, Drosha, RNase III enzyme cleaves the primary miRNA (pri-miRNA) hairpin to the precursor miRNA (pre-miRNA). While the non-canonical pathway is independent of Drosha and pre-miRNAs are generated by the mRNA splicing mechanism. Pre-miRNAs generated by both pathways are transported to the cytoplasm via a nuclear export protein, exportin 5. In the cytoplasm, Dicer, the second RNase III enzyme further processes the pre-miRNAs into duplexes[159]. These miRNA duplexes have a phosphate at the 5' end, a hydroxyl group at the 3', and overhangs of 2 nucleotides[160]. These duplexes are then loaded into a functional ribonucleoprotein complex called the RNA-inducing silencing complex (RISC) comprising Dicer, trans-activation response RNA-binding protein (TRBP), and Argonaute (AGO) proteins. The guide and the passenger strands are identified by the TRBP through thermodynamic properties of the duplex miRNA[159]. Normally, it identifies a strand with a less stable 5' end and is preferentially loaded into the AGO and is known as the guide strand. The guide strand will be unwound from the other strand, known as the passenger strand by means of different mechanisms, depending on the extent of their complementarity[161]. After the strand is selected, the passenger strand leaves the activated RISC and the guide strand (mature miRNA). The 5' end of the mature miRNAs known as seed region (2-8 nucleotides) mediates the binding of mRNA to the miRNA-induced silencing complex[162].

One miRNA can regulate hundreds of different targets at the post-transcriptional level. There are different regulation mechanisms of miRNAs, such as inhibition of translation initiation and mRNA degradation or destabilization[163,164]. The complementarity between miRNA and mRNA determines the mechanism of

regulation. Degradation of mRNA occurs with the 100% complementarity, while inhibition of translation occurs when imperfect complementarity with the characteristic bulges are formed[165].

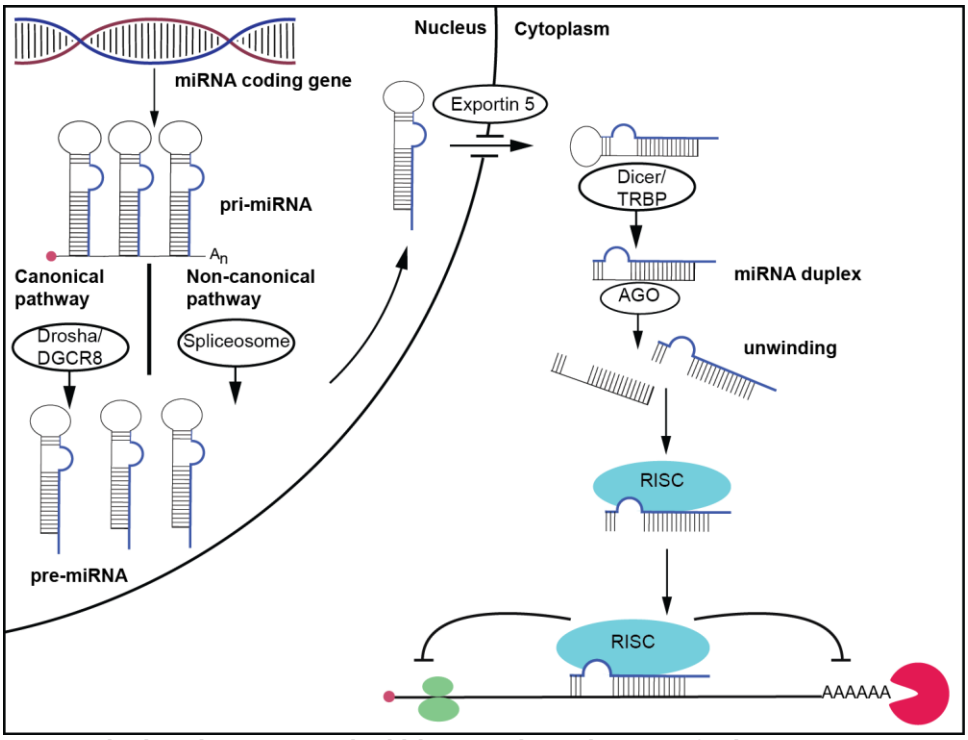

Figure 3.3.1: Canonical and non-canonical biogenesis pathways of miRNA
miRNA coding genes are transcribed into pri-miRNAs transcripts by RNA polymerase II. Pri-miRNAs have a 5' CAP and a poly (A) tail. In the canonical pathway, pri-miRNAs are processed by Drosha-DGCR8 (DiGeorge syndrome critical region 8), RNA III enzyme complex, to pre-miRNAs. Whereas, in the non-canonical pathway pre-miRNAs are generated by mRNA splicing mechanism. Pre-miRNAs of the both pathways are exported to the cytoplasm by exportin 5. Dicer, the RNA III enzyme, further processes the pre-miRNAs to double stranded miRNA duplexes and loads them into an AGO in the RISC and unwound the strands. The guide strand (mature miRNA) is retained in the RISC, while the other strand known as the passenger strand is released. The guide strand mediates and recognizes the target at 3'UTRs of target mRNA for inhibition of translation initiation and mRNA degradation or destabilization (modified from Li *et al.*[159],Stenvang *et al.*[166]).

3.3.2 miRNAs as a therapeutic target

The small size and known sequence of miRNAs are unique characteristics for the development of drug[167]. The other characteristic feature of miRNAs is that the expression level is altered in different disorders such as metabolic diseases, hepatitis C, myocardial infarction, and cancer. Signature patterns of miRNAs are conserved in different diseases e.g., some miRNAs are upregulated and some are downregulated in a particular disease[168]. The fine-tuning of miRNAs through

antisense oligonucleotides (ASO) may have a long-lasting therapeutic effect. The upregulated miRNA can be inhibited by antagomir[166] and the downregulated miRNAs expression can be restored through double-stranded miRNA mimics[169]. Recently, the targeting of miRNAs presents a potent tool for therapeutic intervention in different diseases[167].

3.3.3 Strategies for miRNAs manipulation

There are two main strategies for the manipulation of miRNAs. Depending on the expression level of miRNAs, either the targeted miRNAs expression level needs to be inhibited or restored by re-introducing miRNAs[167].

Restoration or introduction of miRNAs: During the progression of different diseases including cancer, the miRNA expression level was altered or downregulated. The expression level could be restored by transfecting exogenous double-stranded miRNAs or using the vector to express the desired miRNA[167]. Restoration of miRNA-29b in glioblastoma cancer cells has the potential to inhibit the expression of different genes, resulting in anti-cancer effects[170]. Likewise, the delivery of exogenous miRNA-34a with NOV340 liposome resulted in the tumor reduction and prolonged survival in the animal models[171]. The Phase I clinical trial to restore the function of miRNA-34a also showed safety and anti-tumor activity in patients with advanced solid tumors[172].

Antagomir for inhibition of miRNAs: miRNA antagonists (antimiRs) or an antagomir are oligonucleotides having a complementary sequence of endogenous miRNAs[167]. These chemically modified ASO are widely used in the miRNA loss-of-function studies[173]. Chemical modifications are required to increase binding affinity, enhanced nuclease resistance, and *in vivo* delivery[173]. These modifications are classified as first generation, second generation, and third generation modifications. Modifications of the first generation are used to enhance nuclease resistance by the introduction of phosphorothioate (PS) bond in the phosphate

backbone of the ASO **(Figure 3.3.2)**. These modifications also include modulation of the phosphodiester backbone, the sugar moiety, and heterocyclic nucleobase to improve affinity and specificity. The first antisense drug approved by the FDA is Vitravene, a first generation PS-ASO, for the treatment of AIDS-related cytomegalovirus (CMV) retinitis[174]. Unfortunately, Vitravene is discontinued in Europe and the United States due to the development of high-activity anti-retroviral therapy (HAART)[175]. Most drugs based on first generation modifications in Phase I clinical trials are PS modified. However, their binding profile to the target RNA sequence and specificity are less satisfactory with low cellular uptake. The limitations associated with the first generation oligonucleotides are addressed by second generation modification[176].

In the second generation modification, the sugar moiety of nucleobase is modified to improve the binding affinity to the target RNA. The most promising modifications include 2'-O-Methyl (2'-O-Me), 2'-O-methoxyethyl (2'-O-MOE), and Locked Nucleic Acids (LNAs)[176] **(Figure 3.3.2)**. 2'- substitution on the furanose ring of the RNA is one of the structural differences between DNA and RNA. Therefore, the ASO binding affinity to the target RNA may be enhanced by mimicking RNA structures with the 2'- modified nucleosides. The introduction of the 2'-O, 4'-methylene bridge in the sugar-phosphate backbone of the furanose ring locked in the conformation of the RNA mimicking N-type (C3'-endo) in the LNA modified ASO. The other modifications such as substitution of electronegative fluorine and oxygen also affect the furanose ring in the C3'-endo conformation[166]. Meister *et al.*[177] demonstrated for the first time that 2'-O-Me modified oligonucleotides inhibit the sequence-specific miRNA in the cultured mammalian cells for the loss-of-function studies.

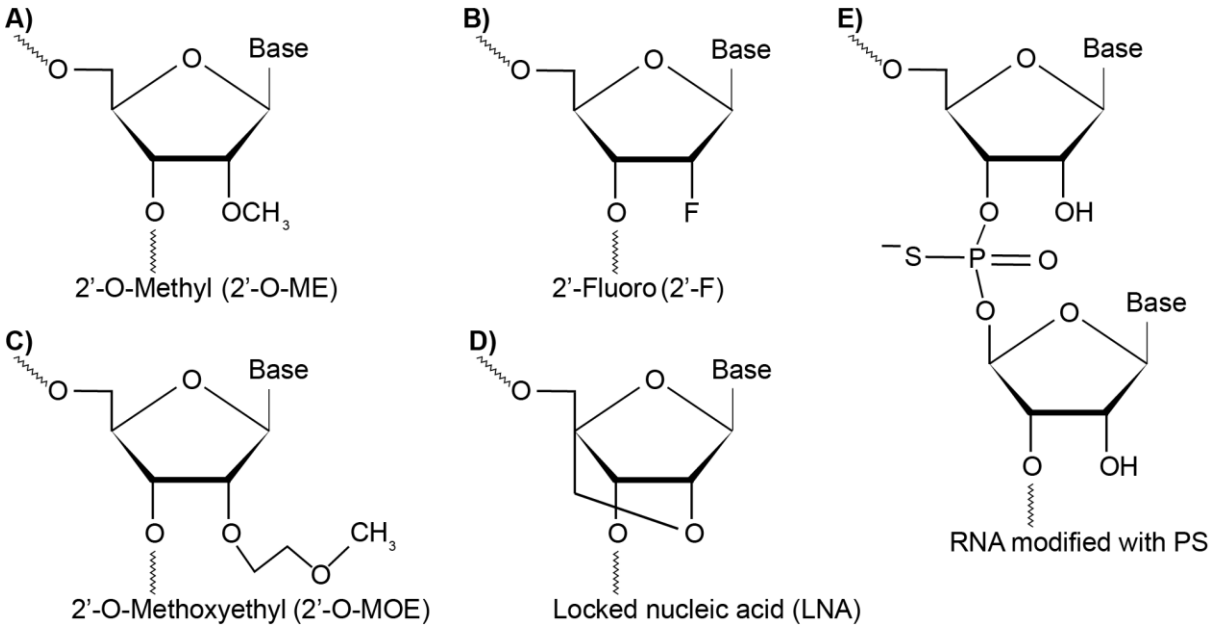

Figure 3.3.2: Chemical modifications of antagomir oligonucleotides
A-D) The sugar backbone of antagomir oligonucleotides is modified to increase the stability and affinity of oligonucleotides. **E)** The phosphate backbone of the oligonucleotides is modified to enhance nuclease resistance by the introduction of phosphorothioate (PS) bond (modified from Stenvang *et al.*[173]).

3.3.4 Mechanism of action of antagomir

Several steps may be targeted during the biogenesis of mature miRNAs for the inhibition or loss-of-function studies. Targets may include pri-miRNA transcripts, intermediate pre-miRNA stem-loop structure or mature miRNA. The most promising target is mature miRNA because two other targets have certain limitations such as the design of antagomir due to thermodynamic challenges and the different complications of *in vitro* studies (e.g., the presence of mature miRNAs in the cytoplasm negatively interferes with the detection of inhibition)[178].

The standard antagomir used to inhibit mature miRNA must be perfectly complementary to the full length of the targeted miRNA[179]. The ideal antagomir has the property to sterically block the target miRNA from binding to the mRNA. The antagomir forms a duplex with a miRNA guide strand and leads to loss-of-function. The potency of an antagomir is increased by chemical modifications that enhance duplex stability and nuclease resistance. The binding affinity of the duplex needs to be significantly higher than that of the miRNA guide and the passenger strand

duplex in order to prevent the unwinding by helicase activity[179,180]. The antagomir needs to bind to the target miRNA either in a single-stranded form or when it is bound to an AGO in the RISC[179]. “Seed region” of miRNA (2-8 nucleotides) at the 5’ UTR is well organised and exposed in the AGO to support the binding to the complementary site to the target mRNA[180,181]. Tiny modified LNA, complementary to the seed region of miRNA, is also capable to inhibiting miRNA and family of miRNA sharing the same seed region[181]. The mechanism of miRNA inhibition by the antagomir oligonucleotides is shown in **Figure 3.3.3**.

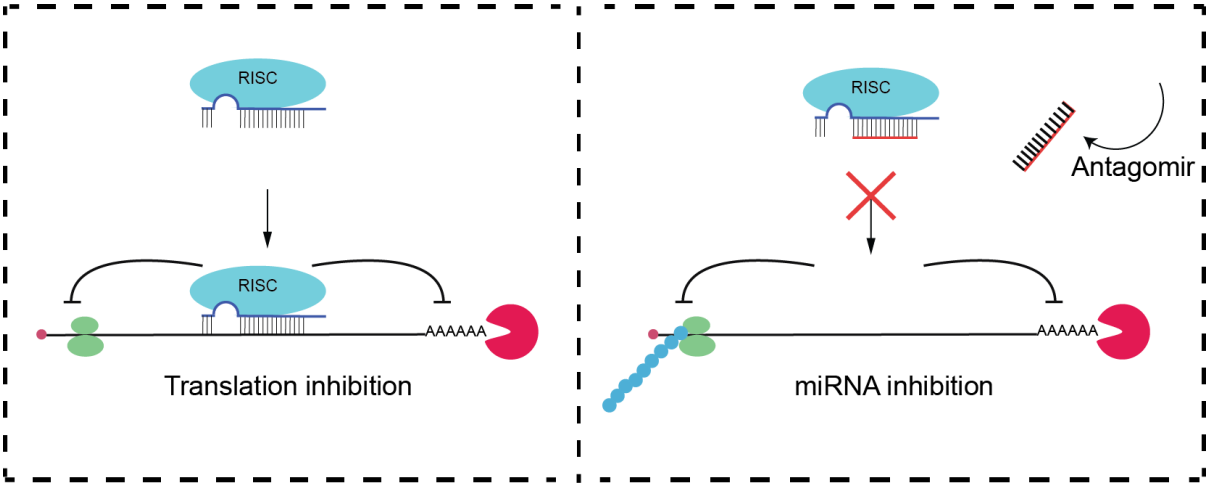

Figure 3.3.3: Mechanism of action of antagomir oligonucleotides
Left: Endogenous miRNA binds to the target mRNA leading to translation inhibition. **Right**: Chemically modified antagomir binds to mature miRNA in competition with the 3’UTR of the cellular target mRNA leading to functional inhibition of the miRNA (modified from Stenvang *et al.*[173]).

3.4 Aims of the thesis

The aim of this study was to investigate the potential role of macrophage-binding aptamer as a delivery tool for delivering antagomir 125a-5p in human baseline macrophages. In particular, we were interested to reprogramming TPP macrophages to other macrophage phenotypes.

The mature miRNAs are from the family of small non-coding RNAs that have a regulatory effect on the expression of various genes. Endogenous miRNAs play a significant role in the fine-tuning of cellular responses. Over the past decades, miRNAs have been known to be an important regulator of macrophage activation and biological response. miRNA 125a-5p is highly upregulated in chronic

inflammatory macrophages (TPP). We hypothesized that inhibition of miRNA 125a-5p could have an impact on the overall polarization state of TPP macrophages. The use of high affinity and complementary nucleic acid (antagomir 125a-5p) can inhibit endogenous miRNA 125a-5p. However, antagomirs have limited therapeutic efficacy due to poor cellular uptake. As a result, various carrier molecules are in use to facilitate transport across the cellular membrane.

In the current study, ssDNA aptamer (DC 12) was used as a carrier molecule for the delivery of antagomir 125a-5p to human baseline macrophages. DC 12 aptamer was covalently linked to the antagomir 125a-5p and thus constructs a chimera known as aptamiR. DC 12 aptamer was screened from the NGS data of BM-DCs cell-SELEX. Potential targeted delivery vehicles have to meet several criteria. They need to bind to their target cells with high affinity and specificity and internalize for the efficient delivery of cargo molecules. Flow cytometry binding assay and confocal microscopy can be used to analyze the binding and internalization of the DC 12 aptamer. The aptamiR 125a-5p chimera interaction with the cells and inhibition of endogenous miRNA 125a-5p was studied. In addition, the carrier properties of DC 12 aptamer were further validated by the aptamer guided delivery of OT-I peptide to DCs for targeted activation of CD8 T cells.

4 Results

The potential of the selected ssDNA aptamer, used as a delivery vehicle in the macrophages and DCs, is described in this chapter. Practically the study was conducted in five phases and so the chapter is also divided into five sections.

The first two **Sections 4.1** and **4.2** describe the characterization of ssDNA aptamers targeting different monocytes/macrophages cell lines, BM-DCs, primary, and differentiated human macrophages. The third **Section 4.3** describes EGFP-4X125a-5p reporter gene construction and investigations using miRNA 125a-5p mimic. The stable cell line was constructed with the reporter gene. The interaction studies were conducted, including inhibition of miRNA 125a-5p in the stable cell line using the antagomir 125a-5p and the binding studies.

Whereas, the fourth **Section 4.4** deals with the construction of the aptamer-antagomir 125a-5p conjugates (aptamiR 125a-5p) and the pharmacological effect of aptamiR on the inhibition of miRNA 125a-5p.

The last **Section 4.5** concludes with the construction of aptamer-peptide conjugates and the targeted delivery of antigen for CD8 T cell activation.

4.1 Analysis of binding capacity (affinity) and specificity of aptamers sequences to macrophages and DCs

Macrophages are immune cells that share a monocyte-macrophage DC progenitor as a common precursor to monocytes and DCs[182]. Macrophages and DCs are professional APCs and might have common cell surface receptors that facilitate this process. In general, macrophage targeting aptamers can be selected through the cell-SELEX approach[183]. BM-DCs cell-SELEX was previously performed in our lab[101] and in the preliminary analysis, the aptamer sequences selected from BM-DCs cell-SELEX showed an affinity towards the macrophages[101]. There might have been some sequences that recognize macrophages as they shared the same progenitor and functions as DCs. The NGS data of BM-DCs cell-SELEX showed that selection cycle 1 contains 100% unique sequences and that the percentage of

unique sequences decreased to 50% in the 10th selection cycle. The complexity of the selection cycle gradually decreased starting from the 3rd selection cycle and certain DNA sequences became more abundant[101].

The NGS data of the BM-DCs cell-SELEX was used and the most abundant sequences **(Table 4-1)** from the 10th selection cycle were tested with macrophage cell lines. To identify the most promising sequence to be used as a delivery vehicle.

Table 4-1: The most abundant sequences identified from the NGS data of BM-DCs cell-SELEX[101]

DC	Random region 5'-3'
4	GGGGAGGTGGGTGGGTTGGCCTTCACGTTATCTTTTGGTGGTT
6	CCAGGGGAGGATGGGAGGGTTTTTTTCGGATTCTTGTCGTGCT
7	CGTGGTATGTGGTGGGTGGTGGGGTGGTAGTTGGGTGGACGGT
8	CAGGGGAGGTGGGTGATTGGGTTGTTTTTCGCGGACGTGAGGT
10	CGAGTTTCTGAGGGTGGGTGGGTGGTTATTAGTCGAGGTTGCA
12	CCAGGGTGGGATGGGTATTTTGAGGTGGAGGTGGGGGTTGGTT
13	GGGTGTTGTGGGGTGGGGCGGTGGGTGTGAGTGTCGGCAGCTG
14	TGTGGTTCGGTAGGTCGGGGAGGGTGGTGGGTTATGCGGCGGG
15	CACAGGGGAGGTCGGGCGGGTTGTCTGCTTTCTTGGGTCGGTT
20	CGTACTTTCACACGGGGAGGTGGGTTGGGTTCTGATTAGGGTT
21	CTGGGTCGGGGGTATTGTTTGCGATATGGGGGGTTTTGGGGTG

4.1.1 Binding of the ssDNA sequences to the J774A.1 cells (mouse macrophages)

The Cherenkov assay was performed to investigate the binding capacity (affinity) of the sequences **(Table 4-1)** towards macrophages **(Figure 4.1.1).** Herein, the J774A.1 cell line (mouse macrophages) was used as a target. Since the sequences were selected from the BM-DCs cell-SELEX, they could recognize mouse macrophages because both express many common molecules[184]. 11 the most abundant sequences **(Table 4.1.1)** were tested in the Cherenkov assay from the NGS data. ^{32}P-DNA was incubated with J774A.1 cells in the DMEM medium supplemented with 10% FCS at 37°C for 10 minutes. The percentage of bound ^{32}P-DNA has been calculated. All the sequences have the potential to bind to J774A.1 cells compared to control (Ctrl 2). Ctrl 2 was used as a non-specific control DNA sequence. This sequence was also used as a control in the characterization of BM-DCs selected aptamers. Ctrl 2 was a scrambled sequence of the CTL#5 aptamer from the protein-SELEX targeting the recombinant protein Fc-CTL[101]. The

percentage of bound DNA greater than Ctrl 2 indicates binding towards macrophages **(Figure 4.1.1).** The sequences (1 pmol of ^{32}P-labeled DNA) showed 6-8% binding to the cells in Cherenkov assay. 6-8% ^{32}P-DNA bound with the cells is considered high because the number of aptamer molecules is greater than the total number of cells used for Cherenkov assay. For instance, 1 pmol contains $6.022x10^{11}$ molecules of the aptamer in Cherenkov assay (1 mole is equal to $6.022x10^{23}$ molecules, Avogadro's number). 6-8% of 1 pmol contains approximately have $3.6x10^{10}$ - $4.8x10^{10}$ molecules of the aptamer bound to the cells ($3.6x10^{10}$ - $4.8x10^{10}$ molecules > $0.5x10^{5}$ cells). Thus, 6-8% of the bound aptamer is considered to be high.

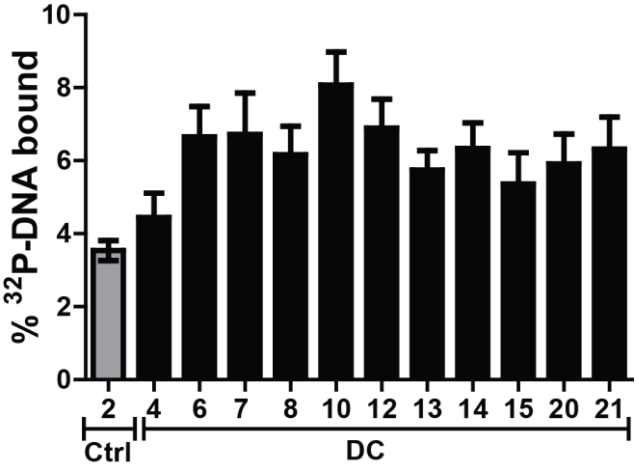

Figure 4.1.1: Binding of the ssDNA sequences to J774A.1 cells (mouse macrophages)
The most abundant NGS sequences from the cell-SELEX of BM-DCs show binding towards mouse macrophages (J774A.1).1 pmol ^{32}P-labeled DNA was incubated with 0.5×10^{5} J774A.1 cells. Liquid scintillation was used to determine the percentage of the bound DNA sequences to the cells. (n=3, mean ± SD).

In order to further confirm the Cherenkov assay, a flow cytometry assay was used to assess the binding to macrophages. Three sequences (DC 7, DC 10, and DC 12) were selected from chenrenkov assay, which had a higher mean percentage of cells bound, to be tested in the flow cytometry assay. 5'-ATTO 647N- labeled Ctrl 2, DC 7, DC 10, and DC 12 were incubated with $4x10^{5}$ cells in the DMEM medium supplemented with 10% FCS at 37°C for 10 minutes.

Table 4-2: Percentage (%) J774A.1 cells bound by ATTO 647N-labeled aptamers and relative mean fluorescence intensity (MFI) in flow cytometry binding assay

Aptamer	% Cells bound	Relative MFI (aptamer/control)
Ctrl 2*	8.60±4.8	1.01±0.16
DC 7	63.6±2.8	3.35±0.76
DC 10	62.8±4.5	3.19±0.67
DC 12	81.3±2.9	3.97±0.59
D#23	81.2±2.6	4.18±0.75

* control

Subsequently, the percentage of cells bound by DNA and the mean fluorescence intensity (MFI) was detected by flow cytometry **(Table 4-2** and **Figure 4.1.2)**. D#23 aptamer was also included in the flow cytometry binding assay as a positive control[101] **(Table 4-2** and **Figure 4.1.2).** D#23 showed the binding ability to BM-DCs as well and it is a two-point mutant of D#7 aptamer. D#7 was a well-characterized aptamer targeting BM-DCs and was used in the aptamer-targeted delivery of antigen to DCs for T cells activation[101].

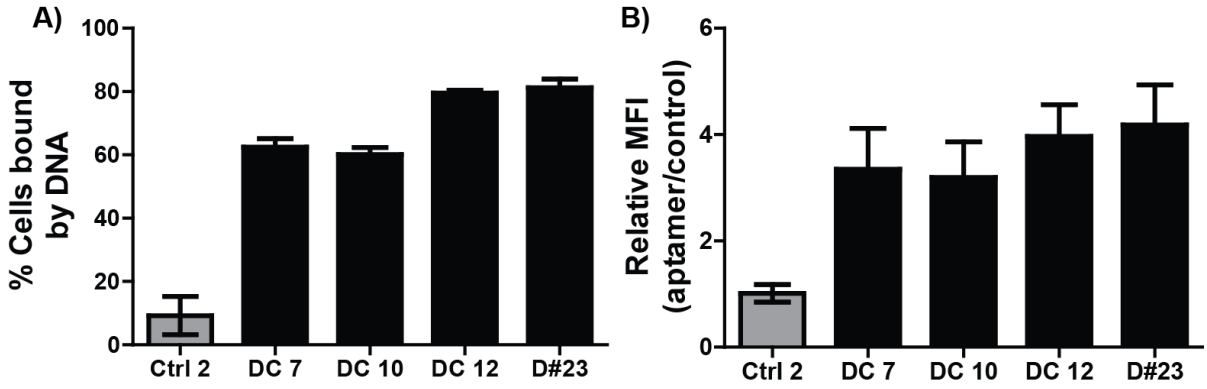

Figure 4.1.2: ATTO 647N-labeled aptamers binds to J774A.1 cells in flow cytometry binding assay

4×10^5 J774A.1 cells were incubated with 250 nM of 5'-ATTO 647N-labeled aptamers at 37°C for 10 minutes.**A)** The percentage of cells bound by aptamers and **B)** relative MFI (aptamer/control) were measured by flow cytometry.(D#23 aptamer was used as a positive control[101]) (n=3, mean ± SD).

4.1.2 Binding of aptamers to THP-1 cells (human monocytic cell line)

The binding potential of the ssDNA sequences was described in the J774A.1 cell binding assay **(Figure 4.1.1** and **Figure 4.1.2)**, resulting in the identification of DC 7, DC 10, and DC 12 aptamers, which showed binding to the mouse macrophages. THP-1 cells were used as target cells to test the binding ability to the human cell line or human origin. Human monocytes have properties to differentiate either as monocyte-derived macrophages or as monocyte-derived DCs[185,186]. Therefore, binding experiments with THP-1 cells are worthwhile. These cells are taken from human sources and are capable of being differentiated into human macrophages and DCs, like cells.

Table 4-3: % THP-1 cells bound by ATTO 647N-labeled aptamers and relative MFI in flow cytometry binding assay

Aptamer	% Cells bound	Relative MFI (aptamer/control)
Ctrl 2*	3.70±1.13	1.0±0.19
D#23	21.7±5.63	2.3±0.58
DC 7	17.8±4.17	2.4±0.63
DC 10	9.70±3.16	1.9±0.42
DC 12	52.4±5.39	3.5±0.64

*control

A flow cytometry assay (**Table 4-3** and **Figure 4.1.3**) was used to analyze the binding of aptamers to THP-1 cells. 5'-ATTO 647N- labeled aptamers Ctrl 2, DC 7, DC 10, and DC 12 were incubated with $4x10^5$ cells in the RPMI 1640 medium supplemented with 10% FCS at 37°C for 10 minutes. The percentage of cells bound by DNA and MFI was detected by the flow cytometry. DC 12 showed 52.4±5.39% cells bound while the other aptamers (DC 7, DC 10, and D#23) showed a lower percentage of bound cells **(Table 4-3)**. THP-1 cells are from the human source and are not well developed/differentiated into macrophages or DCs, which might be the reason for the decrease in the binding of the aptamers. The main aim of this study was to use macrophage-binding aptamer to delivery antagomir 125a-5p into human

baseline macrophages. Therefore, aptamers with a high percentage binding to human cells (THP-1) were chosen for further analysis.

Thus, D#23 and DC 12 were further analyzed because they have a higher potential to recognize human monocytic cells compared to the other two aptamers **(Figure 4.1.3)**.

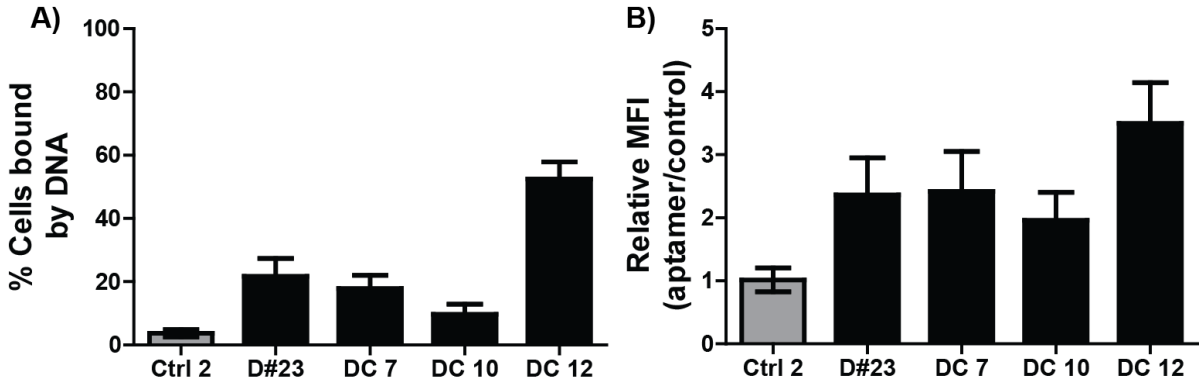

Figure 4.1.3: ATTO 647N-labeled aptamers binds to THP-1 cells in flow cytometry binding assay

4×10^5 THP-1 cells were incubated with 250 nM of 5'-ATTO 647N-labeled aptamers at 37°C for 10 minutes. **A)** The percentage cells bound by aptamers and **B)** relative MFI (aptamer/control) were measured by flow cytometry.D#23 aptamer was used as a positive control[101] (n=4, mean ± SD).

The concentration-dependent binding of DC 12 and D#23 to THP-1 cells, was analyzed using a flow cytometry binding assay. Ctrl 2 (scrambled control), D#23, and DC 12 labeled with 5'-ATTO 647N were incubated with THP-1 cells with the increasing concentration (10 nM - 5000 nM). The cells were incubated with the aptamers at 37°C for 10 minutes. The mean fluorescence intensity (MFI) was measured by flow cytometry **(Table 4-4** and **Figure 4.1.4)**.

Table 4-4: MFI of THP-1 cells bound by ATTO 647N-labeled aptamers in flow cytometry binding assay

Concentration (nM)	MFI		
	Ctrl 2	D#23	DC 12
10	1.60±0.24	2.50±0.64	2.63±0.90
25	1.67±0.27	2.93±1.14	3.49±1.44
50	2.07±0.39	3.39±1.55	4.12±1.71
100	2.15±0.48	5.99±2.90	6.72±3.27
250	2.79±0.85	8.18±5.46	9.68±5.46
500	3.91±0.91	9.43±4.48	14.15±6.24
750	4.06±1.05	12.49±5.97	19.23±7.51
1000	5.09±1.39	11.95±4.76	21.38±5.75
2500	9.75±1.86	21.25±6.20	32.80±8.29
5000	17.10±1.61	33.48±7.84	44.23±8.73

DC 12 was shown to have higher MFI compared to D#23. MFI of the Ctrl 2 was also increased at the last two concentrations but it was still less than aptamers. It might be due to the unspecific uptake of the high concentrated DNA in the surrounding fluid through endocytosis. The concentration-dependent binding curve is not saturated even at the high concentration. It may be due to the continuous internalization of aptamers. As shown in **Figure 4.1.4**, there is an increase in the MFI with increasing the concentration. All aptamers showed the concentration-dependent binding to the human monocytic cell line (THP-1).

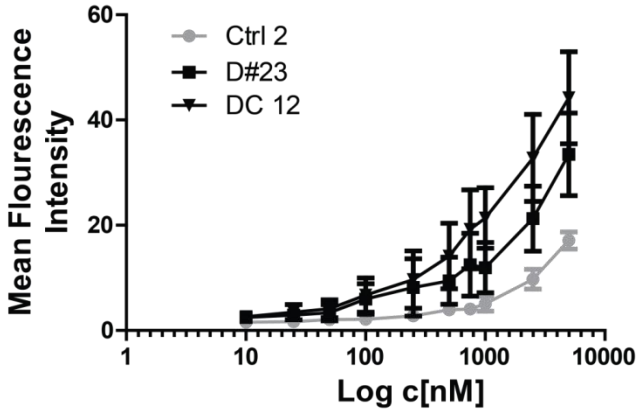

Figure 4.1.4: ATTO 647N-labeled aptamers bind in a concentration dependent manner to THP-1 cells
4×10^5 THP 1 cells were incubated with increasing concentration (10 nM – 5000 nM) of 5' ATTO 647N-labeled aptamers for 10 minutes at 37°C.The mean fluorescence intensity of 5' ATTO 647N-labeled aptamers were measured by the flow cytometry (n=2, mean ± SD).

Taking into account the binding capability of DC 12 aptamer towards mouse macrophages and human monocytes, DC 12 aptamer was selected for further characterization.

4.1.3 Binding of aptamers to BM-DCs

DC 12 aptamer is one of the most abundant sequences from the NGS data of BM-DCs cell-SELEX. In **Section 4.1.1** and **Section 4.1.2**, DC 12 aptamer was identified for binding to macrophages. As DC 12 aptamer was intended to be used as a delivery vehicle for the targeted activation of T cells, the binding to BM-DCs needed to be determined.

Table 4-5: % BM-DCs bound by ATTO 647N-labeled aptamers and relative MFI in flow cytometry binding assay

Aptamer	% Cells bound	Relative MFI (aptamer/control)
Ctrl 2*	9.82±2.14	1.00±0.03
DC 12	72.1±9.85	3.91±1.15
D#23	75.5±9.72	4.00±0.53

*control

For that purpose, the binding of the aptamers to BM-DCs was analyzed by the flow cytometry assay. 5'-ATTO 647N- labeled aptamers Ctrl 2, DC 12, and D#23 were incubated with $4x10^5$ cells in the DC medium supplemented with 10% FCS for 10 minutes at 37°C. The percentage of cells bound by DNA and MFI was detected by the flow cytometry **(Table 4-5** and **Figure 4.1.5)**. DC 12 and D#23 aptamer showed the potential to bind to BM-DCs.

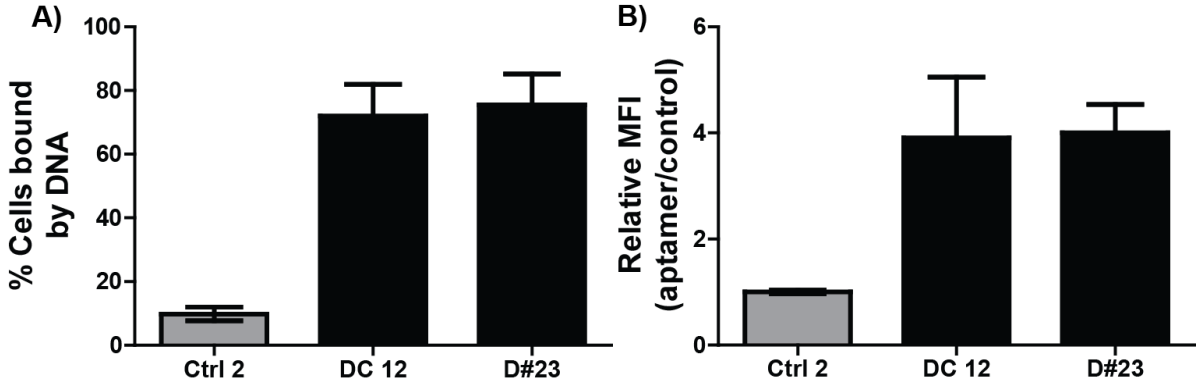

Figure 4.1.5: ATTO 647N-labeled aptamers binds to BM-DCs in flow cytometry binding assay
$4×10^5$ BM-DCs were incubated with 250 nM of 5'-ATTO 647N-labeled aptamers for 10 minutes at 37°C. **A)** The percentage cells bound by aptamers **B)** relative MFI (aptamer/control) were measured by flow cytometry.D#23 aptamer was used as a positive control[101] (n=2, mean ± SD).

4.2 Characterization of DC 12 aptamer

4.2.1 Immunogenicity of aptamers

In order to investigate the immunogenicity of DC 12 and D#23, TNF-α secretion was measured by homogeneous time-resolved fluorescence (HTRF) assay. It was done in collaboration with Prof. Eicke Latz. Immune cells have the ability to detect exogenous or host nucleic acids via pattern recognition receptors (PRRs) e.g., Toll-

like receptors (TLRs). These receptors are expressed both on the cell surface and also in the endosomal compartments. They can detect nucleic acid ligands and activates the signal cascade that results in the secretion of proinflammatory cytokines including TNF-α secretion[187,188].

The basic principle of HTRF assay is established on fluorescence resonance energy transfer (FRET). Anti-TNF-α antibodies were bound with either a FRET donor or an acceptor molecules. These molecules were able to alter the fluorescence emission spectrum in close proximity to antibodies. This change is relative to the concentration of TNF-α in the sample.

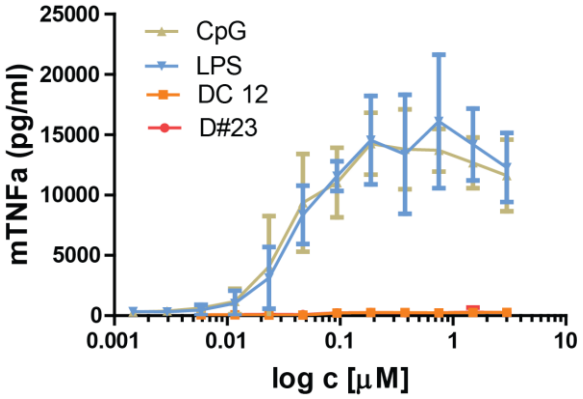

Figure 4.2.1: DC 12 and D#23 do not induce TNF-α secretion in macrophages
Immortalized murine embryonic stem cells derived from macrophages were treated with increasing concentrations of positive controls (LPS and CpG ODN motif), DC 12 and D#23 for 24 hours. TNF-α secretion in the supernatants were determined by HTRF assay (n=5 , mean ± SD). The assays were performed as blinded analysis by James Stunden, member of Prof. Latz group, University Hospitals Bonn.

The TLR activation investigation was performed using immortalized murine embryonic stem cell-derived macrophages. LPS and CpG ODNs, known as TNF-α inducers, were used as positive controls. In general, LPS is considered a key component of the superficial membrane of Gram-negative bacteria.The innate immune response can be initiated even at a minute amount by TLR[189]. Whereas, CpG ODNs are synthetic oligodeoxynucleotides consisting of unmethylated CpG motifs (cytosine-phosphodiester or phosphorothioate-guanosine). These unmethylated motifs elicit cells have TLR 9 and initiate an innate immune response with the production of proinflammatory cytokines and Th1[190]. Both positive controls trigger the cells and activate TNF-α secretion at concentrations in the nanomolar range (**Figure 4.2.1**). The aptamers DC 12 and D#23 showed low TLR activation

even at the highest concentration (**Figure 4.2.1**). As a result, DC 12 and D#23 aptamers have been shown to be less immunogenic and could be used in therapeutic and diagnostic applications for immune cells.

4.2.2 Truncation of DC 12 aptamer and G-quadruplex structure prediction

DC 12 is 80 nucleotides. The structure of DC 12 was predicted using mfold prediction software[191]. The structure consists of a loop, a stem, and a tail on both ends **(Figure 4.2.2A)**. The DC 12 loop and stem might have some impact on the binding behavior of the aptamer. The primer binding site from the 3' (15 nucleotides) and 5' (12 nucleotides) ends was cut and DC 12 was truncated to 53 nucleotides. The truncated structure on the mfold was predicted **(Figure 4.2.2B)**. The parental loop and stem of the DC 12 aptamer were not affected.

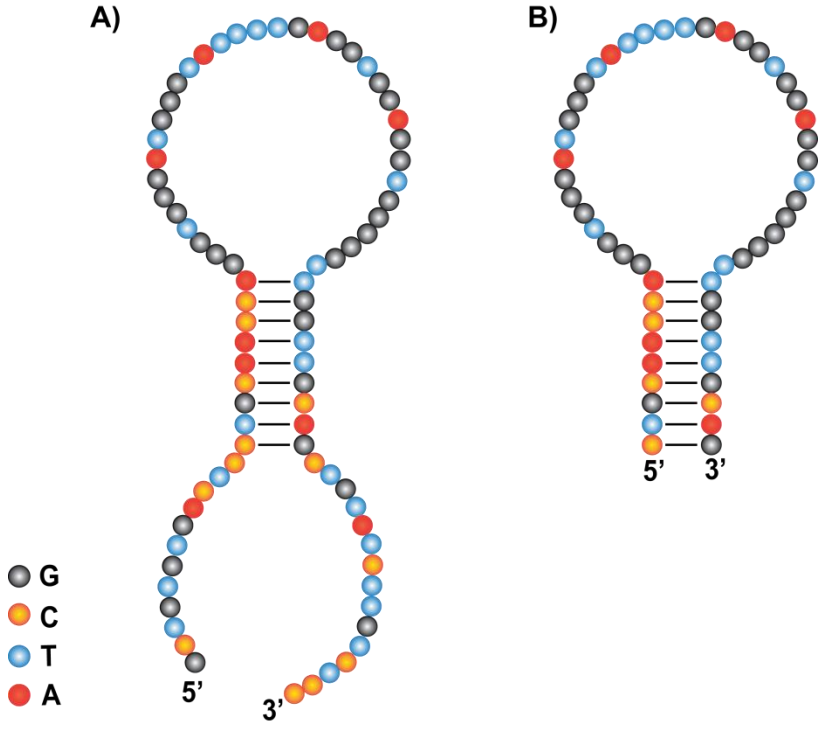

Figure 4.2.2: Truncation of DC 12
Mfold online prediction software has been used to predict the secondary structure of DC 12 aptamer **(A)**. The primer binding site from 3' (15 nt) and 5' (12 nt) end was cut **(B)** to generate DC 12.53.

The aptamer DC 12 is a G-rich sequence and the G-rich sequences have properties for the formation of the G-quadruplex structure. G-quadruplex is one of the most important structures observed in nucleic acids particularly by the ssDNA. The understanding of the G-quadruplex is important for diagnostic and therapeutic applications but also for the structural activity and natural biochemistry of nucleic acids[192].

In order to determine whether DC 12 and DC 12.53 could have a G-quadruplex structure, circular dichroism (CD) was performed. Aptamer C10.36 was used as a positive control. It is folded into a parallel G-quadruplex in DPBS[193]. 10 µM concentration of the aptamers DC 12 and DC 12.53 were prepared in DPBS and in ddH_2O. JASCO J-810 CD spectrometer was used to measure the CD of the aptamers over a wide range of wavelengths. The aptamers (DC 12 and DC 12.53) fold in parallel manner in the DPBS when compared to the positive control C10.36 **(Figure 4.2.3)**. The positive peak ranging from 260-265 nm and the negative peak ranging from 240-245 nm indicates parallel G-quadruplex structure in the CD spectroscopy.

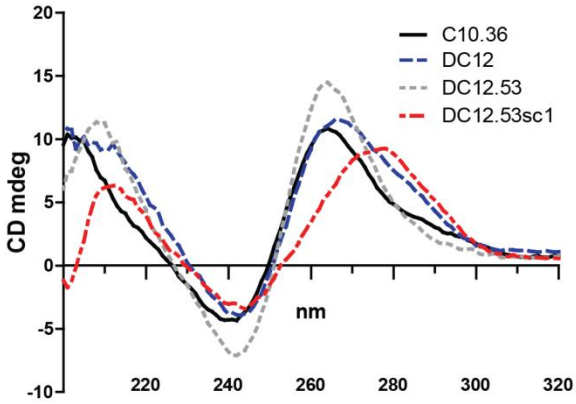

Figure 4.2.3: CD-spectroscopy of the aptamers for the prediction of G-quadruplex structure
10 µM concentration was used to measure the CD spectra of aptamers. C10.36 (black line) was used as a positive control. DC 12 (blue dotted line), DC 12.53 (light grey dotted line), DC 12.53sc1 (red dotted line) in DPBS.

In ddH_2O, both aptamers lose their G-quadruplex structure due to the absence of monovalent cations **(Figure 4.2.4)**. Potassium and sodium ions play a central role in the formation and stability of the G-quadruplex[194], present in DPBS but not in ddH_2O.

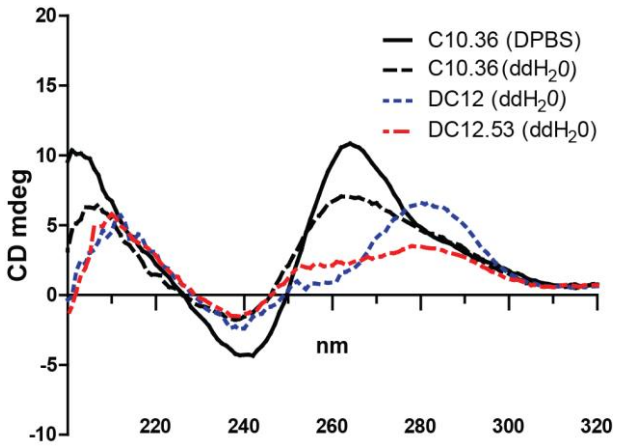

Figure 4.2.4: CD-spectroscopy of the aptamers in the absence of ions
10 µM concentration was used to measure the CD spectra of aptamers in the absence of ions. C10.36 (black line) was used as a positive control. C10.36 (ddH_20) (black dotted line), DC 12 (ddH_20) (blue dotted line), DC 12.53(ddH_20) (red dotted line) in ddH_20.

The binding affinity of DC12.53 aptamer was again tested on both model cell lines J774A.1 **(Table 4-6** and **Figure 4.2.5)** and THP-1 **(Table 4-7** and **Figure 4.2.6)**.

Table 4-6: % J774A.1 cells bound by ATTO 647N-labeled aptamers and relative MFI in flow cytometry binding assay

Aptamer	% Cells bound	Relative MFI (aptamer/control)
Ctrl 2*	12.3±0.3	1.00±0.01
DC 12	86.4±6.9	4.09±0.8
DC 12.53	88.1±7.3	4.07±0.5
DC 12.53sc1**	15.5±2.0	1.00±0.03
DC 12.53sc2	14.9±2.0	0.95±0.08

*control for DC 12
** control for DC 12.53 and DC 12.53sc2

DC 12.53sc1 was a scrambled sequence of DC 12.53 aptamer with the same number of nucleotides and the nucleotide content. DC 12.53sc2 was also a scrambled sequence of DC 12.53 with the same number of nucleotides but with different nucleotides (G was replaced by either A or T, to decrease the stability of the secondary structure). The flow cytometry binding assay with J774A.1 cells showed that ATTO 647N labeled DC 12.53 had the same percentage of cells bound and relative MFI as DC 12 **(Table 4-6** and **Figure 4.2.5).**

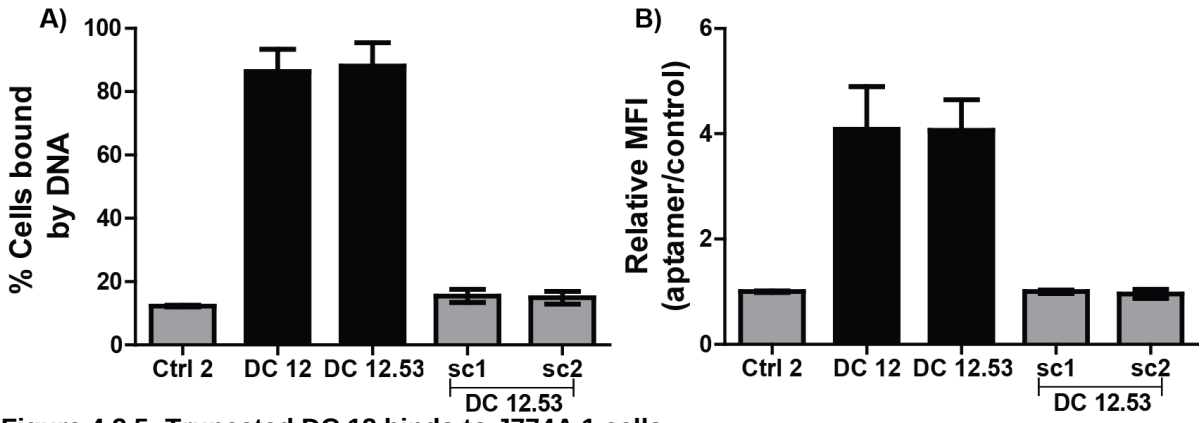

Figure 4.2.5: Truncated DC 12 binds to J774A.1 cells
4×10^5 J774A.1 cells were incubated with ATTO 647N-labeled aptamers. **A)** The percentage cells bound by ATTO 647N labeled aptamers and **B)** relative MFI (aptamer/control) were measured by flow cytometry (n=3, mean ± SD).

Interestingly, DC 12.53 showed almost 40% increase in the binding and relative MFI with THP-1 cells compared to DC 12 **(Table 4-7** and **Figure 4.2.6).** DC 12.53sc1 was used as a control sequence for further experiments because it has the same nucleotide number and nucleotide content.

Table 4-7: % THP-1 cells bound by ATTO 647N-labeled aptamers and relative MFI in flow cytometry binding assay

Aptamer	% Cells bound	Relative MFI (aptamer/control)
Ctrl 2*	3.15±0.6	1.00±0.03
DC 12	57.9±8.3	4.15±0.52
DC 12.53	91.1±3.5	6.61±0.6
DC 12.53sc1**	3.60±1.1	1.01±0.12
DC 12.53sc2	3.19±0.7	0.87±0.13

*control for DC 12
**control for DC 12.53 and DC 12.53sc2

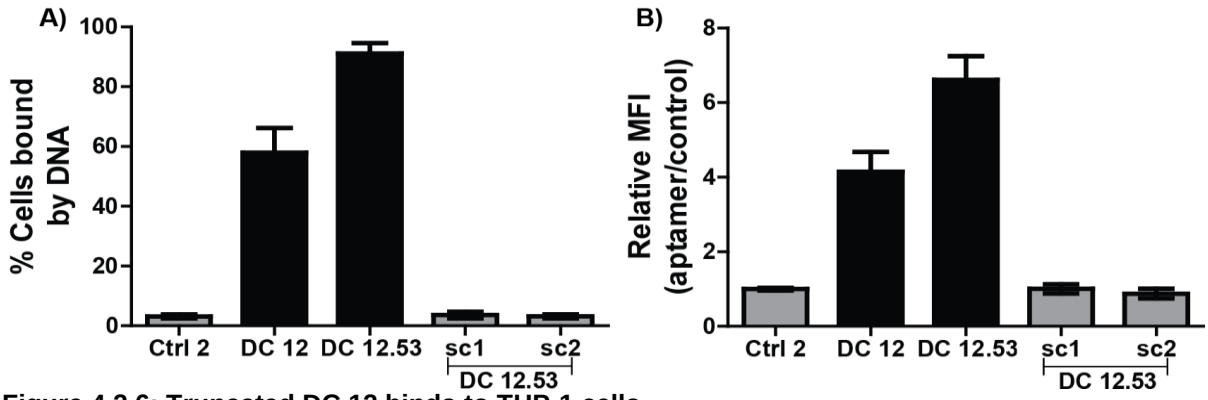

Figure 4.2.6: Truncated DC 12 binds to THP-1 cells
4×10^5 THP 1 cells were incubated with ATTO 647N-labeled aptamers. **A)** The percentage cells bound by ATTO 647N labeled aptamers **B)** relative MFI (aptamer/control) were measured by flow cytometry (n=3, mean ± SD).

4.2.3 Binding of the 3' labeled DC 12 and DC 12.53

In the previous experiments, 5' ATTO 647N-labeled DC 12 and DC 12.53 were characterized for their binding ability to THP-1 and J774A.1 cells. The labeling strategy could affect the folding and binding behavior of the aptamer. In this study, 3' end of the aptamer was also used to conjugate antagomir 125a-5p for the inhibition of miRNA 125a-5p. It is therefore worth investigating the folding behavior of the aptamer after changing the labeling strategy. In order to investigate the impact of the labeling strategy, ATT0 647N-label was introduced into the 3' end instead of the 5'end of DC 12 and DC 12.53.

Table 4-8: % J774A.1 cells bound by ATTO 647N-labeled aptamers and relative MFI in flow cytometry binding assay

Aptamer	% Cells bound	Relative MFI (aptamer/control)
Ctrl 2_5'*	8.87±1.87	1.00±0.09
DC 12_5'	78.7±8.21	3.01±0.64
Ctrl 2_3'**	14.4 ±2.42	1.00±0.08
DC 12_3'	84.1±2.58	2.54±0.24
5'_DC 12.53sc1[#]	12.5±0.38	1.00±0.01
5'_DC 12.53	89.0 ±6.03	4.53±0.24
3'_DC 12.53sc1[##]	14.4±1.68	1.00±0.02
3'_DC 12.53	68.5±2.98	2.62±0.34

DC 12_5' and Ctrl 2_5' was labeled at 5' end and DC 12_3' and Ctrl 2_3' was labeled at 3' end with ATTO 647N. 5'_DC 12.53 and 5'_DC 12.53sc1 was labeled at 5' end and 3'_DC 12.53 and 3'_DC 12.53sc1 was labeled at 3' end with ATTO 647N.
*control for DC 12_5'
**control for DC 12_3'
[#]control for DC 12.53_5'
[##]control for DC 12.53_3'

The binding ability of 3' labeled DC 12 and DC 12.53 were compared to 5' labeled DC 12 and DC 12.53. The aptamers were incubated with $4x10^5$ cells (THP-1 and J774A.1) in the cell culture medium supplemented with 10% FCS at 37°C for 10 minutes. The percentage of cells bound by DNA and MFI were detected by the flow cytometry. 3' ATTO 647N-labeling did not influence the binding behavior of DC 12 aptamer compared to 5' ATTO 647N-labeled DC 12 with J774A.1 cells **(Table 4-8** and **Figure 4.2.7A,B)**. However, 3' ATTO 647N-labeled DC 12.53 showed approximately 20% less binding compared to 5' ATTO 647N-labeled DC 12.53 **(Table 4-8** and **Figure 4.2.7C,D)**. This reduction in the percentage of bound cells by DNA could be due to the stability or alteration of the structure of 3' ATTO 647N-labeled DC 12.53.

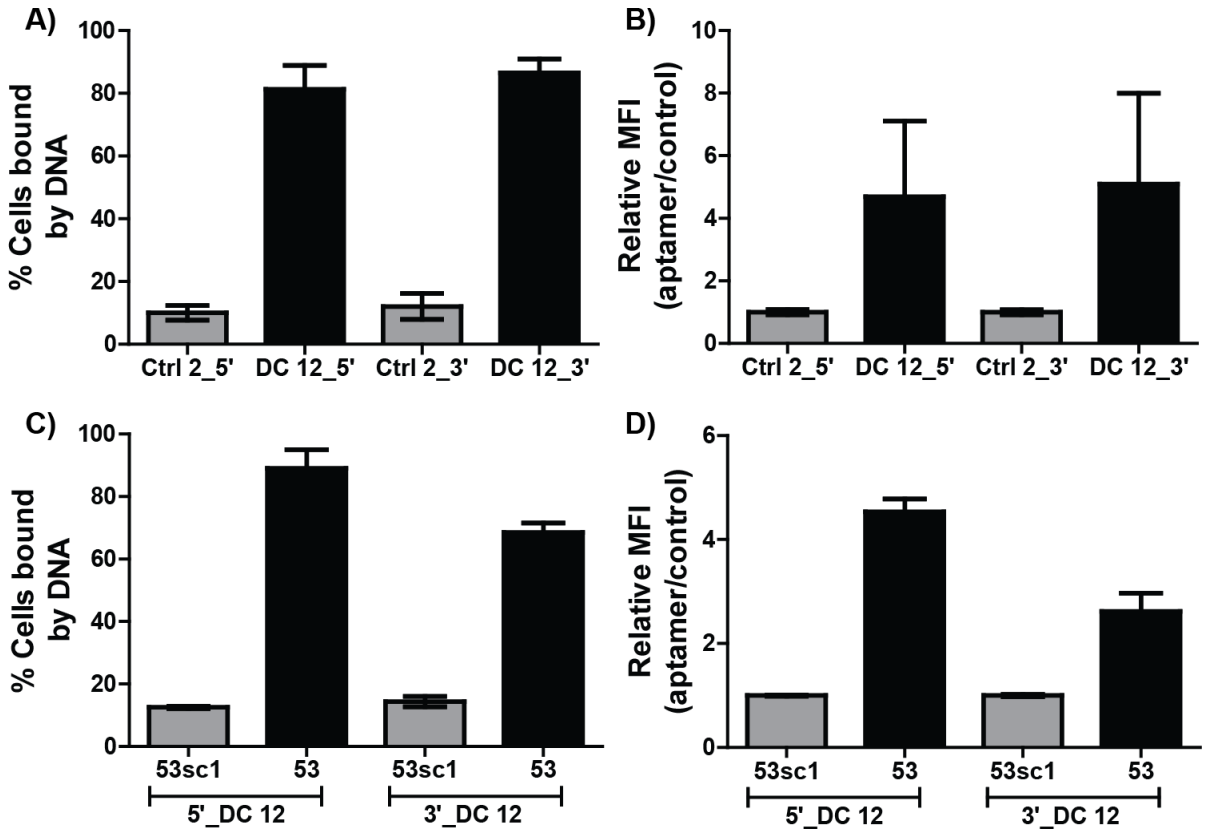

Figure 4.2.7: Comparison of binding of 3' and 5' ATTO 647N-labeled aptamers to J774A.1
A+B) DC 12 and Ctrl 2 was labeled at 5' end (DC 12_5' and Ctrl 2_5') and 3' end (DC 12_3' and Ctrl 2_3') with ATTO 647N. **C+D)** DC 12.53 and DC 12.53sc1 was labeled at 5' end (5'_DC 12.53 and 5'_DC 12.53sc1) and 3' end (3'_DC 12.53 and 3'_DC 12.53sc1) with ATTO 647N.4×10^5 J774A.1 cells were incubated with 250 nM of 3'and 5'-ATTO 647N-labeled aptamers at 37°C for 10 minutes. **A and C)** The percentage of cells bound by aptamers and **B and D)** relative MFI (aptamer/control) were measured by flow cytometry (n=3, mean ± SD).

3' ATTO 647N-labeled DC12 showed 10-15% increase in the binding to THP-1 cells compared to 5' ATTO 647N-labeled **(Table 4-9** and **Figure 4.2.8A,B)**. This increase in the percentage of cell bound by DNA could be due to the stabilization of the structure or an increase in the binding affinity towards the target. However, 3' ATTO 647N-labeled DC 12.53 did not influence the binding behavior of THP-1 cells compared to 5' ATTO 647N- labeled DC 12.53 **(Table 4-9** and **Figure 4.2.8C,D)**. Ctrl 2 and DC 12.53sc1 were used as control sequences, which showed no binding behavior **(Figure 4.2.7** and **Figure 4.2.8).**

Table 4-9: % THP-1 cells bound by ATTO 647N-labeled aptamers and relative MFI in flow cytometry binding assay

Aptamer	% Cells bound	Relative MFI (aptamer/control)
Ctrl 2_5'*	3.74±0.7	1.00±0.1
DC 12_5'	59.9±7.7	4.01±0.5
Ctrl 2_3'**	4.32 ±1.3	1.00±0.09
DC 12_3'	73.3±4.0	3.47±0.3
DC 12.53sc1_5'#	5.29±0.3	1.00±0.1
DC 12.53_5'	94.7±2.7	6.04±1.1
DC 12.53sc1_3'##	5.93±0.7	1.00±0.01
DC 12.53_3'	81.8±9.1	3.30±0.4

DC 12_5' and Ctrl 2_5' was labeled at 5' end and DC 12_3' and Ctrl 2_3' was labeled at 3' end with ATTO 647N. 5'_DC 12.53 and 5'_DC 12.53sc1 was labeled at 5' end and 3'_DC 12.53 and 3'_DC 12.53sc1 was labeled at 3' end with ATTO 647N.

*control for DC 12_5'

**control for DC 12_3'

#control for DC 12.53_5'

##control for DC 12.53_3'

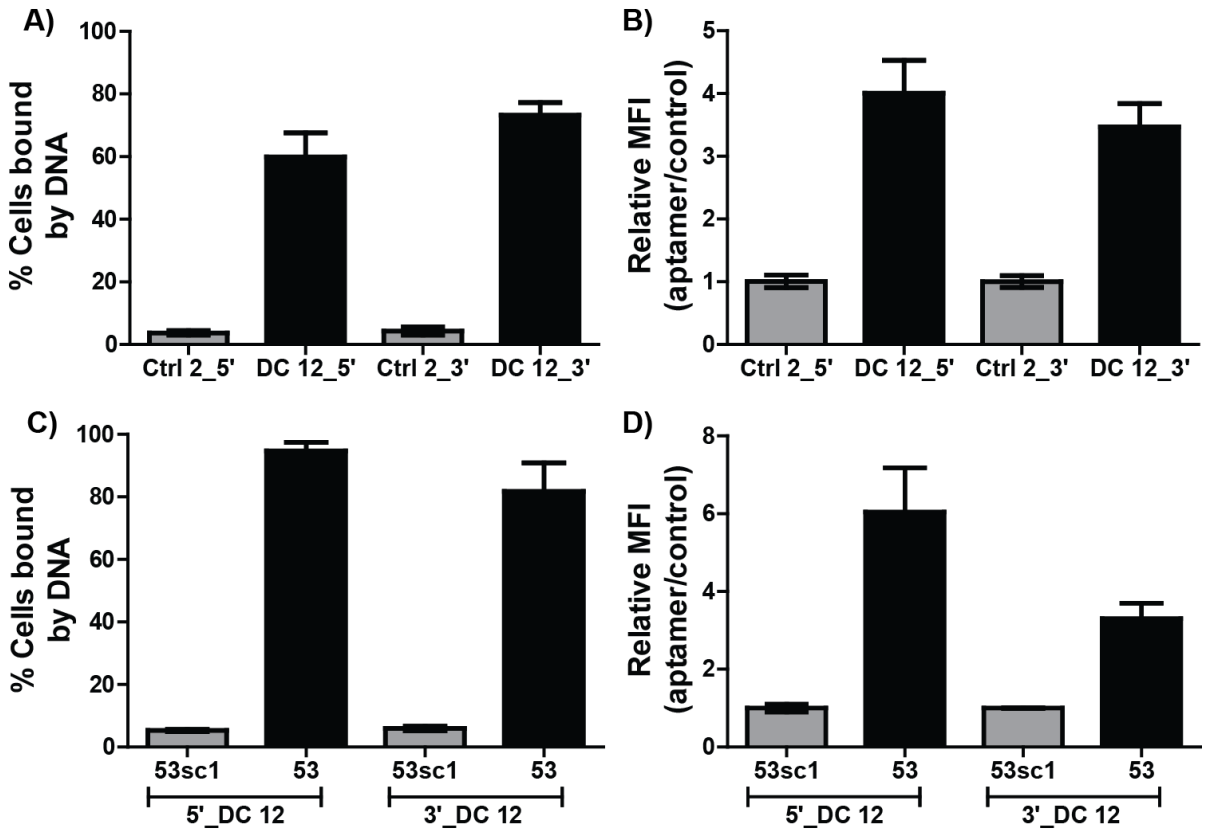

Figure 4.2.8: Comparison of binding of 3' and 5' ATTO 647N-labeled aptamers toTHP-1
A+B) DC 12 and Ctrl 2 was labeled at 5' end (DC 12_5' and Ctrl 2_5') and 3' end (DC 12_3' and Ctrl 2_3') with ATTO 647N. **C+D)** DC 12.53 and DC 12.53sc1 was labeled at 5' end (5'_DC 12.53 and 5'_DC 12.53sc1) and 3' end (3'_DC 12.53 and 3'_DC 12.53sc1) with ATTO 647N.4×10^5 THP-1 cells were incubated with 250 nM of 3'and 5'-ATTO 647N-labeled aptamers at 37°C for 10 minutes. **A and C)** The percentage of cells bound by aptamers and **B and D)** relative MFI (aptamer/control) were measured by flow cytometry (A+B) n=4, C+D) n=2, mean ± SD).

4.2.4 Internalization of aptamers by J774A.1 cells

The aim of the current study was to use DC 12 aptamer as a delivery vehicle. The aptamer must be internalized into the cells in order to become an appropriate delivery vehicle. It was therefore of great importance to test the internalization ability of DC 12 and DC 12.53. Confocal microscopy was used to investigate the internalization of labeled aptamers. 2x10^5 J774A.1 cells were incubated at 37°C for 10 minutes with ATTO 647N-labeled aptamers. The cells were fixed with 4% paraformaldehyde. The cell membrane was stained with the wheat germ agglutinin (WGA) - Alexa fluor 488, which is a membrane marker and the nuclei was stained with 4',6-diamidino-2-phenylindole (DAPI). The slides were prepared and kept overnight. The next day, confocal microscopy images of single cells were acquired

at various depths (Z-stacks). The incubation time of 10 minutes was chosen in accordance with the time used in the selection of these aptamers. DC 12 and DC 12.53 signals were observed in almost every cell **(Figure 4.2.9)**. The red channel was used to acquire the aptamer signal (ATTO 647N-signal), while, less than 2-4 % of cells showed control aptamers signal.

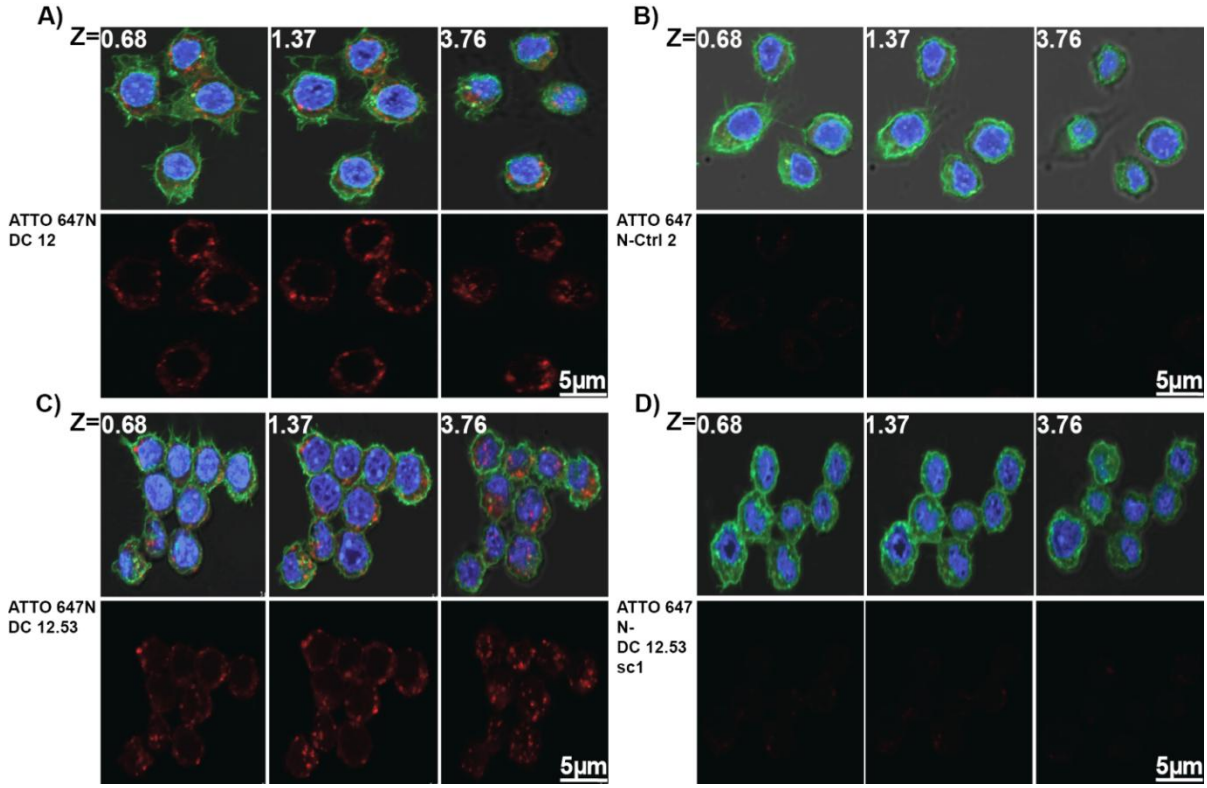

Figure 4.2.9: Internalization of aptamers into J774A.1 cells
2×10^5 J774A.1 were incubated with 250 nM aptamers-ATTO 647N-labeled for 10 min, fixed and co-stained with the membrane marker WGA-Alexa Fluor 488 and nuclear marker DAPI. In laser scanning microscopy (LSM), pictures along the Z-axis were taken (Z numbers are given in µm). **A)** DC 12 **B)** Ctrl 2 **C)** DC 12.53 **D)** DC 12.53sc1.Experiment was performed in duplicate with two independent repeats. 10 pictures of the Z axis were taken from single cell and 8 high dense fields from the slides were selected from all samples.

4.2.6 Binding of aptamers to human primary and TPP macrophages

As described in the previous section, DC 12 and DC 12.53 have the potential to bind to BM-DCs, J774A.1, and THP-1 cells. DC 12 and DC 12.53 were intended to be used as a delivery vehicle to target both human baseline and TPP macrophages. The binding of aptamers to human baseline and TPP macrophages was investigated

for that purpose. TPP macrophages were differentiated from human baseline macrophages. CD14+ monocytes were sorted from the PBMC using the CD14+ magnetic beads according to the manufacturer protocol. CD14+ monocytes were differentiated in the presence of GM-CSF for three days into the baseline macrophages **(Figure 4.2.10)**. After three days, the medium was replaced with fresh medium containing GM-CSF plus stimulants TPP (TNF, PGE_2, and TLR2 Ligand) for the next three days **(Figure 4.2.10)**.

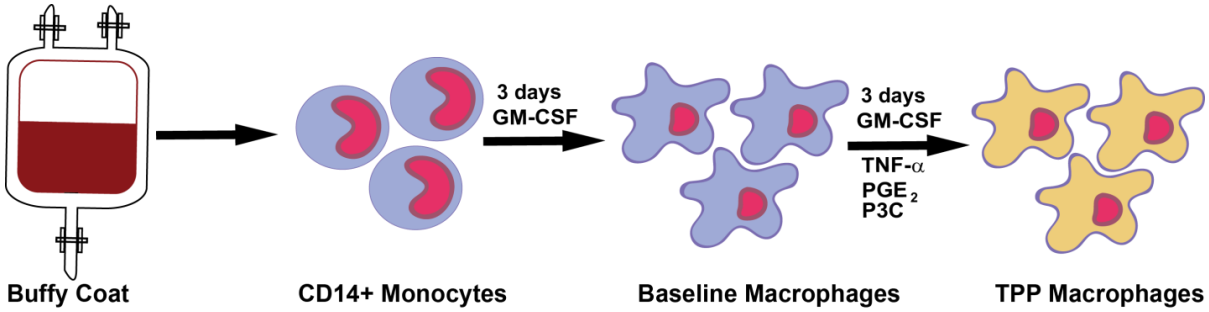

Figure 4.2.10: Schematic representation of isolation and differentiation of TPP macrophages
CD14+ monocytes were isolated from the buffy coats and differentiated into the baseline macrophages in the medium supplemented with GM-CSF for three days. The medium was replaced by fresh medium supplemented with GM-CSF plus TPP (TNF, PGE_2, and TLR2 Ligand) stimulants for the next three days. (Protocol and differentiation scheme taken from Xue *et al.*[114]).

Baseline macrophages have also been differentiated into two other phenotypes IFN-ɤ and IL-4. Surface markers CD14, CD25, CD23, and CD86 were analyzed as described above[114].

Table 4-10: MFI of surface markers (CD23, CD86, CD25, and CD14) of different macrophage phenotypes in flow cytometry

Macrophage Phenotype	MFI			
	CD23	CD86	CD25	CD14
M_b	19.20±3.56	69.3±11.7	3.05±0.44	84.2±27.9
IL-4	192.0±45.8	53.5±16.4	2.42±0.44	26.5±7.98
IFN-ɤ	23.0±9.14	223±72.9	2.98±0.69	60.0±20.1
TPP	23.4±7.17	47.4±15.6	7.40±0.44	213±56.6

CD14 and CD25 have high upregulated surface markers for the TPP chronic inflammatory macrophages **(Table 4-10** and **Figure 4.2.11C,D)**. CD 23 was the highly upregulated surface marker for the IL-4 activated macrophages **(Table 4-10**

and **Figure 4.2.11A)**. CD86 was the highly upregulated surface marker for the IFN-ɣ activated macrophages **(Table 4-10** and **Figure 4.2.11B)**.

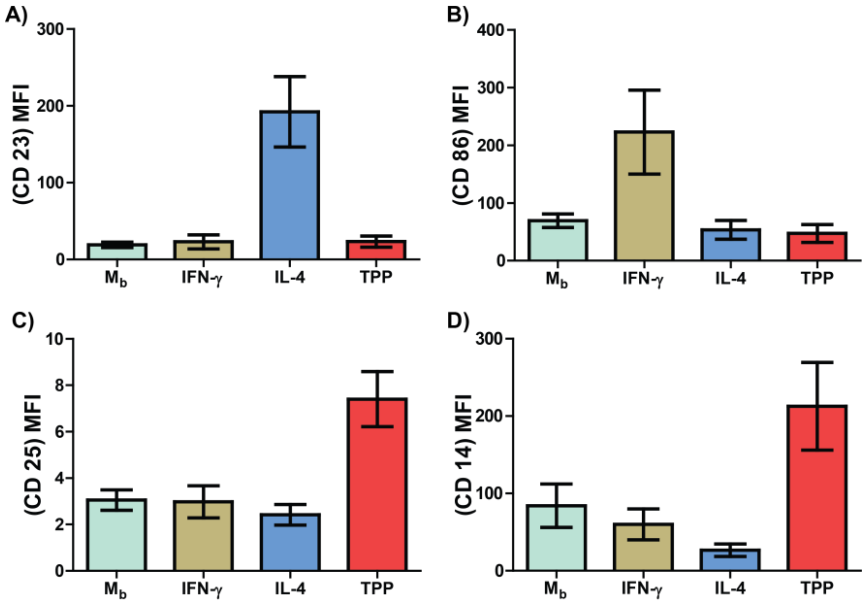

Figure 4.2.11: Phenotypic characterization of macrophages differentiated with IFN-ɣ, IL-4, and TPP (TNF, PGE_2, and TLR2 Ligand)
Flow cytometry of CD14, CD25, CD23, and CD86 in M_b (baseline macrophages), IFN-ɣ, IL-4, and TPP activated macrophages. MFI of one experiment in duplicate (n=3, mean ± SD).

The flow cytometry assay analyzed the binding of aptamers to the human primary baseline **(Table 4-11** and **Figure 4.2.12)** and TPP macrophages **(Table 4-12** and **Figure 4.2.13)**.

Table 4-11: % Human primary macrophages bound by ATTO 647N-labeled aptamers and relative MFI in flow cytometry binding assay

Aptamer	% Cells bound	Relative MFI (aptamer/control)
Ctrl 2*	4.38±0.09	1.00±0.01
DC 12	97.0±1.04	14.2±1.03
DC 12.53	98.2±0.75	14.2±6.24
DC 12.53sc1**	4.81±1.15	1.00±0.01
DC 12.53sc2	2.20±0.88	0.78±0.14

*control for DC 12
**control for DC 12.53 and DC 12.53sc2

5'-ATTO 647N-labeled Ctrl 2, DC 12, DC 12.53, and DC 12.53sc1 were incubated with $4x10^5$ cells in the VLE RPMI 1640 medium supplemented with 10% FCS for 10 minutes at 37°C.

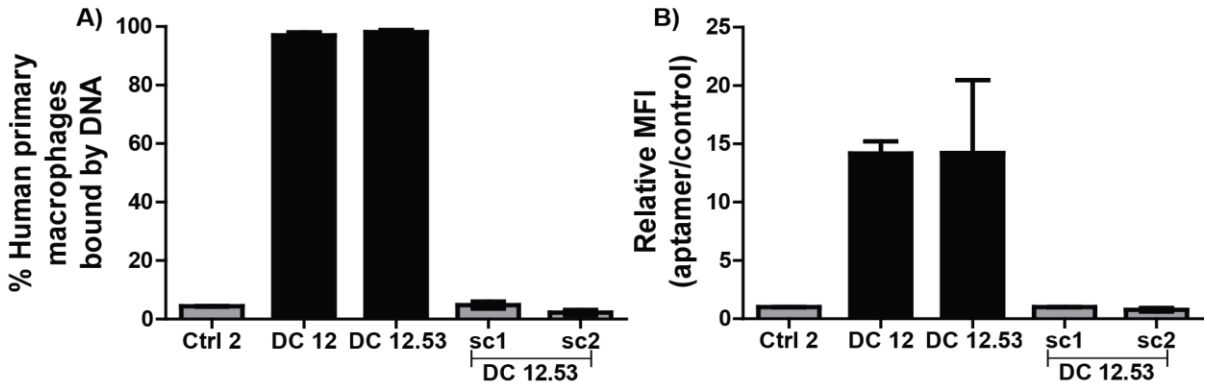

Figure 4.2.12: Binding of the aptamers to human primary baseline macrophages
4×10^5 human primary baseline macrophages were incubated with 250 nM of 5'-ATTO 647N-labeled aptamers at 37°C for 10 minutes. **A)** The percentage cells bound by aptamers and **B)** relative MFI (aptamer/control) were determined by flow cytometry (n=2, mean ± SD).

The percentage of cells bound by DNA and MFI was detected by flow cytometry. DC 12 and DC 12.53 have the potential to bind to human primary baseline and TPP macrophages.

Table 4-12: % TPP macrophages bound by ATTO 647N-labeled aptamers and relative MFI in flow cytometry binding assay

Aptamer	% Cells bound	Relative MFI (aptamer/control)
Ctrl 2*	8.06±0.8	1.0±0.01
DC 12	59±4.2	9.1±4.08
DC 12.53	64.6±5.9	11.8±3.7
DC 12.53sc1**	7.29±1.65	1.0±0.04

*control for DC 12
**control for DC 12.53

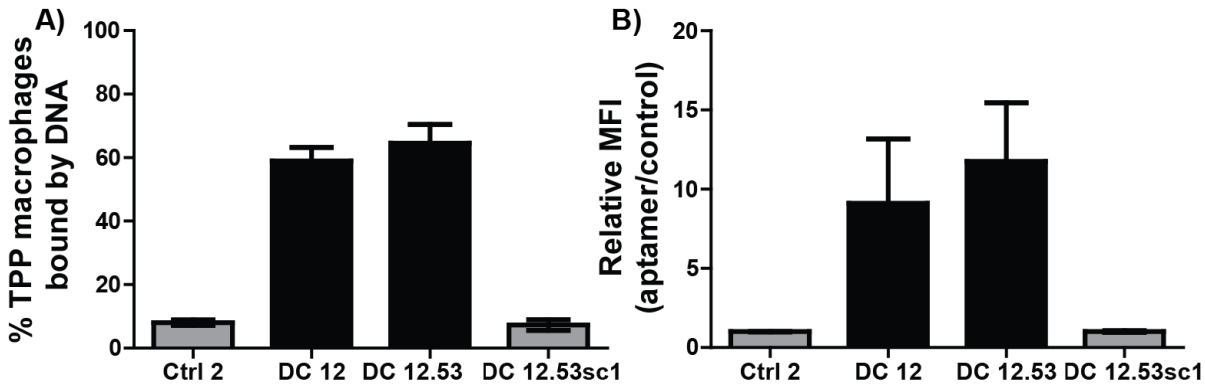

Figure 4.2.13: Binding of the aptamers to TPP macrophages
4×10^5 TPP macrophages were incubated with 250nM of 5'-ATTO 647N-labeled aptamers at 37°C for 10 minutes. **A)** The percentage cells bound by aptamers and **B)** relative MFI (aptamer/control) were determined by flow cytometry (n=2, mean ± SD).

4.2.7 Internalization of aptamers by primary human baseline macrophages

As described in **Section 4.2.4**, DC 12 and DC 12.53 have the ability to internalize into J774A.1 cells. These aptamers to be used as a delivery vehicle in the study in hand, to deliver antagomir 125a-5p into the human baseline macrophages, so the internalization ability of DC 12 and DC 12.53 aptamer into human baseline macrophages was investigated.

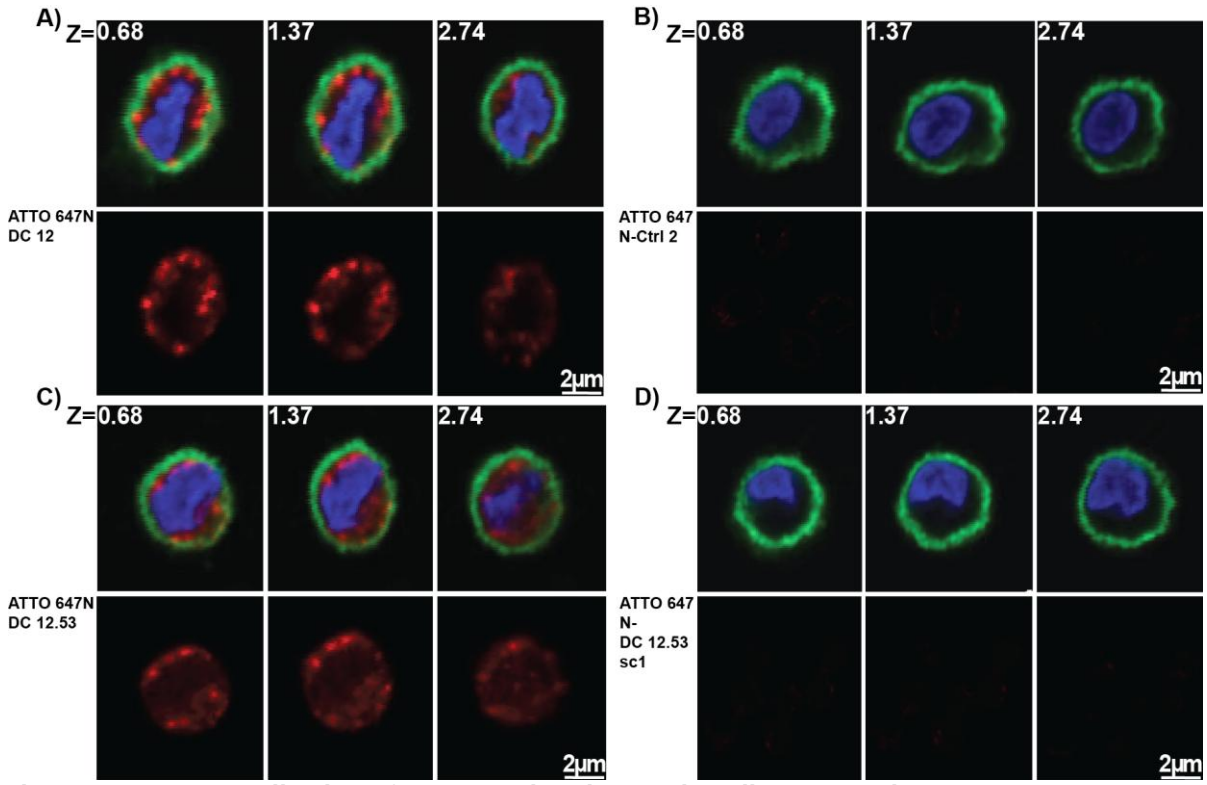

Figure 4.2.14: Internalization of aptamers into human baseline macrophages
2×10^5 human baseline macrophages were incubated with 250 nM aptamers-ATTO 647N labeled for 10 min, fixed and costained with the membrane marker WGA-Alexa Fluor 488 and nuclear marker DAPI. In LSM, pictures along the Z-axis were taken (Z numbers are given in µm). **A)** DC 12 **B)** Ctrl 2 **C)** DC 12.53 **D)** DC 12.53sc1.Experiment was performed in duplicate with two independent repeats.

Confocal microscopy was used to investigate the internalization of labeled aptamers. With ATTO 647N-labeled aptamers, $2x10^5$ three days differentiated human baseline macrophages were incubated at 37°C for 10 minutes. The cells were fixed with 4% paraformaldehyde. The cell membrane was stained with WGA-Alexa fluor 488, which is a membrane marker, while the nuclei was stained with DAPI. The slides have been prepared and kept overnight. Next day, confocal microscopy images of single cells were acquired at various depths (Z-stacks). The DC 12 and DC 12.53 signals were observed in almost every cell (**Figure 4.2.14**). The second image of each aptamer was only the red signal acquired for the aptamer in the microscopy. However, less than 2-4 % of cells showed control aptamers signal.

4.3 Characterization of antagomir 125a-5p in J774A.1 cells

The aim of the project was to use a macrophage-binding aptamer as a delivery tool to deliver antagomir 125a-5p in human baseline macrophages. miRNA 125a-5p is highly upregulated in TPP macrophages **(Figure 3.2.3)**. It could have an impact on the overall polarization state of the TPP macrophages. In the previous section **(Section 4.2)**, DC 12 aptamer was characterized for its binding and internalizing properties towards J774A.1 and human baseline macrophages. Before the construction of aptamer-antagomir 125a-5p conjugates (aptamiR 125a-5p chimera), it was worthwhile to investigate the affinity and specificity of antagomir 125a-5p towards miRNA 125a-5p in the cells. The EGFP reporter gene and a stable cell line were used for the functional validation of antagomir 125a-5p.

4.3.1 Construction of the reporter gene EGFP-4X 125a-5p for validation of antagomir function

miRNA are basically small non-coding RNAs that are generally 18-25 nucleotides in the length. The expression of multiples genes is regulated by a single miRNA through a complementary nucleotide sequence that binds to the 3' UTR[195-197]. The pEGFP-N1 report plasmid was used to validate loss-of-function and gain-of-function studies for miRNA. The most beneficial function of the EGFP plasmid is the visualization and quantification of the green fluorescent protein when transfected into the cells. Therefore, the 4X miRNA 125a-5p target site was cloned into the 3' UTR of mRNA of an EGFP encoding plasmid **(Figure 4.3.1A)** as described previously by Pofahl *et al.*[28] for miRNA 21. The transfection of the plasmid into the eukaryotic cells leads to the transcription of the EGFP mRNA with 4X miRNA 125a-5p target sites at the 3'UTR. These target sites have helped to determine the status of endogenous miRNA 125a-5p in the cells. The presence of miRNA 125a-5p interacts with the 4X miRNA 125a-5p target sites due to Watson Crick base pairing and therefore the translation of EGFP protein is inhibited **(Figure 4.3.1B)**. The interaction between miRNA and the target site can be prevented by antagomir 125a-5p **(Figure 4.3.1C)**. The antagomir is modified RNA and has a high binding affinity to their respective

miRNA[198]. Thus, miRNA interacts with the antagomir, consequently, the EGFP mRNA is translated into protein. The EGFP protein can be visualized through confocal microscopy and quantified by flow cytometry.

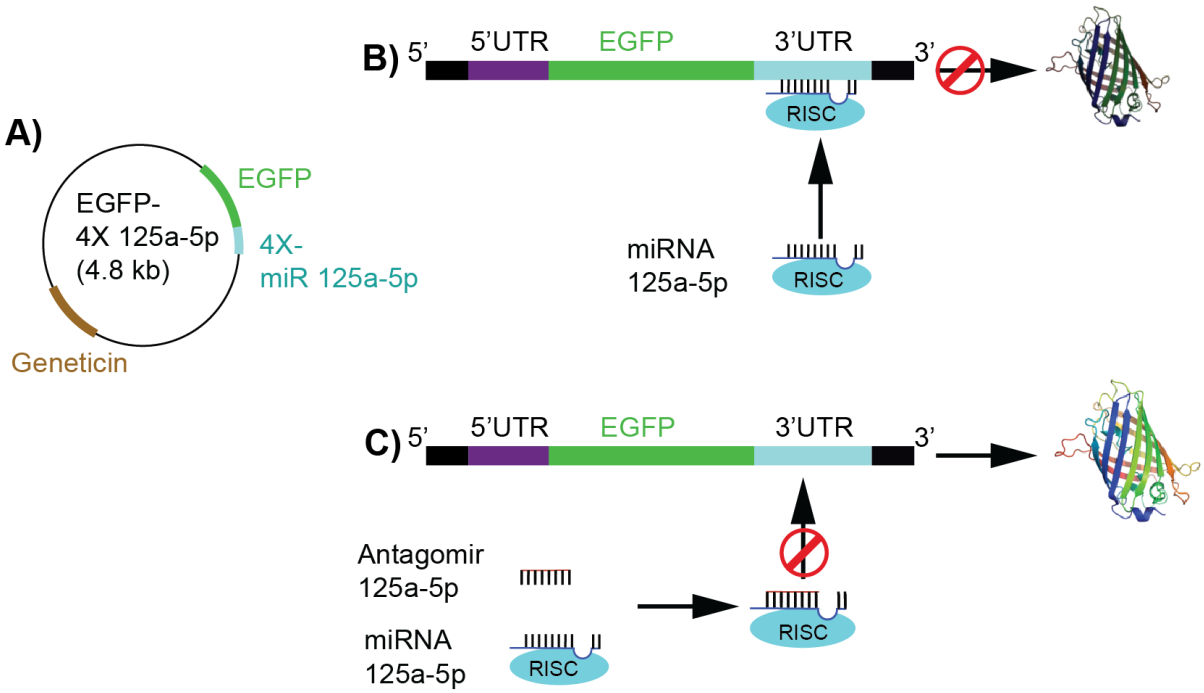

Figure 4.3.1: Schematic representation of the EGFP reporter gene functioning
A) EGFP-4X 125a-5p reporter gene structure **B)** The presence of miRNA 125a-5p interacts with mRNA of the EGFP leading to inhibition of the translation **C)** The interaction of miRNA 125a-5p with mRNA of EGFP is blocked by antagomir 125a-5p (modified from Pofahl Ph.D. thesis[28]).

4.3.2 Functional verification of the reporter gene through miRNA 125a-5p mimic

The functional verification of the reporter gene EGFP-4X 125a-5p was performed by using miRNA 125a-5p mimic. J774A.1 cells were cotransfected with the reporter gene in combination with the miRNA 125a-5p mimic or with the control miRNA mimic. The control plasmid without 4X miRNA 125a-5p target sites was also used in combination with the miRNA 125a-5p mimic or with the control miRNA mimic. Different concentrations of the miRNA 125a-5p mimic and control mimic were used for the functional verification of the reporter system. After cotransfection, the flow cytometry was used to measure the MFI after 24 hours (**Figure 4.3.2** and **Figure 4.3.3**). The effect of miRNA 125a-5p mimic was only observed in the reporter gene EGFP-4X 125a-5p due to the interaction of miRNA 125a-5p mimic with target sites

on the mRNA of EGFP **(Figure 4.3.3)**. This interaction leads to the inhibition of green fluorescent protein.The control mimic did not show any effect **(Figure 4.3.3)**. The transfection of the control plasmid in combination with miRNA 125a-5p mimic or control mimic had no effect on the inhibition of the green fluorescent protein **(Figure 4.3.2)**.

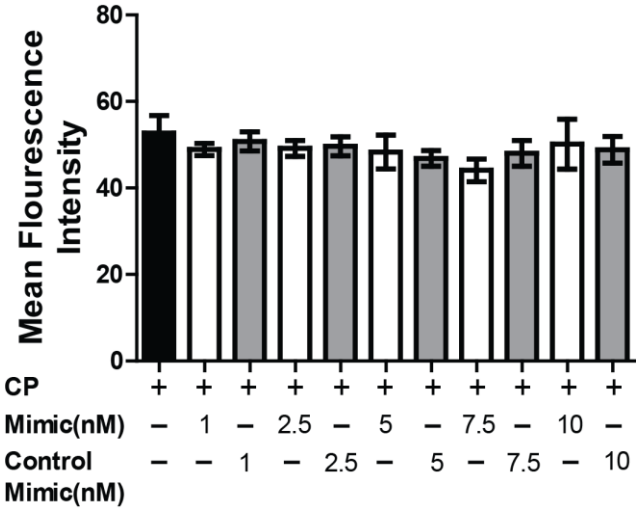

Figure 4.3.2: Transient transfection of miRNA 125a-5p mimic and control mimic with control plasmid (CP)
1×10^5 J774A.1 cells were seeded one day before transfection. 500 ng CP was transiently transfected with miRNA 125a-5p mimic and control mimic at different concentrations (1 nM – 10 nM). Black bar represents only 500 ng CP, white bars represents 500 ng CP transfected with miRNA 125a-5p mimic (1 nM – 10 nM), and grey bars represents 500 ng CP transfected with control miRNA mimic (1 nM – 10 nM). After, 24 hours, the cells were scraped and washed with 1 ml DPBS. The EGFP expression was measured by flow cytometry. The experiment was performed twice (mean ± SD).

It was thus proven that miRNA 125a-5p mimic had a strong influence on the reporter gene EGFP-4X 125a-5p and the 4X target sites of miRNA 125a-5p were functional.

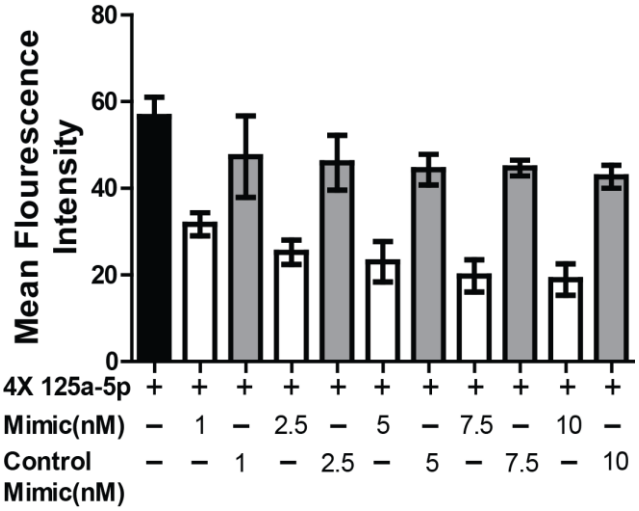

Figure 4.3.3: Transient transfection of miRNA 125a-5p mimic and control mimic with the target site plasmid (4X 125a-5p)
1×10^5 J774A.1 cells were seeded one day before transfection. 500 ng 4X 125a-5p was transiently transfected with miRNA mimic and control mimic at different concentrations (1 nM – 10 nM). Black bar represents only 500 ng 4X 125a-5p, white bars represents 500 ng 4X 125a-5p transfected with miRNA 125a-5p mimic (1 nM – 10 nM), and grey bars represents 500 ng 4X 125a-5p transfected with control miRNA mimic (1 nM – 10 nM). After, 24 hours, the cells were scraped and washed with 1 ml DPBS. The EGFP expression was measured by flow cytometry. The experiment was performed twice (mean ± SD).

Next, a stable cell line was constructed for the transfection independent experiments and for the permanent integration of the EGFP reporter gene into the cells.

4.3.3 Generation of stable J774A.1 cell line with the EGFP-4X 125a-5p reporter gene

In the previous sections **(Section 4.3.1** and **Section 4.3.2)**, the EGFP-4X 125a-5p reporter gene was constructed and functional verification was performed through transfection. The generation of EGFP-4X 125a-5p stable cell line was essential for the transfection independent experiments for aptamer guided delivery of antagomir 125a-5p and for the permanently integrated EGFP plasmid with the 4X 125a-5p target site. For this purpose, 2 µg of the EGFP-4X 125a-5p plasmid was transfected into the J774A.1 cells. The plasmid has a geneticin (G418) resistance gene. Therefore, the selection of cells was based on the G418 gene. Cells without a resistance gene were unable to survive in cell culture medium supplemented with 300 µg/ml G418 antibiotic. After four weeks, the cells were sorted according to the

EGFP expression as monoclonal cells using the cell sorting flow cytometry. Cells with the EFGP expression were sorted in the 96-well plates (single cell/well) and grown in the normal cell culture conditions, DMEM medium supplemented with 10% FCS, 300 µg/ml G418.

4.3.4 Antagomir 125a-5p inhibits endogenous miRNA 125a-5p in stable cell line J774A.1 miRNA 125a-5p

In the previous section **(Section 4.3.3)**, the stable cell line was constructed using the reporter gene. The functional validation of the stable cell line, the mode of action of antagomir 125a-5p, and the endogenous status of miRNA 125a-5p were investigated through antagomir 125a-5p transfection. As a control, a stable cell line with control plasmid without target sites was also constructed in the same way as the EGFP-4X 125a-5p stable cell line. A control antagomir sequence was also used from the earthworm, which has no target gene in both human and mouse species. Stable cell lines were transfected with the antagomir 125a-5p and control antagomir. After 48 hours of transfection, the transfection of antagomir 125a-5p induced an increase in the MFI of the EGFP-4X 125a-5p stable cell line, while the control antagomir did not affect the MFI **(Figure 4.3.5)**. The control stable cell line had no effect either with the antagomir 125a-5p or the control antagomir **(Figure 4.3.4)**.

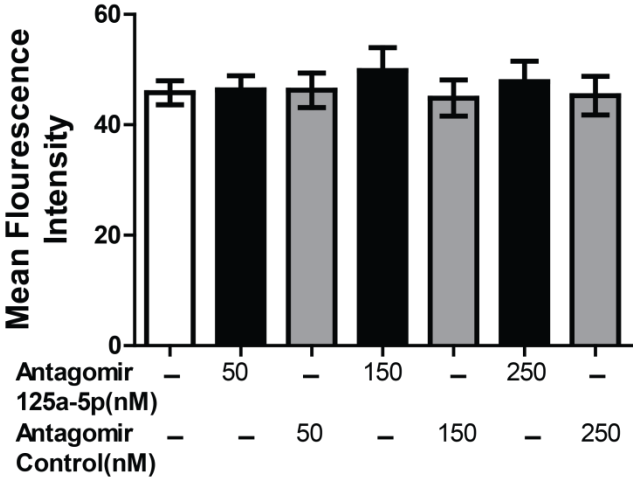

Figure 4.3.4: Transfection of antagomir 125a-5p and control antagomir
4×10^4 control stable cell line J774A.1 cells were seeded one day before transfection. Antagomir 125a-5p and control antagomir had been transfected at three different concentrations. After, 48 hours, the cells were scraped and washed with 1 ml DPBS. The EGFP expression was measured by flow cytometry. The experiment was performed twice (mean ± SD).

As a result, the transfection of antagomir 125a-5p in the EGFP-4X 125a-5p stable cell line resulted in an interaction of antagomir 125a-5p with an endogenous miRNA 125a-5p, so that miRNA 125a-5p did not interact with the mRNA of EGFP. There was an increase in the translation of the EGFP protein, which induced MFI. Therefore, the transfection of antagomir 125a-5p inhibited the endogenous miRNA 125a-5p, as expected.

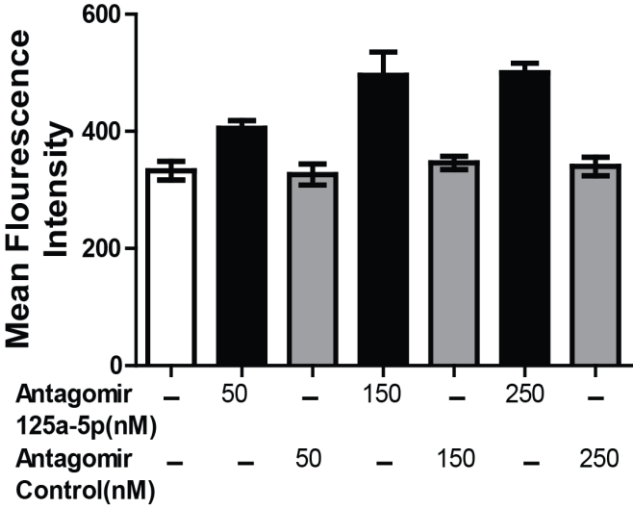

Figure 4.3.5: Transfection of antagomir 125a-5p and control antagomir
4×10^4 EGFP-4X 125a-5p stable cell line J774A.1 cells were seeded one day before transfection. Antagomir 125a-5p and control antagomir had been transfected at three different concentrations. After, 48 hours, the cells were scraped and washed with 1 ml DPBS. The EGFP expression was measured by flow cytometry. The experiment was performed twice (mean ± SD).

Thus, it was shown that the stable cell line J774A.1 miRNA 125a-5p had a certain level of the endogenous miRNA 125a-5p which could be inhibited by antagomir 125a-5p. Thus, this stable cell line was used in transfection independent experiments with aptamiR 125a-5p.

Next, the binding of the aptamers was analyzed for the stable cell line J774A.1 miRNA 125a-5p.

4.3.5 Binding of aptamer to the stable cell line J774A.1 miRNA 125a-5p

The stable cell line has a reporter gene, which is permanently integrated into the cell's genome. This gene could have an impact on the overall machinery of the cells including the endogenous DNA, RNA, proteins, and surface proteins or on the target of the aptamer on the cell surface. The binding of the aptamer was investigated with the stable cell line, to elucidate that the reporter gene did not affect the binding of the aptamer.

Table 4-13: % stable cell line J774A.1 miRNA 125a-5p cells bound by ATTO 647N-labeled aptamers and relative MFI in flow cytometry binding assay

Aptamer	% Cells bound	Relative MFI (aptamer/control)
Ctrl 2*	15.5±1.1	1.0±0.04
DC 12	96.7±0.7	4.0±0.33
DC 12.53	93.0±2.9	4.2±0.10
DC 12.53sc1**	15.9±1.2	1.0±0.02

*control for DC 12
**control for DC 12.53

5'-ATTO 647N- labeled Ctrl 2, DC 12, DC 12.53, and DC 12.53sc1 were incubated with $4x10^5$ cells in the DMEM medium supplemented with 10% FCS for 10 minutes at 37°C. The percentage of cells bound by DNA and MFI was detected by flow cytometry. All of the selected aptamers showed binding to the stable cell line **(Table 4-13** and **Figure 4.3.6)**.

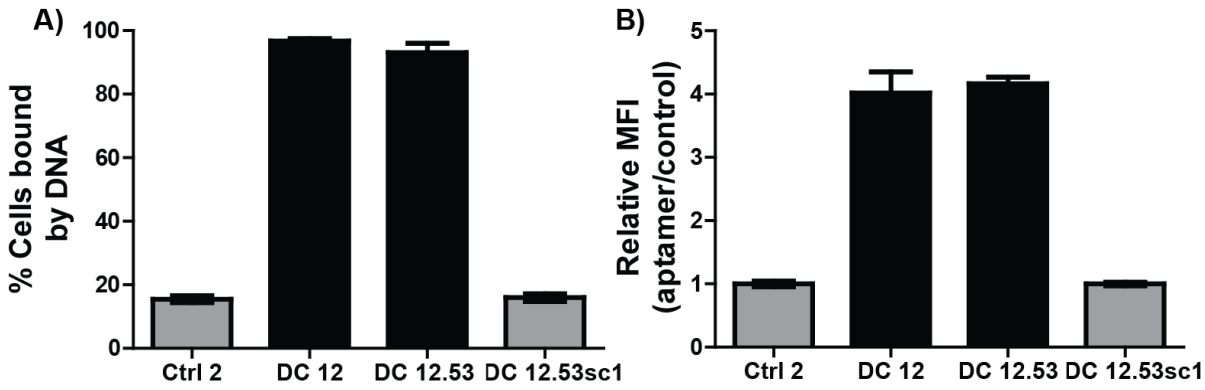

Figure 4.3.6: Binding of the aptamers to the stable cell line J774A.1 miRNA 125a-5p
4×10^5 stable cell line J774A.1 miRNA 125a-5p were incubated with 250 nM of 5'-ATTO 647N-labeled aptamers for 10 minutes at 37°C. **A)** The percentage cells bound by aptamers and **B)** relative MFI (aptamer/control) were measured by flow cytometry (n=2, mean ± SD).

Therefore, it was evident that the reporter gene did not affect the binding potential of aptamers.

4.4 Synthesis and pharmacological characterization of aptamer-antagomir 125a-5p conjugates (aptamiR 125a-5p)

4.4.1 Coupling of aptamers and antagomir 125a-5p

As described in the **Section 4.2.3**, 3' end of the aptamer DC 12 did not influence the binding capability of the aptamer. Thus, the 3' end of the DC 12 aptamer was conjugated with the 5'-maleimide antagomir 125a-5p, to form a chimera known as DC 12 aptamiR 125a-5p. Similarly, 3' end of the Ctrl 2 aptamer was conjugated with the 5'-maleimide antagomir 125a-5p, to form a chimera known as Ctrl 2 aptamiR 125a-5p. The 5'-maleimide antagomir 125a-5p was conjugated through thiol-maleimide chemistry to the 3'-thiol-C6 aptamer sequences (DC 12 and Ctrl 2). Thiol-modified aptamers and maleimide-modified antagomir 125a-5p were deprotected separately and then mixed in DPBS, for 24 hours. Maleimide has the property to react with the sulfhydryl groups and thus to form a stable thioether linkage **(Figure 4.4.1)**.

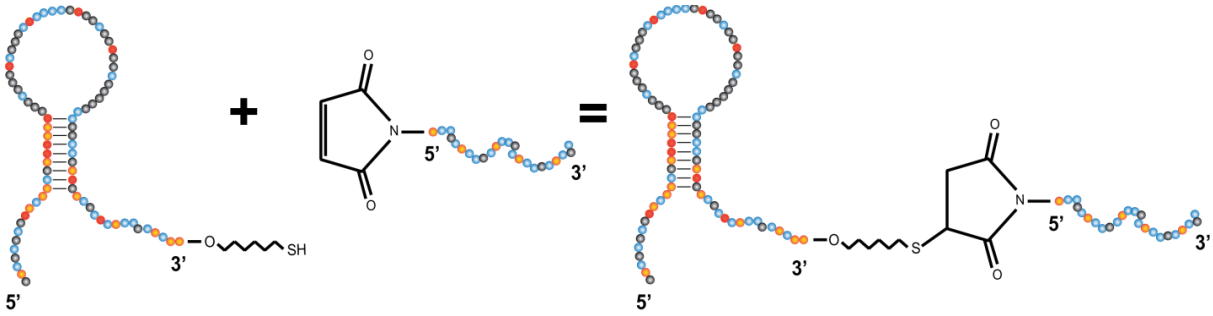

Figure 4.4.1: Overview of thiol-maleimide reaction to synthesize aptamiR 125a-5p
3'modified aptamer was coupled to 5'modified antagomir via thiol-maleimide chemistry (modified from Silvana Ph.D. thesis[101]).

After 24 hours, 4% agarose gel was run to visualize the required product size **(Figure 4.4.2)**.

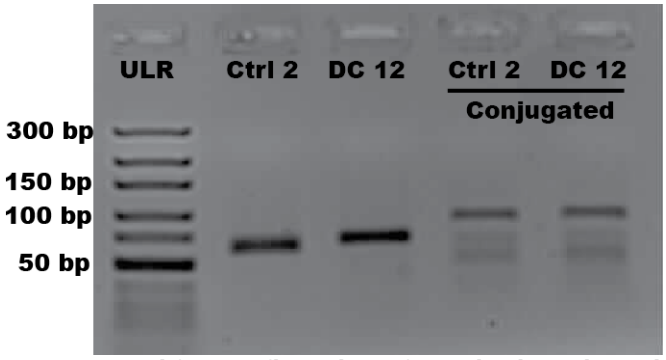

Figure 4.4.2: 4% agarose gel for confirmation of required product size
Ctrl 2 (79 bases), DC 12 (80 bases), Ctrl 2 conjugate (79+24 =103 bases) and DC 12 conjugate (80+24 =104 bases). The smaller bands in the conjugated lines are unconjugated aptamers, which were removed by using 15% PAGE gel.

Following confirmation of 4% agarose gel, the chimeras were purified using 15% PAGE gel and the concentration was measured using nanodrop 2000. They were then characterized by their ability to bind to macrophages.

4.4.2 Binding capability of DC 12 aptamiR 125a-5p

The conjugation of DC 12 aptamer with an antagomir 125a-5p may influence the interaction properties of the aptamer with the cells. It may be possible that the aptamer did not fold in the correct conformation, required to bind to the cells.

Table 4-14: % cells bound by ATTO 647N-labeled aptamers and relative MFI in flow cytometry competition binding assay

Aptamer		% Cells bound	Relative MFI (aptamer/control)
Ctrl 2*		7.01±8.98	1.0±0.12
DC 12+	No competition	63.4±9.23	2.84±0.4
	UN-L DC 12	40.3±7.17	2.13±0.4
	UN-L Ctrl2	65.5±7.28	2.77±0.4
	DC 12 aptamiR	42.1±5.10	2.19±0.2
	CTRL 2 aptamiR	67.7±8.12	2.84±0.2

*control, UN-L= unlabeled (without fluorophore)
UN-L DC 12 (unlabeled DC 12 aptamer), UN-L Ctrl 2 (unlabeled ctrl 2), DC 12 aptamiR (DC 12 aptamer conjugated with antagomir 125a-5p), Ctrl 2 aptamiR (ctrl 2 conjugated with antagomir 125a-5p)

To investigate the binding ability of the aptamiR, a competitive binding assay was performed **(Table 4-14** and **Figure 4.4.3)**.

$8x10^4$ THP-1 cells were co-incubated with 50 nM ATTO 647N-labeled aptamers and eight-fold molar excess unlabeled aptamers (without fluorophore) and aptamiR 125a-5p in RPMI 1640 supplemented with 10% FCS at 37°C for 10 minutes. The percentage of cells bound to the labeled DC 12 was decreased in the presence of unlabeled DC 12 and DC 12 aptamiR 125a-5p. Whereas, no competition was observed in the presence of unlabeled Ctrl 2 and Ctrl 2 aptamiR 125a-5p. Ctrl 2 aptamiR 125a-5p had functional antagomir 125a-5p domain but Ctrl 2 aptamer domain was not functional and could not bind to the cells. Hence, DC 12 aptamiR 125a-5p retains the binding properties with the cells and may be able to deliver antagomir 125a-5p.

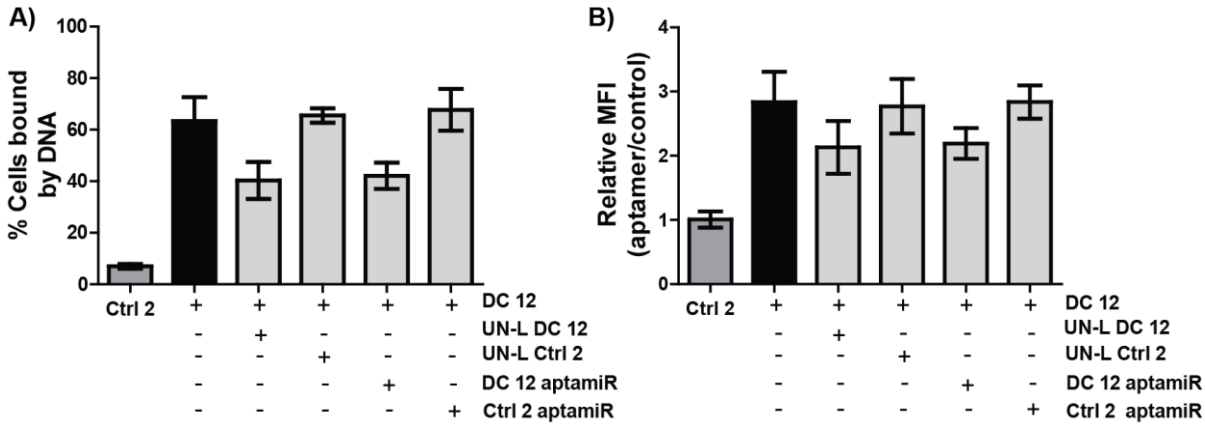

Figure 4.4.3: Binding capability of aptamiR 125a-5p is maintained
8×10^4 THP-1 cells were incubated with 50 nM ATTO 647N-labeled DC 12 in the presence of 400 nM competitors (grey bars) and analyzed by flow cytometry (n=2, mean ± SD). UN-L DC 12 represents unlabeled DC 12 aptamer, UN-L Ctrl 2 represents unlabeled Ctrl 2 aptamer, DC 12 aptamiR represents DC 12 conjugated with antagomir 125a-5p, and Ctrl 2 aptamiR represents Ctrl 2 conjugated with antagomir 125a-5p.

4.4.3 Transfection of aptamiR 125a-5p

The conjugation of aptamer with the antagomir 125a-5p may influence the interaction properties of the antagomir 125a-5p with an endogenous miRNA 125a-5p. It may be possible that the folding or size of aptamer domain limits the interaction of antagomir 125a-5p with the miRNA. The transfection of aptamiR 125a-5p was performed to investigate the interaction of antagomir 125a-5p with miRNA. AptamiR 125a-5p were transfected in the stable cell lines, control stable cell line and EGFP-4X 125a-5p stable cell line. Different controls were included in the experiments such as DC 12 and Ctrl 2 un-conjugated, antagomir 125a-5p and antagomir control. A concentration of 50 nM was selected as it showed significant increase in the EGFP expression **(Figure 4.3.5)**.

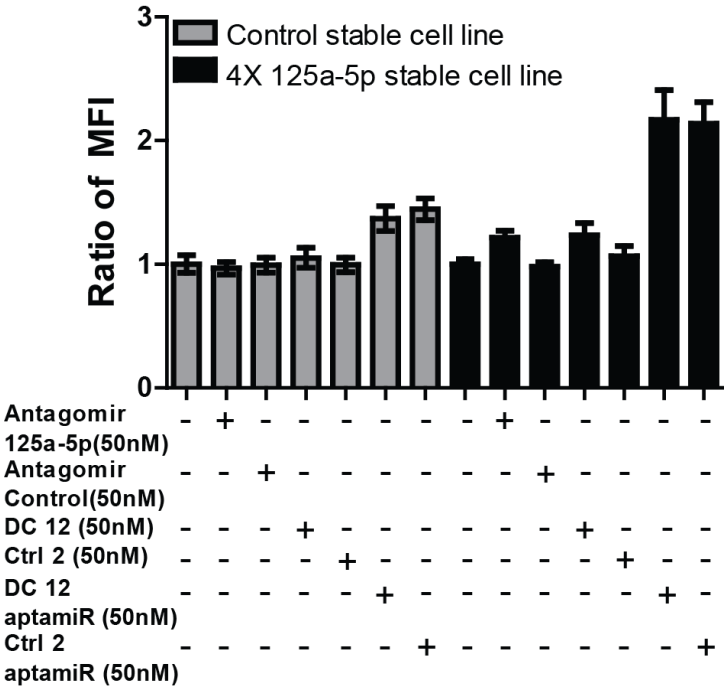

Figure 4.4.4: Transfection of aptamiR 125a-5p (Ratio of MFI)
4×10^4 control stable cell line (light grey bars) EGFP-4X 125a-5p stable cell line (black bars) cells were seeded one day before transfection. AptamiR 125a-ap and controls (50 nM) were transfected using lipofectamine 2000. After, 48 hrs cells were scraped and washed with 1 ml DPBS. The ratio of MFI was measured by flow cytometry. The experiment was performed twice (n=2, mean ± SD).

The cells were transfected with aptamiR 125a-5p and controls. After 48 hours of transfection, DC 12 and Ctrl 2 aptamiR 125a-5p with the functional antagomir 125a-5p showed an increase in MFI and also an increase in the EGFP expressing cells in the EGFP-4X 125a-5p stable cell line **(Figure 4.4.4** and **Figure 4.4.5)**. The antagomir 125a-5p did not have similar effect when compared to the conjugated antagomir 125a-5p, which could be due to the transfection efficiency of the small RNAs with lipofectamine 2000. This problem could be encountered or avoided by using a transfecting agent for small RNAs. The aptamiR 125a-5p showed an increase in MFI and EGFP expressing cells in the control stable cell line. This effect could be due to the non-specific effect of aptamiR 125a-5p and it could be considered as non-significant compared to the EGFP-4X 125a-5p stable cell line **(Figure 4.4.4** and **Figure 4.4.5)**.

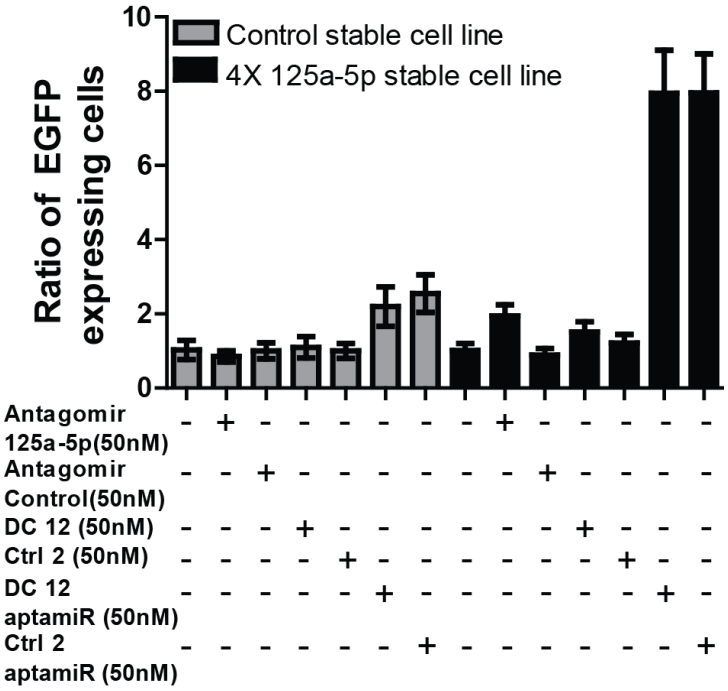

Figure 4.4.5: Transfection of aptamiR 125a-5p (Ratio of EGFP expressing cells)
4×10^4 control stable cell line (light grey bars) EGFP-4X 125a-5p stable cell line (black bars) cells were seeded one day before transfection. AptamiR 125a-5p and controls (50 nM) were transfected using lipofectamine 2000. After, 48 hours, the cells were scraped and washed with 1 ml DPBS. EGFP expressing cells were measured by flow cytometry. The experiment was performed twice (n=2, mean ± SD).

The antagomir 125a-5p domain of the aptamiR 125a-5p has thus been shown to retain its interaction properties with the miRNA. The aptamer domain did not affect the functionality of the antagomir 125a-5p after the conjugation.

4.4.4 Effect of aptamiR 125a-5p on the reporter gene expression

The functionality of aptamiR 125a-5p was tested in **Section 4.4.2** and **Section 4.4.3** above. In order to investigate the ability of DC 12 aptamer to deliver antagomir 125a-5p into the cytoplasm, aptamiR 125a-5p was incubated with the EGFP-4X 125a-5p stable cell line. DC 12 aptamiR 125a-5p and Ctrl 2 aptamiR 125a-5p were diluted in the cell culture medium and incubated with a reporter gene stable cell line. As a positive control 50 nM of aptamiR 125a-5p was also transfected using lipofectamine 2000 **(Section 4.4.3)**.

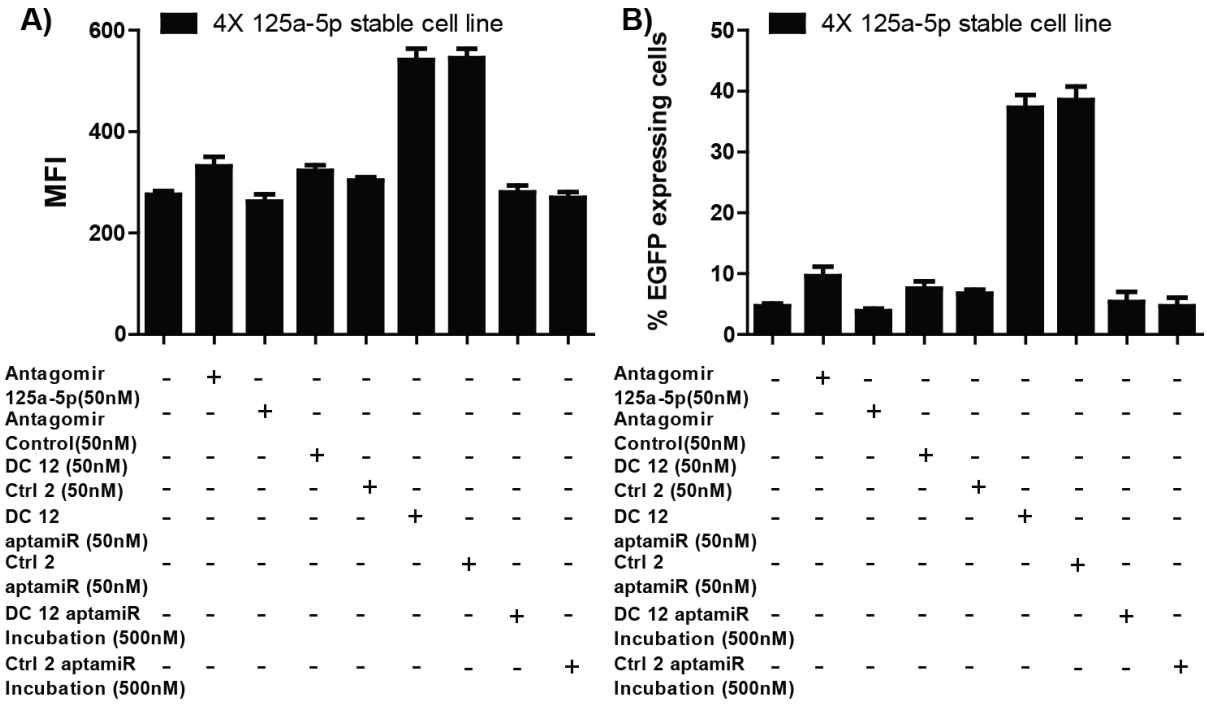

Figure 4.4.6: Aptamer-targeted delivery of antagomir 125a-5p in stable cell line
4×10^4 EGFP-4X 125a-5p stable cell line (black bars) cells were seeded one day before aptamer-antagomir 125a-5p incubation and transfection. AptamiR 125a-5p (500 nM) were incubated and positive controls (50 nM) were transfected using lipofectamine 2000. After, 48 hrours, the cells were scraped and washed with 1 ml DPBS. **A)** The MFI and **B)** EGFP expressing cells were measured by flow cytometry. The experiment was performed twice (n=2, mean ± SD).

After 48 hours, the cells were scraped and washed with 1 ml of DPBS. The MFI of the cells and the percentage of EGFP expressing cells were determined using flow cytometry. Incubation with DC 12 aptamiR 125a-5p and Ctrl 2 aptamiR 125a-5p showed no increase in the EGFP expression compared to untreated cells **(Figure 4.4.6)**. Transfection of the aptamiR 125a-5p showed an increase in the MFI and an increase in the percentage of EGFP expressing cells. It meant that the DC 12 mediated delivery of antagomir 125a-5p into the cytoplasm was limited. It might be possible that the aptamiR 125a-5p are entrapped in the endosomal or lysosomal compartments.

4.4.5 Pharmacological effects of aptamiR 125a-5p on human baseline macrophages

DC 12 aptamer was able to recognize and bind to both human baseline and TPP macrophages **(Figure 4.2.12** and **Figure 4.2.13)**. The main distinct property of the TPP macrophage phenotype was the upregulation of miRNA 125a-5p (see **Figure 3.2.3** in the introduction section). DC 12 aptamer was successfully conjugated with the antagomir 125a-5p **(Section 4.4.1)** to inhibit miRNA 125a-5p. The domains of DC 12 aptamiR 125a-5p were functional in terms of targeting macrophages and inhibiting miRNA 125a-5p via transfection in the reporter gene assay **(Section 4.4.2** and **Section 4.4.3)**. Unfortunately, DC 12 guided uptake of aptamiR 125a-5p did not show any effect on the EGFP expression on the stable cell line. Non-effected expression may be due to the entrapment of the antagomir in the endosomes or lysosomes **(Figure 4.4.6)**. It may be possible that the human baseline macrophages have different uptake pathways for DC 12 or that they might not have sufficient endosomes for entrapment of DC 12.

Table 4-15: MFI of surface markers (CD23, CD86, CD25, and CD14) of different macrophage phenotypes and TPP treated groups in flow cytometry

Macrophage Phenotype		MFI			
		CD23	**CD86**	**CD25**	**CD14**
M_b		49.6±1.98	68.2±1.95	6.5±0.43	155±2.06
IL-4		250±93.5	20.3±9.37	5.9±0.37	37.5±3.63
IFN-ɤ		57±0.83	233±113	7.42±1.25	89.6±3.99
TPP+	No treatment	63.5±0.55	62.7±7.96	32±2.69	353±195
	DC 12 (500nM)	59.1±0.95	57±11.7	27.4±3.05	376±198
	Ctrl 2 (500nM)	60.5±1.45	59.9±8.46	29.5±2.28	384±215
	Ctrl 2 aptamiR (500nM)	58.6±0.38	61.4±10.9	27.4±4.76	381±190
	DC 12 aptamiR (500nM)	57.4±1.84	75.4±24.3	30±3.54	395±237

In order to investigate inhibition of upregulated miRNA 125a-5p in TPP macrophages through DC 12 aptamiR 125a-5p, baseline macrophages were

incubated with aptamiR 125a-5p. 500 nM aptamiR 125a-5p, DC 12, and Ctrl 2 unconjugated have been incubated with the human baseline macrophages for 30 minutes under standard cell culture conditions. Then, the supernatant was replaced with fresh medium containing TPP macrophage stimulants. As the control baseline, IL-4, and IFN-ɤ macrophage stimulants were also incubated with baseline macrophages for the next three days. The cells were stained with surface marker antibodies (CD14, CD25, CD23, and CD86) and the MFI was measured using flow cytometry.

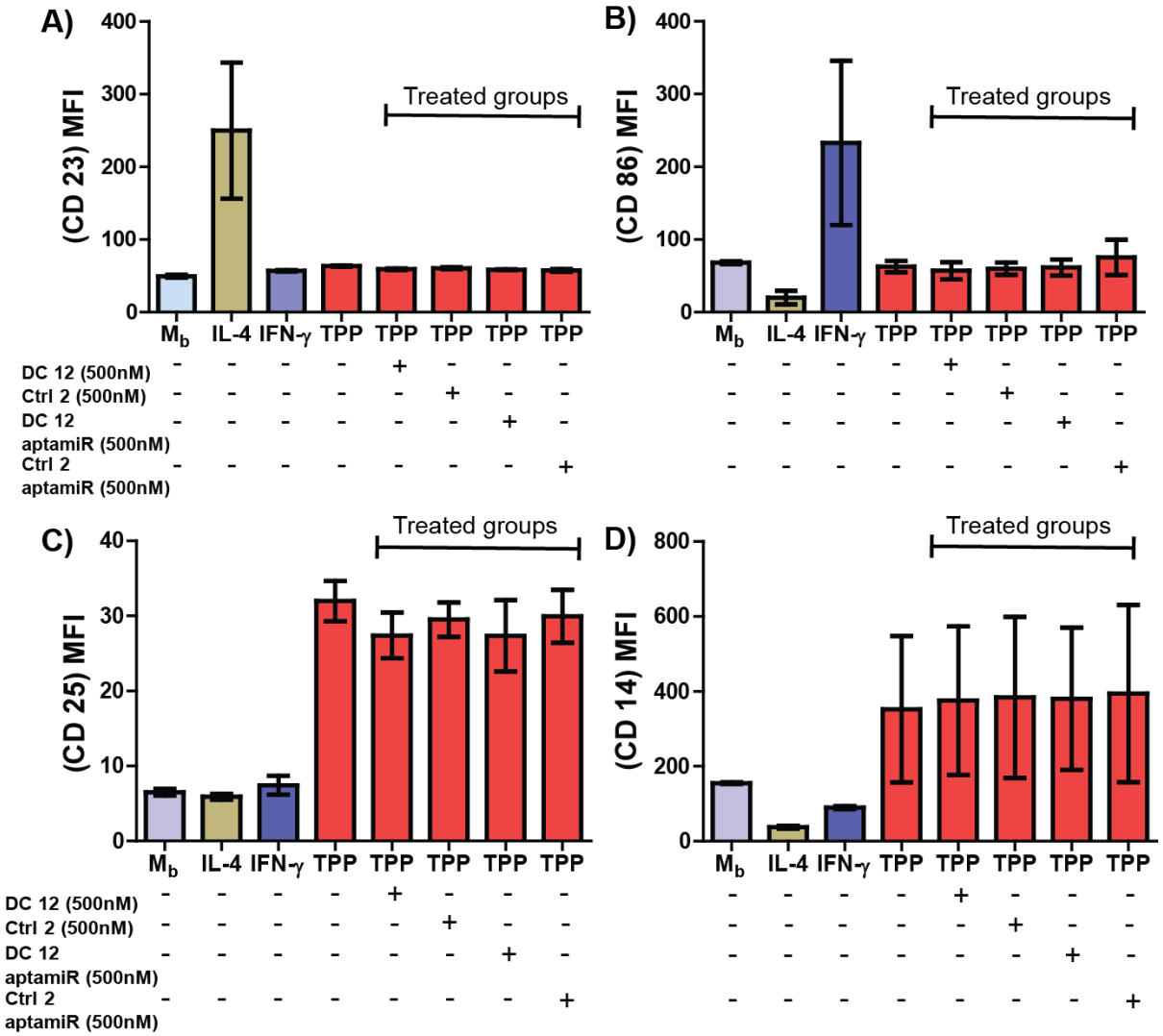

Figure 4.4.7: Aptamer-targeted delivery of antagomir 125a-5p in human baseline macrophages
4×10^6 human baseline macrophages were treated with aptamiR 125a-5p for 30 minutes. Then, the medium was replaced with fresh medium containing TPP stimulants. As positive control, untreated cells, IL-4, and IFN-ɤ macrophages were also differentiated for the next three days. After 72 hours, cell surface markers profiles were determined through flow cytometry (n=2, mean ± SD). The treatment of 500 nM DC12 aptamiR (DC 12 aptamer-antagomir 125a-5p) showed similar MFI

compared to untreated TPP macrophages, Ctrl 2 aptamiR (Ctrl 2 aptamer-antagomir 125a-5p), DC 12 (unconjugated DC 12), and Ctrl 2 (unconjugated Ctrl 2).

The expression level of TPP stimulated macrophages showed similar MFI regardless of treatment **(Table 4-15** and **Figure 4.4.7)**. The results were consistent with the previous experiments of the reporter gene **(Figure 4.4.6)**. The entrapment of DC12 aptamiR 125a-5p limited its interaction with the endogenous miRNA 125a-5p.

4.5 Aptamer-targeted activation of CD8 T cells

In the previous sections of this chapter, DC 12 aptamer was selected from the NGS data of BM-DCs cell-SELEX. DC 12 aptamer was shown to binds to J774A.1, THP-1, human baseline macrophages, and dendritic cells. DC 12 aptamer has also been internalized into J774A.1 and human baseline macrophages and be non-immunogenic. DC 12 aptamer meets all requirements to function as a suitable carrier molecule.

In the last **Section 4.4**, DC 12 aptamer was successfully conjugated with antagomir 125a-5p for endogenous inhibition of miRNA 125a-5p and its functionality was tested. Unfortunately, DC 12 aptamer guided delivery of antagomir 125a-5p may have entraped into the endosomes and limited its inhibitory activity. Therefore, the carrier properties of DC 12 aptamer was further illustrated by an OVA model system. This system was widely used and most feasible model to study aptamer-based delivery of antigenic OVA peptides to DCs for T cell-mediated immunity[101]. It is well known that OVA possesses binding sites MHC I $OVA_{257-264}$ (MHC I peptide) and MHC II $OVA_{323-339}$ (MHC II peptide)[199,200]. Transgenic mouse models were established to produce OVA-specific CD8 or CD4 T cells. These models produce either CD8 T cells that identify MHC I bound $OVA_{257-264}$ or CD4 T cells that recognize MHC II bound $OVA_{323-339}$[201,202].

Isolated MHC I or MHC II peptides are capable of binding to MHC molecules expressed on the cell surface. Thus, DC 12 aptamer was conjugated with prolonged OVA peptide ($OVA_{249-272}$, known as OT-I peptide), expanded with MHC I recognition

sequence for targeted delivery to DCs for targeted activation of CD8 T cells. OT-I peptide was covalently bound to DC 12 aptamer by thiol-maleimide chemistry.

4.5.1 Coupling of aptamers and OT-I ($OVA_{249-272}$) peptide

5' thiol-modified aptamers were conjugated through thiol-maleimide chemistry to MHC I- restricted OT-I OVA peptide. Aptamers modified with 5'-thiol were reduced to thiol derivatives and mixed with N-terminal maleimide MHC I-restricted OVA peptide. Maleimide has the ability to react with the sulfhydryl groups and forms a stable thioether linkage **(Figure 4.5.1B)**.

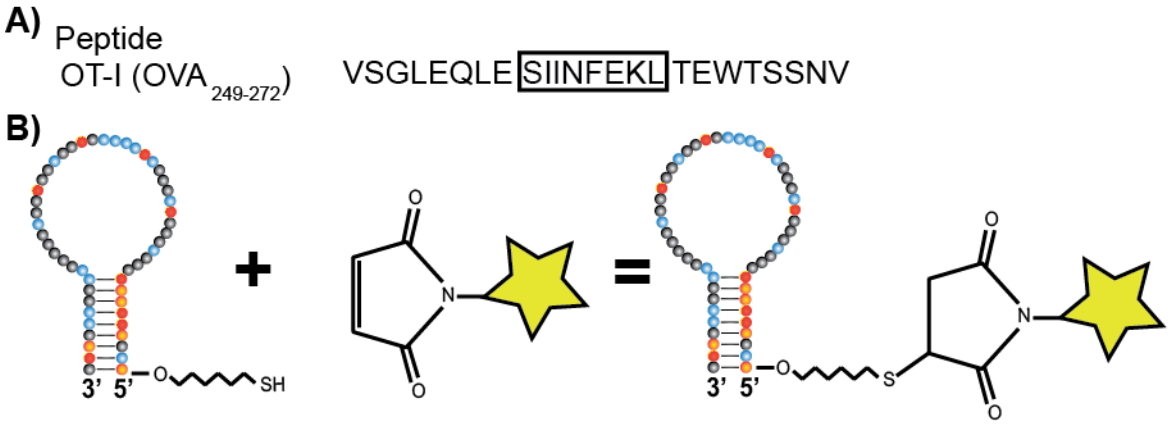

Figure 4.5.1: Overview of thiol-maleimide reaction to synthesize aptamer-OT-I ($OVA_{249-272}$) conjugates
A) MHC I peptide OVA $_{257-264}$ is highlighted in the box. The OVA peptide expanding MHC I recognition sequence was used for coupling with aptamers. **B)** 5' thiol-modified aptamer was coupled to N-terminal maleimide functionalized peptide (yellow star) (Figure modified from Silvana Ph.D. thesis[101]).

Reverse phase high performance liquid chromatography (RP-HPLC) was performed to purify the conjugates.

4.5.2 Aptamer-targeted delivery of OT-I peptide for CD8 T cells activation

In order to investigate aptamer-OT-I conjugates mediated targeted activation of CD8 T cell, an *in vitro* proliferation assay was selected. This assay was established by Dr. Silvana Haβel in LIMES, University of Bonn, Germany for the aptamer-targeted

activation of T cells[101] and was also performed by Dr. Silvana Haβel, University of Bonn, Germany. Genetically modified murine OVA-specific CD8 T cells[203] were able to recognize $OVA_{257-264}$ presented on MHC I molecules on the cell surface of BM-DCs. Briefly, $5x10^4$ murine BM-DCs cells were counted and treated with either MHC I or OT-I peptides and aptamer-OT I conjugates in the DC cell medium at 37°C for 10 minutes. As a positive control, D#7 aptamer conjugated with OT-I was used, a known activator of CD8 T cell[101]. D#7 aptamer was selected and characterized by Dr. Silvana Haβel for targeted activation of T cells[101]. Transgenic mice were used for isolation of OVA-specific CD8 T cells. $1x10^5$ cells were isolated, labeled with CFSF and incubated with treated BM-DCs for 72 hours.

Carboxyfluorescein succinimidyl ester (CFSE) is considered to be an ideal dye for cell division measurement. Normally, when a CFSE-treated cell proliferates, its daughter cells are equally endowed with dye and thus each cell division can be determined by analyzing the reduction of cell fluorescence through the flow cytometry[204].CD8 T cells activation was assessed by the CFSE proliferation assay by flow cytometry and quantified through a ranged gate tool.

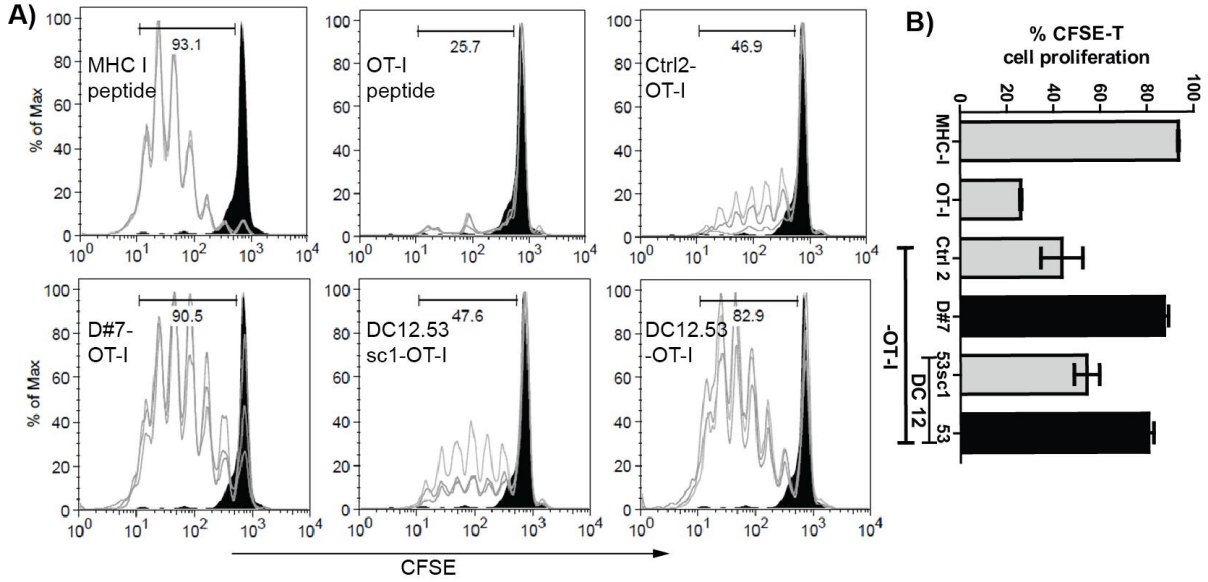

Figure 4.5.2: Aptamer-targeted delivery of OT-I peptide for CD8 T cells activation
$1×10^5$ OVA-CD8 specific T cells were stained with fluorescent staining dye (CFSE) and incubated with $5×10^4$ BM-DCs treated with 100 nM of aptamer-conjugates, OT-I peptide and 1 nM of MHC I peptide. **A)** Black area shows non-treated cells in all histograms. CFSE profiles were determined by flow cytometry and the proliferated population was gated by ranged gate tool. **B)** The ranged gate percentage of CFSE T cell proliferation of triplicates (mean ± SD) was plotted (n=1 in triplicates). For more information see supplementary Figure S 9.3.1. The assay was performed by Dr.Silvana Haβel.

The black bars are non-proliferative populations **(Figure 4.5.2A)**. This population was obtained by adding T cells to non-treated BM-DCs. MHC I peptide ($OVA_{257-264}$) was able to bind directly to the MHC I molecules on the surface of BM-DCs because it consists only of the OVA MHC I recognition amino acid sequence **(Figure 4.5.1A)**. Therefore, 1 nM MHC I peptide was able to induce strong CD8 T cells activation compared to 100 nM OT-I peptide, which needs to be processed by the endosomal compartments for presentation on the surface of BM-DCs. DC 12.53 aptamer-OT-I has the potential to deliver OT-I peptide and activates CD8 T cells compared to the D#7-OT-I **(Figure 4.5.2B)**. As expected, Ctrl 2-OT-I and DC 12.53sc1-OT-I were unable to induce CD8 T cell proliferation compared to D#7-OT-I and DC 12.53-OT-I **(Figure 4.5.2** and **Figure S 9.3.1)**. In conclusion, DC 12.53 aptamer has the capability to deliver OT-I peptide into the required endosomal compartment for processing and presentation on the surface of BM-DCs. Upon presentation, it was able to induced CD8 T cell proliferation **(Figure 4.5.2** and **Figure S 9.3.1)**.

5 Discussion

Aptamers are promising alternatives to protein-based target approaches as they are considered to have some advantages over antibodies[20] **(Table 5-1)**. Cell-targeting aptamers have a high specificity and affinity to their specific targets and are also capable of delivering cargo molecules[25-29]. They are cheaper, easy to synthesize, chemically stable, relatively smaller in size, low or non-toxic, and less immunogenic than other carrier molecules[16-19,196]. Hence, they can be used to target immune cells in a variety of different therapeutic and diagnostic applications.

Table 5-1: Advantages and disadvantages of aptamers and antibodies (modified from Ganji *et al.*[205])

Aptamer		**Antibody**	
Advantages	Disadvantages	Advantages	Disadvantages
1. Chemically synthesis (*in vitro* selection) 2. Low-immunogenic 3. No viral or bacterial contamination 4. High specificity and affinity 5. No batch-to-batch variation 6. Small size (easy penetration into biological compartment) 7. Heat stability (reversible denaturation) 8. Produced against non-immunogenic molecules	1. Small size (renal filtration) 2. Susceptible to nuclease degradation 3. Short half-life	1. Large size (without renal filtration) 2. Long half-life (prevent from filtration because of binding to neonatal Fc receptor for IgG (FcRn) and large size) 3. High specificity and affinity 4. Resistance to nuclease degradation	1. Hybridoma technology (*in vivo* selection) 2. Immunogenic 3. Viral and bacterial contamination 4. Large size (low penetration into biological compartment) 5. Batch-to-batch variation 6. Heat susceptibility (irreversible denaturation)

The aim of the study is to find out whether aptamers targeting immune cells have been able to inhibit endogenic miRNA 125a-5p through targeted delivery of antagomir to macrophages. In the first phase, NGS data from BM-DCs cell-SELEX was used to identify the most promising sequences that will bind to J774A.1 and THP-1 cells, as a result, DC 12 aptamer was selected, characterized and truncated to 53 nucleotides. In the second phase, the EGFP reporter system and human baseline macrophages were used to study the inhibition of miRNA 125-5p through DC 12 targeted delivery of antagomir. Unfortunately, DC 12 guided uptake did not have sufficient effect on miRNA 125-5p inhibition. In parallel, the functionality of DC 12 as a carrier molecule for targeted activation of CD8 T cell was tested by an OVA model system. Consequently, the aptamer-OT-I conjugate was found to have the potential to activate T cell-mediated immunity.

5.1 Screening of sequences for binding to macrophages and DCs

In general, cell-targeting aptamers can be obtained by using the cell-SELEX approach without prior knowledge of the target on the cell surface[13]. As described above, cell-targeting aptamers have certain advantages over other pharmacological molecules such as low toxicity, little or non-immunogenicity, easy to synthesize, no batch to batch variation, thermal stability, easy to modify, and internalization into the cells upon binding[21-24,206].

With their originally targeted cells, depending on the surface expression of aptamer-target on other cells, the cell-SELEX related aptamers might also have the ability to recognize cell surface targets on other cells. For example, aptamers obtained from breast cancer cell-SELEX also have the ability to recognize and bind to different solid tumor-derived cancer cells (H460, A549, and MCF7)[207]. Taking this property of cell-targeting aptamers into account, the NGS data of BM-DCs cell-SELEX[101] was screened to obtain aptamers targeting macrophages. The aptamers obtained from BM-DCs cell-SELEX have the potential to recognize and bind to DCs, which were subsequently used for aptamer-targeted delivery of antigen to DCs for T cells

activation[101]. In this study, the most abundant sequences from NGS data of the 10th selection cycle were used to screen macrophage targeting aptamers. Macrophages and DCs are the immune cells and latter are professional APCs. They have the same progenitor precursor and have overlapping properties[182]. Various studies have shown that BM-DCs, human monocyte-derived DCs, and Langerhans cells (LCs) have significant similarity in transcriptional level and similar ontogenetic origin with macrophages[208]. Since cell-SELEX was performed on mouse DCs it was worthwhile to screen these sequences with mouse macrophages.

5.1.1 Binding to mouse macrophages and DCs

BM-DCs and the mouse macrophage cell line (J774A.1) have many similar targets on their cell surfaces[184]. In this study, the most abundant sequences from the NGS data of BM-DCs cell-SELEX showed the potential to recognize and bind to the mouse macrophage cell line (J774A.1) **(Figure 4.1.1** and **Figure 4.1.2)**. DC 7, DC 10, and DC 12 aptamers were tested in mouse macrophages and DC 12 was characterized to deliver antagomir 125a-5p to J774A.1 cells, expressing stable EGFP reporter gene and human primary baseline macrophages.

During BM-DCs cell-SELEX, the complexity of the library decreased to 50% in the 10th round of selection[101]. The selection showed enrichment of the DCs targeting sequences. DC 12 aptamer was also enriched in the selection procedure and was able to bind to BM-DCs **(Figure 4.1.5** and **Figure S 9.1.1)**. In the present work, the truncated version of DC 12 was used for the targeted delivery of antigen to DCs for the activation of CD8 T cells. Previously, the full length (80 nucleotides) D#5 and D#7 aptamers were used for the targeted activation of CD8 T cells[101].

Untill now, various DCs targeting molecules have been studied using numerous targeting agents to use in therapeutic purposes[205]. As stated in **Table 5-1,** aptamers have more advantages than antibodies, aptamer 16, generated through SELEX against recombinant DC-specific intercellular adhesion molecule (ICAM)-3 grabbing non-integrin (DC-SIGN) was as specific as anti-DC-SIGN monoclonal antibody[209].

Cell-SELEX generated DNA aptamer pools can distinguish between mature and immature DCs. Later these pools were used for the discovery of biomarkers from DCs [210].

5.1.2 Binding to human monocytes and macrophages

As outlined in **Section 3**, human monocytes and macrophages have the same progenitors and have many similar properties as DCs. Herein, DC 12 aptamer was identified, which recognizes and binds to human monocytic cell line (THP-1) **(Figure 4.1.3)**, human primary baseline macrophages **(Figure 4.2.12)**, and chronic inflammatory macrophages (TPP) **(Figure 4.2.13)**.

THP-1 cells are the most widely used cell line for the study of monocytes and macrophages biology, drug transport, and signaling pathways[211]. DC 12 aptamer might provide an opportunity to study these parameters in detail. As, Dou *et al*.[212] have shown, aptamer-drug conjugate can provide better efficacy and tolerability due to aptamer-targeted delivery of the drug compared to the unconjugated drug. Thus, DC 12 can be conjugated with drugs for the treatment of various monocytes-related diseases.

THP-1 cells are also considered difficult to be transfected by non-viral approaches to the study of different biological processes[213]. Transfection of plasmids, DNA, and siRNA may be possible by using liposomes in combination with DC 12 aptamer, as liposomes provide encapsulation of therapeutic molecules and aptamers for targeting the cells[214]. Simple conjugation or coupling with DC 12 could be possible but a high concentration was required for endosomal escape. In general, the main limitation of the aptamer used as a delivery vehicle is the endosomal pathway[215]. In this study, DC 12 conjugated antagomir 125a-5p was used to delivery antagomir 125a-5p to human baseline macrophages. The binding and transfection of conjugates have shown that both domains of conjugates are functional. DC 12 after conjugation recognized and bound to the cells and antagomir 125a-5p was able to bind to the endogenous miRNA 125a-5p via transfection. However, DC 12 guided

uptake limited the release of antagomir 125a-5p into the cytoplasm and could be entrapped in the endosomes.

5.2 Immunogenicity of aptamer targeting immune cells

Nucleic acid-based drug products are used in different novel treatment strategies for several medical conditions. These products range from single-stranded antisense oligonucleotides to complex ribozymes including aptamers[216]. Nucleic acid-based drug products are usually designed to act within a cell, a distinctive property different from conventional drugs[216]. Thus, the assessment of immunogenicity is usually essential for pharmacological agents used in treatment strategies. They may induce an immune response or the production of antibodies to the product that interferes with the mechanism of action or leads to unwanted side effects[217]. Oligonucleotides based therapeutics are structurally in close resemblance to the endogenous nucleic acids, particularly endogenous DNA, which could be surprisingly immunogenic once it has moved its usual nuclear location and is found in the bloodstream[218]. Therefore, DNA aptamers might stimulate an immune response when sensed by the DNA sensors. It usually depends on the physicochemical properties and protein association of the DNA. TLR 9 is the most prominent internal DNA sensor, which stimulates an immune response[216].

In the present study, the immunogenicity of DC 12 and D#23 aptamer was determined by the TNF-α HTRF assay **(Figure 4.2.1)**. CpG ODNs and LPS, considered to stimulate the immune response, have been used as positive controls. The concentration of TNF-α was measured from the supernatant of the treated cells. In general, nucleic acid ligands were sensed by the internal DNA sensors such as TLR3, 7/8, 9 or 13[219] and signal cascades were activated for secretion of TNF-α. LPS and CpG ODNs induced a strong TNF-α secretion even in a minute amount but DC 12 and D#23 showed very low to no secretion even at a very high concentration **(Figure 4.2.1)**. Consequently, these aptamers did not appear to be immunogenic.

These results are consistent with previous studies by Haßel[101] and Fülle *et al.*[220]. Both studies used the TNF-α HTRF assay to investigate the immunogenicity of the aptamers and showed that aptamers were non-immunogenic.
Thus, it provided strong evidence that these aptamers can be used to target immune cells in therapeutic and diagnostic applications without activating the immune response.

However, *in vivo* information on the toxicity and immunogenicity of aptamers is very limited[221]. Introduction of unnatural nucleotides may cause serious chemical adverse effects or become immunogenic. LNA-modified nucleic acids cause severe hepatotoxicity in animal models[222]. To date, adverse events are very rare in the clinical evaluation of aptamers but may arise from continuous or repeated administration of aptamer therapeutics, polyanionic effects, intensive chemical modification, non-specific immune activation or unexpected tissue accumulation[223-225]. Potential hepatotoxicity often results from the non-specific liver uptake of highly lipophilic molecules[226].

5.3 Characterization of DC 12 aptamer

The native properties of aptamers as targeting molecules enable them to be used as a delivery vehicle for therapeutic agents. The structures of aptamers are easily predictable and can be modified by chemical modifications. These chemically modified aptamers can be easily linked to the cargo molecules for the development of diagnostic or therapeutic tools[227]. Several studies have shown that aptamers are promising molecules for targeting tumor cells when used as a delivery vehicle for small molecules such as siRNA, proteins, and drugs, even though the microvasculature of the tumor[227,228].

In the present study, the DC 12 aptamer structure was predicted using mfold[191] **(Figure 4.2.2A)**, it is 80 nucleotides in length **(Table 6-8)**. The DC 12 variant with 53 nucleotides was generated and termed as DC 12.53. DC 12.53 retained the parental

loop and stem in the structure prediction **(Figure 4.2.2B)**. DC 12.53 was able to recognize and bind to J774A.1 **(Figure 4.2.5)**, THP-1 **(Figure 4.2.6)**, human primary macrophages **(Figure 4.2.12)**, and TPP macrophages **(Figure 4.2.13)**. The scramble of DC 12.53 showed no binding and no recognition property. DC 12.53 was used in this study for the targeted delivery of antigen to DCs for CD8 T cell activation **(Figure 4.5.2** and **Figure S 9.3.1)**. Previously, two aptamers from the BM-DCs cell-SELEX without truncation were used to activate T cells[101]. The truncated aptamers are less expensive than the full-length aptamers. They are easy to synthesize with the solid phase synthesis of DNA with high yield.

The other factor, which may influence the binding of the aptamer is the coupling or conjugation of the molecules at the 5' or 3' end. In this study, ATTO 647-N (red absorbing fluorophore) was conjugated at the 5' and 3' ends of the aptamers DC 12 and DC 12.53. The conjugation of the fluorophore at either the 5' or 3' end of the aptamers showed that the aptamers retained the binding properties with the cells **(Figure 4.2.7** and **Figure 4.2.8)**. DC 12 was also synthesized with an extra 28 nucleotides through solid phase synthesis, which showed that it bound to the cells in a competition binding assay **(Figure S 9.2.1)**. These characterization studies provided a clue that DC 12 and DC 12.53 could be used as a delivery vehicle for the delivery of the small molecules. Cargo molecules can be conjugated to either ends of the aptamers. In the present study, DC 12 and DC 12.53 were further characterized regarding their uptake and internalization. Upon binding these aptamers were taken up by the cells and successfully internalized into the cells **(Figure 4.2.9** and **Figure 4.2.14)**.

The G-quadruplex is another important structure frequently seen in ssDNA aptamers[192]. In the current study, CD spectroscopy revealed that DC 12 and DC 12.53 could be folded into parallel G-quadruplex in the presence of ions **(Figure 4.2.3)**. Several experimental techniques are normally used to observe G-quadruplex such as atomic force microscopy, electron microscopy, sedimentation velocity analysis, UV melting etc but CD spectroscopy is considered to be a comprehensive

technique to observe G-quadruplex topology[192]. Further investigation will be needed to understand the G-quadruplex of DC 12 and DC 12.53. This could help in the therapeutic and diagnostic applications and even contributes to the natural biochemistry of G-rich nucleic acids[192]. The aptamer structure usually consists of stems, loops, and bulges but G-quadruplex structures often act as a motif to recognize the target as seen in many aptamers[229]. G-quadruplexes structure is one of the secondary structures to form well-defined tertiary structures of aptamers. Thus, it often increases the specific binding of aptamers and acts as a binding motif[229]. The secondary structures e.g., G-quadruplexes, T-junctions, bulges, pseudoknots, hairpins or their combinations forms a well-defined binding shapes. These shapes facilitate and enhance the binding properties through electrostatic interactions, π-π stacking interactions, and hydrogen bonds among aptamers and their targets. The structural properties of aptamers including G-quadruplexes help to elucidate patterns, principles, and diversity related to nucleic acids structural design, molecular recognition, and the adaptive binding behaviors[229,230].

5.4 Targeted delivery of aptamer-conjugates

5.4.1 Aptamer-targeted inhibition of miRNA 125a-5p

Aptamer-based targeted delivery and the amount of cargo that can reach successfully to the cytoplasm depends primarily on the following factors: The number of targeted protein on the cell surface, the ability to escape from the endosomal compartment, and the endocytic pathway[215]. In the study at hand, aptamer-targeted inhibition of miRNA 125a-5p was studied. DC 12 aptamiR 125a-5p had both the aptamer and antagomir domains functional. DC 12 aptamer domain was able to recognize and bind to the cells **(Figure 4.4.3)**. Antagomir 125a-5p domain was able to inhibit the endogenous miRNA 125a-5p via transfection in the stable cell line **(Figure 4.4.4** and **Figure 4.4.5)**. The DC 12 guided uptake of the aptamiR 125a-5p showed no interaction or inhibition of the miRNA 125a-5p **(Figure 4.4.6)**. It could be possible that the endocytic pathway for internalization of DC 12 aptamer ends up in the endosomes or lysosomes. This could have limited the

delivery efficiency of the aptamer and antagomir 125a-5p would not have been able to interact with the endogenous miRNA 125a-5p in the cytoplasm. Thus, diminishes the inhibitory activity of antagomir 125a-5p. Normally, the aptamer-based delivery system internalizes through an endocytic mechanism and gets entrapped in the endosomes[215]. However, it has often been observed that the delivery efficiency, usually required for therapeutic activity by aptamer guided uptake was limited and far from optimal yet[28].

Thiel *et al.*[231] selected an RNA aptamer through 'cell-internalization SELEX' to deliver siRNA into the cells of interest. Aptamer-siRNA chimeras have been internalized and released into the cytoplasm through receptor-mediated internalization. The chimera was able to interact with the RNAi machinery in the cytoplasm. However, they did not know the uptake kinetics or the pharmacological mechanisms by which these aptamer-siRNAs chimeras usually escape from the endosomes[231]. Cell-internalization SELEX strategy could be used to identify aptamer targeting macrophages to efficiently deliver antagomir 125a-5p into the cytoplasm.

However, in the current study, the characterization of DC 12 aptamer provided strong reasons for using it as a delivery vehicle. Antagomir 125a-5p was conjugated at the 3' end of the DC 12 aptamer and it may also be possible to use the free end of the aptamer or antagomir 125a-5p for endosomal escape purposes. These ends can be used for the introduction or conjugation of certain protein tags[232], peptides[233], polyethyleneimine[234], and nanoparticles[235] to facilitate the endosomal escape. These agents act through proton sponge effect and cause disruption or lysis of the endosomes[232].

Furthermore, the treatment of TPP macrophages with DC 12 aptamiR 125a-5p did not show any alteration in the surface marker analysis **(Figure 4.4.7)**. 500 nM aptamiR 125a-5p were incubated with the human baseline macrophages for 30 minutes and the medium was replaced with the fresh medium containing TPP stimulants for the next three days. The surface marker analysis showed no difference when compared to untreated cells. Relatively low concentration of aptamiR 125a-5p (500 nM) was used to prevent the non-specific binding and cellular

uptake of the non-internalizing oligonucleotides, which tend to internalize at relatively high concentrations of ≥1.0 µM[236,237].

These results indicated that further characterization of DC 12 aptamer was required for endosomal escape strategies. It would also be possible to use a protein or peptide with the aptamiR 125a-5p to facilitate endosomal escape. The 5-8 µM concentration of the aptamiR might have an inhibitory effect[23] or may change the endocytotic pathway of aptamer guided uptake.

5.4.2 Aptamer-targeted delivery of OT-I peptide for CD8 T cells activation

T-cell receptors (TCRs) are expressed by CD8 T cells that are activated by binding to the peptide bound to MHC class I molecules in a highly sensitive manner. These peptide ligands are degraded products of the endogenous polypeptide and are loaded on MHC I molecule in most cells. Upon recognition of the peptide, the T cell is activated and leads to the eradication of the target cell[238]. DCs are capable of proficiently presenting the ingested antigens to MHC I molecules. This process is known as cross-presentation and plays a significant role in the development of an immune response[239].

In the study at hand, DC 12.53 aptamer was used for the targeted delivery of OT-I peptide to DCs for CD8 T cell activation. The results showed that DC 12.53 was effective in delivering OT-I peptide and derived strong CD8 T cell activation **(Figure 4.5.2** and **Figure S 9.3.1)**. As discussed in the previous section **(Section 5.4.1)**, that aptamiR 125a-5p was entrapped in the endosomes, resulting in limited therapeutic efficiency, and provided evidence that aptamers were co-localized in the endosomal compartments. Therefore, aptamer-targeted delivery of OT-I peptide was also endocytosed, processed in these compartments, and loaded on MHC I molecule through cross-presentation to derive strong CD8 T cell activation.

These results are consistent with Haßel[101], where they used DNA aptamer D#7 (80 nucleotides) for targeted activation of T cell with OVA peptide. In another study, DEC-205 RNA aptamer was selected which binds specifically to DEC205, which is

mainly expressed by DCs. DEC-205 aptamer conjugated with OVA has the capability to trigger T cell activation[240]. These studies and the study at hand shows that aptamer-based vaccine design for targeted delivery of the antigen can be a promising alternative to protein-based targeting strategies. Cell-targeting aptamers also have several advantages over antibodies as described in the previous section **(Section 3.1.3)**.

5.5 Perspective for future research

The study at hand showed that aptamers have the potential to replace protein-based targeting approaches and be used as a delivery vehicle. Nevertheless, questions remain open for antagomir 125a-5p delivery.

If the high concentration (5-10 µM) of DC 12 aptamiR 125a-5p is able to reach the cytoplasm? In the previous work, 5 µM concentration of aptamiR-21 was required to inhibit the endogenous miRNA-21[28]. By increasing the concentration, it may be possible to inhibit miRNA, but conditions still need to be optimized by selecting new aptamers for macrophages or by facilitating endosomal escape.

Which chemical modification for antagomir could be used to inhibit miRNA efficiently? The most promising modifications to inhibit endogenous miRNAs are 2'O-methyl and LNA. LNA has some advantages over 2'O-methyl modification. Tiny LNA (8 nucleotides) complementary to the seed region of miRNA is capable of inhibiting the target miRNA and miRNA family sharing the same seed region[181].

Which endosomal escape facilitating agent can be used to delivery aptamiR 125a-5p efficiently into the cytoplasm? What other pharmaceutical formulations can be developed using these aptamers as targeting domain with endosomal escape properties? AptamiR 125a-5p may be combined or formulated with endosomal escape facilitating agents such as protein tags[232], peptides[233], polyethyleneimine[234], and nanoparticles[235] to facilitate the endosomal escape or rupture of the endosome

in order to release the cargo into the cytoplasm. However, these agents need to be characterized in terms of toxicity and immune response for clinical use.

What are the optimal conditions for inhibiting the endogenous miRNA 125a-5p through aptamiR 125a-5p in TPP macrophages? AptamiR 125a-5p can be administered during or after differentiation of human baseline macrophages into TPP macrophages. The treatment duration and time of administration are also critical parameters during the development of the therapeutics. Therefore, different optimal treatment conditions have to be determined, which have the maximum inhibitory effect on the endogenous miRNA 125a-5p.

What is the role of these aptamers targeting THP-1 cells in basic and applied research in the immunological context? Are these aptamers capable of helping immunologists to use THP-1 cells for their research? DC 12 aptamer can be combined with drugs to further study the effect of targeted-drug delivery on monocytes or macrophages. DC 12 aptamer can be used as transfection agent for THP-1 cells, which are considered to be difficult to be transfected using non-viral approaches[201].

For in vivo use, further characterization of aptamer-based delivery of antigen to DCs will be required.

5.6 Concluding remarks

The study at hand demonstrates that aptamers have the potential to be used as a carrier molecules and provides a basis for further investigation of endosomal escape of aptamiR chimera for the reprogramming of macrophages.
DC 12 aptamer was characterized from the NGS data of the previously performed BM-DCs cell-SELEX. DC 12 and DC 12.53 aptamers are valuable tools for our understanding of aptamers as a delivery vehicle. Selected aptamers are limited to delivering cargo into the cytoplasm. The reason for this is the endocytic pathway of

aptamer, which ends up in the endosomes and lysosomes. It could be improved by the use of different endosomal escape facilitating agents or design of special pharmaceutical formulations with aptamer as a targeting domain.

These results were further verified by delivering the antigen through aptamer into the endosomes (processing compartments) for efficient presentation of antigen and CD8 T cell activation. These aptamers contribute to the field of aptamer-based DC vaccines for potent T cell activation. In general, aptamers can be used as a delivery vehicle and are promising molecules as an alternative to protein-based targeting approaches. The doors are still open for improvement in this field, in order to regulate the pathway of internalization and endosomal escape of cell-targeting aptamers.

6 Materials

6.1 Equipment

Table 6-1 Equipment

Equipment	Manufacturer
FACS Canto II	BD
Genoplex UV transilluminator	VWR
HPLC 1260 series, C18 Eclipse column	Agilent
JASCO J-810 CD spectrometer	Jasco
Liquid scintillation counter WinSpectral 1414	Perkin Elmer
LSM 710 confocal laser scanning microscopy	Zeiss
MACS multistand	Miltenyi Biotec
Magnetic separator	Miltenyi Biotec
Nanodrop 2000c Spectrophotometer	Thermo Scientific
PCR Mastercycler personal	Eppendorf
Phosphorimager FLA-3000	Fujifilm
Pipets	Eppendorf
Water purification system	TKA/Thermo Scientific

6.2 Consumables

Table 6-2 Consumables

Consumable	Supplier
Amicon Ultra-0.5 Centrifugal Filter Devices 10 K	Millipore
Cell culture plates	Sarstedt; TPP; Greiner Bio One
FACS tubes, 5 ml, 12 mm	Sarstedt
Falcon cell strainer 40 µm	Sarstedt
G25 Columns	GE Healthcare
LS Columns	Miltenyi Biotec
Nunclon culture plates	Thermo Scientific
Pre-separation filters (30 µM)	Miltenyi Biotec
Reaction tubes	Sarstedt;Eppendorf

6.3 Commercially available kits

Table 6-3 Commercially available kits

Kit	Supplier
NucleoSpin Extract II Gel and PCR Clean-up	Macherey and Nagel
NucleoSpin plasmid	Macherey and Nagel

6.4 Cell culture

Table 6-4 Cell culture

Cell culture	Manufacturer
Fetal bovine serum	Sigma Aldrich
Geneticin G418	ThermoFisher
Gibco PBS 1x	ThermoFisher
Gibco RPMI 1640	ThermoFisher
Gibco DMEM	ThermoFisher
Gibco 0.05% Trypsin/EDTA	ThermoFisher
Human pancoll, density 1.077g/ml	Pan Biotech
Lipofectamine 2000	ThermoFisher
VLE-RPMI 1640 (Very Low Endotoxin) Liquid medium with stable glutamine	Merck
Penicillin [10000 U/ml]/Streptomycin [10 mg/ml]	PAA
Cyroprotective medium	Lonza

6.5 Antibodies

Table 6-5 Antibodies

Antibody	Manufacturer
PE anti Human CD25	Biolegend
Pacific Blue anti Human CD14	Biolegend
APC anti Human CD86	Biolegend
FITC anti Human CD23	Biolegend
CD14 Positive Selection Microbeads, Human	Milteny Biotech

6.6 Cytokines

Table 6-6 Cytokines

Cytokine	Manufacturer
TLR2 Ligand (Pam3CSK4)	InvivoGen
rh human GM-CSF	ImmunoTools
IFN gamma	Immuno Tools
rh IL-4	Immuno Tools
rh TNF –alpha	Immuno Tools
Prostaglandin E2	Sigma Aldrich

6.7 Chemicals and reagents

Table 6-7 Chemicals and reagents

Reagent	Supplier
1,4-Dithiothreitol (DTT)	Roth
4',6-diamidino-2-phenylindole (DAPI)	Sigma Aldrich
Acetic acid	Merck
Acetonitril	Fluka
Agar	Sigma Aldrich
Agarose	Merck; Genaxxon
Ammoniumperoxodisulfate (APS)	Roth
Bis-Acrylamid, Rotiphorese	Roth
Bovine serum albumin (BSA, nuclease and protease free)	Calbiochem
Bromophenol blue	Merck
DNA ladders	Fermentas;Thermo Scientific
dNTPs/NTPs	Larova
DPBS	Gibco
Ethanol abs.	Sigma Aldrich
Ethdiumbromide	Roth
Ethylendiamintetraacetic acid (EDTA)	AppliChem
Fluorogel mounting medium	EMS
Formaldehyde	Fluka
ɣ-32P-ATP	Perkin Elmer
Isopropanol	Merck
Magnesium chloride-hexahydrate	AppliChem
N,N,N',N'-tetramethylethylendiamide (TEMED)	Roth
Phenol	Roth
Potassium chloride (KCl)	Gruessing
Rotiphorese sequencing gel concentrate	Roth
Pwo polymerase	Genaxxon
Sodium chloride (NaCl)	AppliChem
Sodium dodecylsulfate (SDS)	Roth
Sodium acetate	Gruessing
T4 polynucleotide kinase (PNK)	NEB

Taq polymerase In house production;	Promega
Tricine	Roth
Triethylamine (TEA)	Sigma Aldrich
Triethylammonium acetat (TEAA)	Sigma Aldrich
Tris	Roth
Triton-X 100	Merck
Trypsin [0.05%]/EDTA [0.5M]	Thermo Scientific
Wheat germ agglutinin-Alexa Fluor 488	Invitrogen

6.8 Oligonucleotides

Table 6-8 Oligonucleotides

Name	Sequence 5'-3'
Ctrl 2	GCTGTGTGACTCCTGCAAGTGGTGTTAAGAGGTGAGGTATAACGCGGAATGG TGCGAGGCGCAGCTGTATCTTGTCTCC
D#23	GCTGTGTGACTCCTGCAACGTGGGCGGGTTTATATTTGGTGGTGGTGGGG GTGGTACTGTTGCAGCTGTATCTTGTCTCC
DC 4	GCTGTGTGACTCCTGCAAGGGGAGGTGGGTGGGTTGGCCTTCACGTTATC TTTTGGTGGTTGCAGCTGTATCTTGTCTCC
DC 6	GCTGTGTGACTCCTGCAACCAGGGGAGGATGGGAGGGTTTTTTTCGGATT CTTGTCGTGCTGCAGCTGTATCTTGTCTCC
DC 7	GCTGTGTGACTCCTGCAACGTGGTATGTGGTGGGTGGTGGGGTGGTAGTT GGGTGGACGGTGCAGCTGTATCTTGTCTCC
DC 8	GCTGTGTGCTCCTGCAACAGGGGAGGTGGGTGATTGGGTTGTTTTTCGCGGA CGTGAGGTGCAGCTGTATCTTGTCTCC
DC 10	GCTGTGTGACTCCTGCAACGAGTTTCTGAGGGTGGGTGGGTGGTTATTAGTC GAGGTTGCAGCAGCTGTATCTTGTCTCC
DC 12	GCTGTGTGACTCCTGCAACCAGGGTGGGATGGGTATTTTGAGGTGGAGGTGG GGGTTGGTTGCAGCTGTATCTTGTCTCC
DC 13	GCTGTGTGACTCCTGCAAGGGTGTTGTGGGGTGGGGCGGTGGGTGTGAGTG TCGGCAGCTGGCAGCTGTATCTTGTCTCC
DC 14	GCTGTGTGACTCCTGCAATGTGGTTCGGTAGGTCGGGGAGGGTGGTGGGTTA TGCGGCGGGGCAGCTGTATCTTGTCTCC
DC 15	GCTGTGTGACTCCTGCAACACAGGGGAGGTCGGGCGGGTTGTCTGCTTTCTT GGGTCGGTTGCAGCTGTATCTTGTCTCC
DC 20	GCTGTGTGACTCCTGCAACGTACTTTCACACGGGGAGGTGGGTTGGGTTCTG ATTAGGGTTGCAGCTGTATCTTGTCTCC
DC 21	GCTGTGTGACTCCTGCAACTGGGTCGGGGGTATTGTTTGCGATATGGGGGGT TTTGGGGTGGCAGCTGTATCTTGTCTCC
DC 12.53	CTGCAACCAGGGTGGGATGGGTATTTTGAGGTGGAGGTGGGGGTTGGTTGCA G
DC 12.53sc1	GGCGGTAGGGAGTGAGGTGGAGTGGCTTGTGAGGTCCGTGATAGCGTTTAG GT
DC 12.53sc2	GAACTCAAGACCCGGAGTTCCATTTCGAGTGAAGACTGTCGGAGTAGTGCATA
miRNA 125a-5p	UCCCUGAGACCCUUUAACCUGUGA
Antagomir 125a-5p	UCACAGGUUAAAGGGUCUCAGGGA

4X miRNA 125a-5p target site	GACGAGCTGTACAAGTAAAGCGGCCGCCTAATCACAGGTTAAAGGGTCTCAG GGACTAATCACAGGTTAAAGGGTCTCAGGGACTAATCACAGGTTAAAGGGTCT CAGGGACTAATCACAGGTTAAAGGGTCTCAGGGACGACTCTAGATCATAATCA GCCATACC
Fwd primer target site	GACGAGCTGTACAAGTAAAGCG
Rev primer target site	GGTATGGCTGATTATGATCTAGAGTCG

6.9 Mouse strains

Table 6-9 Mouse strains

Mouse strains	Description
C57BL/6J	Wildtype strain
OTI Rag2$^{-/-}$	C57/BL6 background, CD8 T cells express TCR specific for $OVA_{257-264}$ on MHC I, deficient in recombinant activating gene 2 (Rag2), therefore no endogenous TCR expression

6.10 Proteins

Table 6-10 Ovalbumin (OVA) peptides

Protein	Sequence (N-C)	Supplier
MHC I peptide ($OVA_{257-264}$)	SIINFEKL	Tebu-Bio
OT-I peptide	VSGLEQLESIINFEKLTEWTSSNV	Panatecs

6.11 Buffers and solutions

6.11.1 Gel electrophoresis

1 x TBE

90 mM Tris pH 8.0, 90 mM Borat, 2 mM EDTA

1 x DNA loading buffer

25 mM Tris pH 8.0, 25 % glycerol, 25 mM EDTA, bromophenol blue

1 x RNA loading buffer

50 % formamide, 0.013 % SDS, 0.25 mM EDTA, bromophenol blue

10 x PAA loading buffer

60 % formamide, 5 % SDS, 0.25 mM EDTA, bromphenol blue

6.11.2 Binding assay

Wash Buffer

DPBS, 1 mM $MgCl_2$, 1 mM $CaCl_2$

6.11.3 Isolation of CD14+ cells and staining

MACS buffer

1L DPBS, 2mM EDTA, 5ml FCS

6.11.4 Bacteria culture

Agar plates w/ kanamycin

7.6 g Agar, 10 g LB broth, 500 ml ddH_2O, 50 µl 100 mg/ml Kanamycin

LB medium w/ kanamycin

10 g LB broth, 500 ml ddH_2O, 50 µl 100 mg/ml Kanamycin

7 Methods

7.1 Working with nucleic acids

7.1.1 Synthesis and storage of nucleic acids

All nucleic acids have been purchased from ELLA-Biotech GmbH. They were dissolved in ddH_20 as described in the manufacturer certificate of analysis. All oligonucleotides have been stored at -20°C.

7.1.2 Quality control and concentration measurement

The concentration of nucleic acids was determined by nanodrop 2000. The required size of the oligonucleotides and the quality was checked by agarose gel electrophoresis.

The ATTO 647N-labeled DNA concentration was also determined by nanodrop 2000 using the micro-array option. The labeling efficiency was determined by gel electrophoresis and the fluorescence was analyzed by Phosphorimager FLA-3000 (Fujifilm).

7.1.3 Agarose gel electrophoresis

Usually, 4% agarose gels were used to monitor purchased nucleic acids, PCR products and 1% agarose gels were used for plasmid DNA. For this, agarose powder was dissolved in 1 x TBE buffer and boiled in a microwave for several minutes. 4 µl of ethidiumbromide has been added to 40 ml of this solution which is 1:10000 dilutions. This solution was thoroughly mixed and poured into the gel cast. The nucleic acid samples were diluted in a DNA or RNA loading buffer, 2 x RNA loading buffer was used for ssDNA and heated to 65°C for 5 minutes to prevent the secondary structures. The diluted samples were loaded into the gel wells. The gel was run for 15-20 minutes in the presence of 1 x TBE buffer at 130 V. The samples were run towards the positive charge and separated on the basis of their size. The

UV transilluminator (Genoplex, VWR) was used to visualize the separate oligonucleotides and the band size was determined by comparison with the DNA ladder.

7.1.4 Polyacrylamide gel electrophoresis (PAGE)

PAGE gel was used to analyze the labeling efficiency of radioactive labeled nucleic acids (^{32}P). The receipt of the gel (10%) was described in **Table 7-1** and was poured between the two glass plates of the chamber. The gel was stored for at least 45-60 minutes for polymerization. After polymerization, the glass plates were carefully adjusted in the running chamber and filled with 1 x TBE buffer. The gel was pre-run at 370 V for 30 minutes. After pre-run, the wells of the gel were rinsed with 1 x TBE buffer using the syringe. Nucleic acid samples were diluted in PAA loading buffer and heated at 95°C for 3 minutes. The gel was run for approximately 1 hour at 370 V.

Table 7-1 Recipe for one PAGE gel

Solution	Volume (10%)	Volume (15%)
Rotiphorese sequencing gel concentrate	28 ml	42 ml
8.3 M Urea	35 ml	21 ml
8.3 M Urea in 10 x TBE	7 ml	07 ml
TEMED	28 µl	28 µl
10 % APS	560 µl	560 µl

7.1.5 Thiol-maleimide conjugation

The 5'-maleimide antagomir 125a-5p and 3'-thiol-C6 oligonucleotides were purchased from Ella-Biotech, dissolved in dd$H_2$0 as indicated in the certificate of analysis to obtain a final concentration of 100 µM.

The concentration required for coupling of antagomir 125a-5p and oligonucleotide was calculated. The required concentration was aliquot in a clean screw cap vial and freeze-dried overnight using a freeze dryer. Then next day, 2 ml of anhydrous acetonitrile (Acros Organics) was added to the vial. A screw cap with a hole was used and a septum was placed. The center of the septum was pierce with a 16

gauge needle, at a slight angle. The vial was placed in a 100 ml round bottom glass flask and connected to the schlenk line. The schlenk line provides the possibility of vacuum and dry argon flashing. Vacuum was gently increased to avoid bumping. Wait until the anhydrous acetonitrile has completely evaporated. The vacuum was released by dry argon. Then, 2 ml of anhydrous toluene (Acros Organics) was added to the vial via 16-gauge needle and completely evaporated, by increasing the vacuum. Electromagnetic hot plate was used to maintain temperature at 37°C with a sand bath. A further 2 ml of anhydrous toluene was added and evaporated again. The residue of the antagomir 125a-5p was visible after the evaporation. The vial was removed from the flask. Again, 2 ml of anhydrous toluene was added and a 16-gauge needle was removed from the vial. The vial was placed in the sand bath at 90°C for four hours. The vial was cooled at room temperature for 15 minutes and the 16-gauge needle was inserted again. Anhydrous toluene was evaporated and the residue was dissolved in DPBS. The antagomir 125a-5p was ready for conjugation with the 3'-thiol-C6 oligonucleotides.

The 3'-thiol-C6 oligonucleotides were reduced with 1:2000 DTT, 100 mM DTT was freshly prepared in 1 M TEAA pH 8.3 - 8.5. The oligonucleotides with DTT were heated at 70°C for 3 minutes and incubated at room temperature for 1 hour. Reduced oligonucleotides were desalted with the aid of 10 K Amicon column into dd$H_2$0.

Subsequently, reduced oligonucleotides were mixed with a 5 times molar excess of maleimide antagomir 125a-5p. The mixture was incubated at 4°C for 24 hours and then loaded into 4% agarose gel to confirm reaction between thiol and maleimide oligonucleotides.

Similarly, for the conjugation of N-maleimide peptide with 5'-thiol-C6 oligonucleotides, thiol-C6 oligonucleotides were reduced as mentioned above and incubated with a 40-fold molar excess of N-maleimide peptide. Subsequently, the mixture was incubated at 4°C, overnight. The conjugates were purified via RP-HPLC on a C18 column with a linear gradient of 10 mM TEA and 100 Mm HFIP. The concentration was measured using nanodrop 2000 and analyzed by LC-MS.

7.1.6 Purification of aptamer-antagomir conjugates

For the purification of aptamer-antagomir conjugates (aptamiR), 15% PAGE gel was prepared. The gel was pre-run at 175 V for 15 minutes. Aptamer-conjugates were carefully mixed with the 2:1 loading buffer. Samples were mixed, then centrifuged. After cleaning the wells, the samples were loaded into the wells with 1 x TBE buffer. The gel was run at 175 V for about 1.5-2 hours until the loading buffer had reached more than 2/3 of the gel. The gel was wrapped in the plastic wrap to visualize separation of the bands. Separated bands were visualized with UV-light at 254 nm, using a fluorescent TLC plate (TLC Silica gel 60 F254) under the wrapped gel. The upper band was marked by drawing a box around, under the UV light. The gel was carefully cut with a plastic wrap using a sterile scalpel. After removing the plastic wrap, the gel pieces were transferred into the 2 ml reaction tube. The bands were crushed into small pieces with a blue pipette tip. 0.3 M sodium acetate pH 5.4 was also added to the reaction tube, so that the crushed gel pieces could move freely. The reaction tube was placed in the thermomixer at 65°C for a minimum of 1.5 hours. Then, the supernatant was filtered to remove the gel pieces using a 5 ml syringe filled with glass wool. The gel pieces in the reaction tube were washed twice with 100 µl of 0.3 M sodium acetate pH 5.4. Absolute ethanol was pre-cooled at -20°C and added to the sample volume three times. For better precipitation of the conjugates, 1 µl of glycogen has been added. Samples were incubated at -80°C for 15 minutes and, centrifuged at 4°C at 21130 xg for 45 minutes. The supernatant was discarded and the pellet was washed with 100 µl of 70% ethanol. The samples were centrifuged at 21130 xg for 10 minutes at room temperature. The supernatant was discarded again. The pellet was air-dried under the hood and was resuspended with ddH_2O. Conjugates concentration was measured using the nanodrop 2000 ssDNA option.

7.1.7 Polymerase chain reaction (PCR)

For the amplification of the 4X miRNA 125a-5p target site that was later inserted into the EGFP reporter gene, the pipetting scheme and program are shown below.

Table 7-2 Pipetting scheme for amplication of target site

Reagent	Stock concentration	Volume (µl)	Final
Pwo reaction buffer	10 x	10	1x
dNTPs	25 mM each	0.8	0.2 mM
miRNA 125a-5p fwd	100 µM	1	1 µM
miRNA 125a-5p rev	100 µM	1	1 µM
Pwo polymerase	2.5 U/µl	2.5	5 U
DNA template			1-10 nM
ddH_20		Q.S=50 µl	

Q.S= quantity sufficient

Table 7-3 PCR program for amplication of target site

Step	Time (min)	Temperature (°C)
Activation of Pwo (first cycle)	5	95
Denaturation	1	95
Annealing	1.5	57
Elongation	1.5	72
Final elongation (after last cycle)	3	72
Storage	∞	4

Restriction enzymes were used to make sticky ends of the PCR product for cloning. After restriction digestion, nucleospin clean-up kit from Machery and Nagel was used to purify the product.

7.1.8 ^{32}P- labeling of ssDNA

The ssDNA was labeled with ^{32}P at the 5' end using the enzyme T4 polynucleotide kinase (PNK) for a radioactive binding assay. All reagents (**Table 7-4**) were mixed and incubated at 37°C for 1 hour. The mixture was then desalted using G25 column.

Table 7-4 PCR program for amplication of target site

Reagent	Stock concentration	Volume (µl)	Final
T4 PNK reaction buffer	10 x	2	1 x
ɣ-32P-ATP	10 µCi/µl	1	10 µCi
ssDNA	1 µM	10	10 pmol
T4 PNK	10 U/µl	2	20 U
ddH_20	--	5	--

7.2 Working with bacteria and bacterial plasmids

7.2.1 Preparation of antibiotic stock solution

50 mg/ml Kanamycin antibiotic stock solution in ddH_20 was prepared for LB and LB agar plates. The antibiotic stock solution was aliquoted and stored at -20°C.

7.2.2 LB medium and agar plates

For agar plates, 7.6 g agar and 10 g LB broth were mixed with 500 ml deionized water and autoclaved at 121°C for 15 minutes. After cooling the solution at room temperature, 50 µl Kanamycin antibiotic stock solution was added in 500 ml at a final concentration of 50 µg/ml. The solution was poured into the petri dishes. The plates had been stored at 4°C.

LB medium was prepared by mixing 10 g LB broth with 500 ml deionized water and then autoclaved. The solution has been stored at room temperature. All procedures have been performed under sterile conditions to prevent contamination. The bacterial culture hood was used for the preparation of agar plates.

7.2.3 Transformation of E.coli (Competent cells)

Competent cells were used for transformation of E. coli with EGFP-4X miRNA 125a-5p plasmid. For this purpose, cells were thawed on the ice for 4-5 minutes. 50 ng/µl plasmid DNA or ligated plasmid with the reporter gene was added to 50 µl competent cells. The cells had been incubated on the ice for 30 minutes. Then, the cells were exposed to a heat shock at 42°C for 90 sec. 450 µl ice-cold LB medium was added and the cells were incubated at 37°C at 800 rpm for 1 hour. The mixture was then plated on LB-kanamycin agar plates and incubated at 37°C overnight. The next day, bacterial colonies were picked and placed overnight in the LB medium for plasmid isolation.

7.2.4 Liquid bacterial culture

For the preparation of glycerol stock and isolation of plasmid, 25 ml autoclaved LB medium with 25 µl kanamycin was mixed in 50 ml falcon under sterile condition. One bacterial colony from the LB-kanamycin agar plate was picked with the help of a yellow pipette tip and placed in the falcon. The falcon was placed in the shaking incubator at 37°C and at 150 rpm overnight.

7.2.5 Preparation of bacterial glycerol stock

For long term storage of bacteria, 500 µl of the liquid bacterial culture was mixed with 500 µl of 50% glycerol in a 2 ml screw reaction tube and gently mixed. The reaction tubes were then transferred to the -80°C freezer.

7.2.6 Isolation of plasmid from liquid bacterial culture

Plasmids were isolated from the liquid bacterial culture using the Nucleospin Plasmid kit from Machery and Nagel according to the manufacturer's protocol.

7.2.7 Construction of the reporter gene plasmid

5'-TCACAGGTTAAAGGGTCTCAGGGACTAATCACAGGTTAAAGGGTCTCAGGGACTAATCACAGGTTAAAGGGTCTCAGGGACTAATCACAGGTTAAAGGGTCTCAGGGA-3' target sites have been cloned in the 3'UTR of the pEGFP-N1 plasmid. Briefly, the control pEGFP-N1plasmid was cut using two restriction enzymes NotI and XbaI. 4X miRNA 125a-5p target sites were amplified with these restriction sites. The amplified PCR product was subjected to double digestion with these enzymes to produce the sticky ends (**Table 7-5**). Then, the linearized plasmid and the PCR products with sticky ends were then ligated (1:3) overnight using NEB ligation protocol. Transformation into E.coli was performed the following day and was plated on the agar plates containing kanamycin antibiotic for the selection of positive

colonies. The liquid culture was prepared with a positive colonies and the plasmid was purified. The purified plasmid was sent to the Sanger sequencing for confirmation of the 4X miRNA 125a-5p target site at the 3'UTR of pEGFP-N1.

Table 7-5 Pipetting scheme for double restriction digestion

Reagents	Plasmid volume (µl)	PCR insert Volume (µl)
Restriction Buffer Neb 3.1	2	2
Acetylated BSA 10 µg/µl	0.2	0.2
DNA 1 µg	8.7	8.7
Mix by pipetting		
NotI	0.5	0.5
Xbal	0.5	0.5
Sterile ddH_2O	Upto 20	Upto 20
*Incubate at 37°C for 1 hour. Heat inactivation at 65°C for 15 minutes		

Table 7-6 Pipetting scheme for ligation reaction

Reagents	Volume (µl)
T4 DNA ligase buffer (10X)	2
Linearized plasmid	4
PCR insert	16
Nuclease free water	1.5
T4 DNA ligase	1.5
*Incubate at 17°C overnight. Next day, Heat inactivation at 65°C for 10 minutes	

7.3 Working with mice and cells

7.3.1 Mice

OTI RAG2-/- and C57BL/6J mice have been used in this study. Animals were bred, maintained, and nourished in the central animal facility of the LIMES Institute at the University of Bonn under a specific pathogen-free environment. All experimental procedures and protocols were used in accordance with the local animal guidelines.

7.3.2 Cell culture

All the cell lines and primary cells were handled under a sterile hood using sterile devices and materials. Cells were grown under normal cell culture conditions (37°C, 5% CO_2, 95% humidity). Mycoplasma PCR (Minerva Biolabs) was performed for all cell lines every three months to determine mycoplasma contamination. Cell lines were cultivated for a maximum period of two months and then replaced by a new culture.

7.3.3 Cell lines

THP-1 cells (human monocytes) and J774A.1 cells (mouse macrophages) were kindly provided by Prof. Dr. Albert Haas of the University of Bonn, Germany. THP-1 cells were cultured in RPMI 1640 while J774A.1 cells were cultured in DMEM, high glucose, GlutaMAX™ (ThermoFischer) supplemented with fetal bovine serum (Sigma) 10% at 37°C. THP-1 and J774A.1 cells were maintained in culture by routine passage every 2-3 days and cultivated for a maximum period of two months.

7.3.4 Isolation and cultivation of bone marrow-dervied dendritic cells

After isolation and cultivation, BM-DCs were kindly provided by Dr. Silvana Haβel (AK Mayer) and Dr. Maria Embgenbroich (AK Burgdorf), LIMES Institute Bonn. In brief, wildtype mice were sacrificed to extract the femur and the tibia. The bone cavity was flushed with PBS and the bone marrow cells were filtered through a 40 µm nylon membrane. Cells have been cultivated in DC-medium for 7 days. After 3-4 days, the medium was changed.

7.3.5 Isolation and differentiation of human macrophages

Buffy coats were obtained from the University of Bonn Hospital. IL4, IFN-ɤ, and TPP macrophages were isolated and cultured as described above[109]. In brief, Buffy coat

was cut with scissors on one of the two hoses. Blood was collected in the T175 flask and diluted with DPBS at 1:1. Four falcons were prepared with 35 ml of diluted blood. The pipette was filled with 14 ml ficoll (at room temperature) and the pipette was carefully placed touching the bottom of the falcon. The final volume of each falcon was 49 ml. The density gradient centrifugation was then performed at room temperature for 25 minutes with 615 xg without brake and 9 acceleration. Carefully, the top serum layer had been discarded. The white blood cell ring fraction was carefully transferred to a new 50 ml falcon tube. The volume was adjusted to 50 ml with DPBS and the falcon tubes were rotated 2 x at 200 xg for 10 minutes at room temperature (thrombocyte wash). The supernatant was discarded and the cell pellet was resuspended at a defined volume of MACS buffer or DPBS (20 ml). Cells were counted with dilution of 1:40 (5 µl cell suspension + 195 µl trypan blue). The cell pellet was resuspended in 80 µl per 10^7 cells of MACS buffer (count and calculate- about 1.5 to 3 ml), 200 µl of MACS CD14 microbeads were added, well mixed and incubated in the fridge (4°C) for 15 minutes. The cells have been resuspended with 25 ml MACS buffer. The cells were centrifuged at 6°C for 8 minutes at 300 xg. At the same time, columns have been prepared using 1 LS column per donor. The MidiMACS-Magnet was placed in the cell culture hood and washed to equilibrate the column with 3 ml of the MACS buffer. 30 µm presorting filter was placed on the LS-column and a 50 ml falcon was placed under the LS-column to collect the $CD14^-$ cell fractions. After centrifugation, the supernatant was discarded, and the cell pellet was resuspended in 3 ml MACS buffer. On the separation filter, 3 x 1ml of the suspended cells were filtered. 3 ml of the MACS buffer was added on the remaining cells in the 50 ml falcon to suspend the remaining cells and applied to the filter. The column was washed with 3 ml fresh MACS buffer and the filter was discarded before the final washing step. The column was removed from the magnetic separator for the elution of $CD14^+$ cells. The column was placed on an appropriate collection tube prefilled with 10 ml DPBS, pipette 5 ml of MACS buffer onto the column and $CD14^+$ cells were flushed using the plunger. Then the volume was adjusted up to 50 ml with DPBS. The cells were counted with appropriate dilution with trypan blue (20 µl cell suspension + 80 µl trypan blue).

Monocytes were seeded with the density of $2x10^6$ cells/ml in 6 well NUNC plates (2 ml/well) with VLE RPMI 1640 medium supplemented with 10% FCS. The differentiated scheme has been described in (**Table 7-7**).

After d3, the cells were observed under the microscopy. The cells were scraped and counted. The cells were spun down to 6 minutes at 1200 rpm to discard the old media. The cells were seeded in 6 well NUNC plates (2 ml/well) with VLE RPMI 1640 medium supplemented with 10% FCS and GM-CSF 500 U/ml plus the stimulants described in **Table7-7**.

Table7-7 Differentiation to the baseline macrophages d0 to d3

Cell Phenotype	**Cell number**	**Stimulants**	VLE RPMI 1640 medium+ 10% FCS and GM-CSF 500U/ml
Baseline macrophages	$2x10^6$ cells/ml	GM-CSF 500U/ml	
d3 to d6 differentiation			
IL-4	$2x10^6$ cells/ml	rh IL-4 :1000 U/ml	GM-CSF 500U/ml VLE RPMI 1640 medium+ 10% FCS and GM-CSF 500U/ml
IFN-ϒ	$2x10^6$ cells/ml	IFN : 200 U/ml	
TPP	$2x10^6$ cells/ml	TNFα :800U/ml PGE_2 :1µg/ml Pam_3 :1µg/ml	

7.3.6 Surface markers analysis of differentiated macrophages

The plates **(Section 7.3.5)** were taken out from the incubator, stored at room temperature for 5 minutes and the media was allowed to cool down. The supernatant was pipetted out into a 15 ml falcon and stored on the ice. 1 ml of 2 mM EDTA in DPBS (room temperature) was immediately pipetted to the cells that remained adherent. After 10 minutes, the cells were checked. They were still attached to the plate, but they were round and contracted. The cells were carefully resuspended by pipetting them with 1 ml pipette 3-5 times. The cell fraction was combined with the previous one and stored on the ice. Immediately 2 ml cold DPBS

was added to the remaining cells of the plate and carefully scraped. The scrap cell fractions have been combined and stored on ice. The plate was washed with cold DPBS once or twice. All fractions were combined and the falcon was centrifuged at 4°C for 5 minutes at 280 to 300 xg. The supernatant was discarded and the cell pellet was carefully resuspended in the MACS buffer. The cells suspension was adjusted according to the protocol $1x10^6$ cells/ml in the MACS buffer. In the four FACS tubes, 100 µl of cells suspension was added. The stained and unstained samples proceeded in a parallel manner/fashion. The unspecific antibody binding was blocked by the MACS buffer at 4°C for 20 minutes. The antibody mixture was prepared as described in **Table 7-8.**

Table 7-8 Pipeting scheme for antibody mixture

Antibody	**1X**
CD14	0.1 µl
CD23	0.5 µl
CD25	0.1 µl
CD86	0.1 µl
Mix	=0.8 µl

The cells were stained with an antibody mixture in the fridge for 30 minutes. The cell suspension was washed with 2 ml cold DPBS and centrifuged at 300 xg. The supernatant was discarded and the pellet was resuspended in 200 µl DPBS.

Five FACS tubes were prepared with the compensation beads with 100 µl of MACS buffer. 0.5 µl of each antibody was added. They were also incubated in the fridge for 30 minutes.

7.3.7 Cells binding assays

7.3.7.1 Radioactive binding assay using the Cherenkov protocol

J774A.1 cells were seeded at a density of $0.5x10^5$ in 24 well plates one day before the Cherenkov assay. On the day of the binding assay, the cells were washed with wash buffer (DPBS, 1 mM $MgCl_2$, 1 mM $CaCl_2$) and then incubated with 1 pmol ^{32}P-DNA in 500 µl cells growth medium (DMEM, 10% FCS) for 10 minutes at 37°C. 4x1.5 ml reaction tubes/well was prepared with 500 µl ddH_20. After the incubation time, the supernatant was collected in a 1.5 ml reaction tube (fraction I). The cells were washed twice with 500 µl wash buffer and collected in a 1.5 ml reaction tube (fractions II and III) each time. The cells were carefully detached in the presence of trypsin/EDTA and collected in a 1.5 ml reaction tube (fraction IV). The Cherenkov protocol was used to measure the radioactivity of all the fractions in Liquid scintillation counter WinSpectral (Perkin Elmer).

The percentage of bound 1 pmol ^{32}P-DNA was calculated using the following formula:

$$\%\ bound\ DNA = \left[\frac{fraction\ IV}{fraction\ I + fraction\ II + fraction\ III + fraction\ IV}\right] * 100$$

7.3.7.2 Flow cytometry binding assay

THP-1 cells were counted and resuspended at a density of $4x10^5$ in the FACS tubes. The cells were incubated with ATTO 647N-labeled aptamers diluted in 100 µl cells growth medium (RPMI 1640, 10% FCS) for 10 minutes at 37°C and 5% CO_2. Then 2 ml wash buffer (DPBS, 1 mM $MgCl_2$, 1 mM $CaCl_2$) was added to the FACS tubes. The FACS tubes were centrifuged at 200 xg for 5 minutes and the supernatant was discarded. The cell pellet was resuspended with 1 ml wash buffer and then centrifuged. Approximately 800 µl supernatant was discarded and the remaining buffer was used to measure the percentage of cells bound by DNA. The percentage of cells bound by DNA was measured by BD FACS Canto II and the results were

analyzed by FlowJo software (BD). The binding assay for human baseline macrophages and TPP macrophages were done as explained above for THP-1 cells.

Binding assay for J774A.1 cells was also done as explained above for THP-1 cells, except that $2x10^5$ J774A.1 cells were counted and seeded in 24-well plates one day before the binding assay. On the day of binding assay, cells were washed twice with 500 µl wash buffer. The cells were then incubated with ATTO 647N-labeled aptamers diluted in 200 µl cells growth medium (DMEM, 10%FCS) for 10 minutes at 37°C and 5% CO_2. The cells were scraped and transferred into the FACS tubes containing 2 ml wash buffer. The FACS tubes were centrifuged at 200 xg for 5 minutes and the supernatant was discarded. The cell pellet was resuspended with 1 ml wash buffer and then centrifuged again. Approximately 800 µl supernatant was discarded and the remaining buffer with the cells was used to find the percentage of cells bound by the DNA. The percentage of cells bound by the DNA was measured by BD FACS Canto II and the results were analyzed by the FlowJo software (BD).

The aptamiR 125a-5p binding was determined through a competition binding assay. $8x10^4$ THP-1 cells were counted and resuspended in the FACS tubes. The cells were incubated with 50 nM ATTO 647N-labeled aptamers in the presence and absence of 400 nM competitors at 37°C for 10 minutes. The cells were washed and analyzed as stated above for THP-1.

7.3.8 Confocal microscopy

$2x10^5$ cells were counted and seeded onto coverslips. Coverslips were cleaned with absolute ethanol and dried before being placed in a 12-well plate. Cells have been incubated for one day under standard cell culture conditions. Next day, the cells were washed with wash buffer (DPBS, 1 mM $MgCl_2$, 1 mM $CaCl_2$) and followed by incubation with 250 nM ATTO 647N-labeled DC12, DC 12.53 and their respective controls at 37°C for 10 minutes. The cells were washed three times with wash buffer

and subsequently washed once with 1 ml DPBS. Then the cells were fixed by using 4% paraformaldehyde diluted in DPBS at 4°C for 30 minutes. The cells were then washed thrice with DPBS and the membranes were stained with WGA-Alexa fluor 488 (100 µg/ml in 500 µl DPBS) for 10 minutes. The cells were washed again thrice and finally, the nuclei were stained with 1:1000 (1 mg/ml) DAPI in DPBS for 5 minutes and washed thrice with DPBS, once with 2 ml ddH_2O. The coverslips were carefully mounted onto the slides with the fluorogel mounting medium. The slides were placed in the dark overnight at room temperature and on following day microscopy data of the slides were acquired using LSM 710 confocal laser scanning microscopy (Zeiss).

7.3.9 Cell transfection

7.3.9.1 Transient transfection of reporter gene plasmid with miRNA 125a-5p mimic and control mimic

J774A.1 cells were transiently transfected with 500 ng of the control pEGFP-N1 plasmid (CP) and EGFP-4X 125a-5p plasmid (4X 125a-5p) with different concentration of miRNA 125a-5p mimic (miRNA 125a-5p mimic, Sigma-Aldrich) and control miRNA mimic (miRNA negative control 1, Sigma-Aldrich). Briefly, $1x10^5$ cells were plated one day before the transfection in 24-well plate. On the day of the transfection, two reaction mixtures were prepared separately and mixed together.

Mixture A: 500 ng CP and 4X 125a-5p plasmids with the different concentrations of miRNA mimic and control mimic were diluted in Opti-MEM, respectively.

Mixture B: In a second reaction tube, the same volume of Opti-MEM was supplemented with 1.5 µl lipofectamine 2000 (transfection agent) and incubated at room temperature for 5 minutes.

Then mixture A and mixture B were mixed and incubated for another 20 minutes according to the manufacturer protocol. The cells were washed with DPBS once and replaced with fresh medium. After the incubation period, the mixture was slowly transferred into wells for 24 hours. After 24 hours, the cells were scraped and

washed with 1 ml DPBS in the FACS tubes. The supernatant was discarded and the MFI of the cells ($1x10^5$ cells) was measured in flow cytometry using FITC-A channel for the EGFP.

7.3.10 Generation of stable cell line J774A.1 miRNA 125a-5p

7.3.10.1 Stable transfection of EGFP-4X 125a-5p plasmid

Stable cell line J774A.1 miRNA 125a-5p was generated with permanent integration of the EGFP-4X 125a-5p plasmid. For that 2 µg of the plasmid was transiently transfected with lipofectamine 2000 according to the manufacturer protocol as described in the transient transfection section above (**Section 7.3.9.1**). After 2 days, the positive cells selection of EGFP-4X 125a-5p plasmid was started by adding 300 µg/ml G418 to the cell culture medium. After four weeks of the positive selection, the surviving cells were used for the isolation of monoclonal cell lines. As a control, EGFP plasmid without target sites has also been transiently transfected as for EGFP-4X 125a-5p plasmid.

7.3.10.2 Isolation of monoclonal cells

Surviving cells from the stable transfected EGFP-4X 125a-5p plasmid (**Section 7.3.10.1**) showed fluorescence compared to untransfected J774A.1 cells. Cell sorting was performed using a flow cytometer with cell sorting function (BD FACS-Aria, Flow cytometry core facility, University of Bonn). The cells were individually placed on a 96-well plate for both the control and the EGFP-4X 125a-5p plasmid. 96-well plates were placed in an incubator with standard cell culture conditions for two weeks. After two weeks, each well was observed under a fluorescence microscopy for cell growth and cell fluorescence. Cells that grew in monolayer with 80-90% confluency and had fluorescence were transferred into 24-well plates. Then these cells were placed in T25 flask when they showed 80-90% confluency in 12-

well and 6-well plates. These cells were maintained in the culture with DMEM, 10% FCS and 300 µg/ml G418. They were cultivated for a period of not more than 2 months and with a passage after every 2-3 days.

7.3.11 Transfection of the stable cell line J774A.1 miRNA 125a-5p with antagomir 125a-5p

Stable cell line J774A.1 miRNA 125a-5p cells and control stable cell line were transfected with different concentrations of antagomir 125a-5p (Ella-Biotech) and control antagomir (Ella-Biotech). Briefly, $4x10^4$ cells were plated in a 24-well plate one day before the transfection. On the day of the transfection, two reaction mixtures were prepared separately and then mixed together.

Mixture A: Different concentrations of antagomir 125a-5p and control antagomir were diluted in Opti-MEM, respectively.

Mixture B: In a second reaction tube, the same volume of Opti-MEM was supplemented with 1.5 µl lipofectamine 2000 (transfection agent) and incubated for 5 minutes.

Then, mixture A and mixture B were mixed and incubated for another 20 minutes according to the manufacturer protocol. The cells were washed once with DPBS and replaced with 300 µl Opti-MEM. After the incubation period, the mixture was slowly transferred into the wells for 4 hours. After 4 hours, the Opti-MEM was replaced with fresh medium (DMEM, 10% FCS) for the next 48 hours. The cells were scraped and washed with 1 ml DPBS in FACS tubes. The supernatant was discarded and the MFI of the cells was measured in the flow cytometry using the FITC-A channel for the EGFP.

In aptamiR 125a-5p transfection, 50 nM concentration of the aptamiR was prepared in a manner similar to mixture A preparation.

7.3.12 Antagomir and peptide delivery assays

7.3.12.1 Aptamer-targeted delivery of antagomir 125a-5p

Stable cell line J774A.1 miRNA 125a-5p cells were treated with aptamiR 125a-5p. Briefly, $4x10^4$cells were plated in a 24-well plate one day before treatment. On the day of treatment, the cells were washed once with DPBS and replaced with 200 µl DMEM medium containing 10% FCS and 500 nM aptamiR 125a-5p for four hours. Subsequently, the medium was replaced with fresh medium (DMEM, 10% FCS) for the next 48 hours. The cells were scraped and washed with 1 ml DPBS in FACS tubes. The supernatant was discarded and the MFI of the cells was measured in flow cytometry using the FITC-A channel for EGFP. As a positive control, cells were transfected as described in **Section 7.3.11** for aptamiR 125a-5p.

For human baseline macrophage treatment, CD14+ monocytes have been differentiated into human baseline macrophages as described in **Section 7.3.5**. After 3 days, $4x10^6$ cells were counted and treated with aptamiR 125a-5p, control aptamers for 30 minutes. Then, the medium was replaced by fresh medium containing TPP stimulants. As a positive control, untreated cells, IL-4, and IFN-ɤ macrophages have also been differentiated for the next three days **(Section 7.3.5)**. After 72 hours, the profiles of the cell surface markers were determined through flow cytometry as described in **Section 7.3.6**.

7.3.12.2 *In vitro* proliferation assay

Dr. Silvana Haβel (AK Mayer), University of Bonn, Germany, performed *In vitro* proliferation assay. Briefly, $5x10^4$ BM-DCs were counted and seeded in 96-well plates and incubated for one hour under standard cell culture conditions. OT-I T cells (OVA-specific CD8 T cells) have been isolated from spleen and incubated with 1 µM CFSE in PBS at 37°C for 15 minutes. The T cells were washed thrice with cold PBS at 4°C and centrifuged. In the meantime, MHC I peptide, aptamer-peptide conjugates, and OT-I peptides were diluted in DC-medium and added to the BM-DCs, incubated at 37°C for 10 minutes. Subsequently, the supernatants from BM-

DCs were removed and $1x10^5$ OT-I T cells in 100 µl T cell medium was added. Cells were incubated for 24 hours. After 24 hours, 200 µl T cell medium was added per well and incubated for another 48 hours. The T cells were stained with an anti-CD8 alpha antibody conjugated with fluorophore and analyzed with flow cytometry. The anti-CD8 antibody was diluted 1:400 in the FACS buffer supplemented with mouse serum 1:100.

7.3.13 Statistical Analysis

The flow cytometry data was analyzed using FlowJo software (TreeStar, USA). All results were presented as mean ± SD, as described in tables and figures legends using GraphPad prism 5 (GraphPad Software, San Diego, USA).

8 References

1 Krüger, A., Zimbres, F., Kronenberger, T. & Wrenger, C. Molecular Modeling Applied to Nucleic Acid-Based Molecule Development. *Biomolecules* 8, 83-100 (2018).

2 Zhou, J. & Rossi, J. Aptamers as targeted therapeutics: Current potential and challenges. *Nat Rev Drug Discov* 16, 181-202 (2016).

3 Wolter, O. & Mayer, G. Aptamers as valuable molecular tools in neurosciences. *J Neurosci* 37, 2517-2523 (2017).

4 Kong, H. Y. & Byun, J. Nucleic Acid aptamers: new methods for selection, stabilization, and application in biomedical science. *Biomol Ther (Seoul)* 21, 423-434, doi:10.4062/biomolther.2013.085 (2013).

5 Ellington, A. D. & Szostak, J. W. In vitro selection of RNA molecules that bind specific ligands. *Nature* 346, 818-822 (1990).

6 Tuerk, C. & Gold, L. Systematic evolution of ligands by exponential enrichment: RNA ligands to bacteriophage T4 DNA polymerase. *Science* 249, 505-510 (1990).

7 Robertson, D. L. & Joyce, G. F. Selection in vitro of an RNA enzyme that specifically cleaves single-stranded DNA. *Nature* 344, 467-468 (1990).

8 Raddatz, M. S. L. *et al.* Enrichment of cell-targeting and population-specific aptamers by fluorescence-activated cell sorting. *Angew Chem Int Ed* 47, 5190-5193 (2008).

9 Hamedani, N. S. *et al.* Capture and Release (CaR): a simplified procedure for one-tube isolation and concentration of single-stranded DNA during SELEX. *Chem Commun* 51, 1135-1138 (2015).

10 Rhie, A. *et al.* Characterization of 2′-fluoro-RNA aptamers that bind preferentially to disease-associated conformations of prion protein and inhibit conversion. *J Biol Chem* 278, 39697-39705 (2003).

11 Darmostuk, M., Rimpelova, S., Gbelcova, H. & Ruml, T. Current approaches in SELEX: An update to aptamer selection technology. *Biotechnol Adv* 33, 1141-1161 (2015).

12 Dua, P., Kim, S. & Lee, D. K. Nucleic acid aptamers targeting cell-surface proteins. *Methods* 54, 215-225, doi:10.1016/j.ymeth.2011.02.002 (2011).

13 Chen, M. *et al.* Development of Cell-SELEX Technology and Its Application in Cancer Diagnosis and Therapy. *Int J Mol Sci* 17, E2079, doi:10.3390/ijms17122079 (2016).

14 Morris, K. N. *et al.* High affinity ligands from in vitro selection: complex targets. *Proc Natl Acad Sci U S A* 95, 2902-2907 (1998).

15 Sefah, K. *et al.* Development of DNA aptamers using Cell-SELEX. *Nat Protoc* 5, 1169-1185, doi:10.1038/nprot.2010.66 (2010).

16 Morita, Y. *et al.* Aptamer Therapeutics in Cancer: Current and Future. *Cancers (Basel)* 10, E80, doi:10.3390/cancers10030080 (2018).

17 Tang, Z. *et al.* Generating aptamers for recognition of virus-infected cells. *Clin Chem* 55, 813-822 (2009).

18 Hamula, C. L., Le, X. C. & Li, X.-F. DNA aptamers binding to multiple prevalent M-types of Streptococcus pyogenes. *Anal Chem* 83, 3640-3647 (2011).

19 Mercier, M.-C., Dontenwill, M. & Choulier, L. Selection of nucleic acid aptamers targeting tumor cell-surface protein biomarkers. *Cancers (Basel)* 9, E69 (2017).

20 Pei, X., Zhang, J. & Liu, J. Clinical applications of nucleic acid aptamers in cancer. *Mol Clin Oncol* 2, 341-348, doi:10.3892/mco.2014.255 (2014).

21 Xiang, D. *et al.* Superior Performance of Aptamer in Tumor Penetration over Antibody: Implication of Aptamer-Based Theranostics in Solid Tumors. *Theranostics* 5, 1083-1097, doi:10.7150/thno.11711 (2015).

22 Hicke, B. J. *et al.* Tumor targeting by an aptamer. *J Nucl Med* 47, 668-678 (2006).

23 Xiang, D. *et al.* Nucleic acid aptamer-guided cancer therapeutics and diagnostics: the next generation of cancer medicine. *Theranostics* 5, 23-42, doi:10.7150/thno.10202 (2015).

24 Gopinath, S. C. *et al.* Cell-targeting aptamers act as intracellular delivery vehicles. *Appl Microbiol Biotechnol* 100, 6955-6969, doi:10.1007/s00253-016-7686-2 (2016).

25 Thiel, K. W. & Giangrande, P. H. Intracellular delivery of RNA-based therapeutics using aptamers. *Ther Deliv* 1, 849-861, doi:10.4155/tde.10.61 (2010).

26 Chu, T. C. *et al.* Aptamer: toxin conjugates that specifically target prostate tumor cells. *Cancer Res* 66, 5989-5992 (2006).

27 Kim, M. W. *et al.* Cancer-targeted nucleic acid delivery and quantum dot imaging using EGF receptor aptamer-conjugated lipid nanoparticles. *Sci Rep* 7, 9474 (2017).

28 Pofahl, M., Wengel, J. & Mayer, G. Multifunctional nucleic acids for tumor cell treatment. *Nucleic Acid Ther* 24, 171-177 (2014).

29 Xiang, D. *et al.* Transforming doxorubicin into a cancer stem cell killer via EpCAM aptamer-mediated delivery. *Theranostics* 7, 4071 (2017).

30 Mayer, G., Pofahl, M., Schöler, K. M. & Haßel, S. Cell-Specific Aptamers for Nano-medical Applications. *Nucleic Acid Nanotechnology* 2014, 261-283 (2014).

31 Iaboni, M. *et al.* Aptamer-miRNA-212 Conjugate Sensitizes NSCLC Cells to TRAIL. *Mol Ther Nucleic Acids* 5, e289, doi:10.1038/mtna.2016.5 (2016).

32 Esposito, C. L. *et al.* Multifunctional Aptamer-miRNA Conjugates for Targeted Cancer Therapy. *Mol Ther* 22, 1151-1163, doi:10.1038/mt.2014.5 (2014).

33 Dassie, J. P. *et al.* Systemic administration of optimized aptamer-siRNA chimeras promotes regression of PSMA-expressing tumors. *Nat Biotechnol* 27, 839 (2009).

34 Wu, X. *et al.* Second-generation aptamer-conjugated PSMA-targeted delivery system for prostate cancer therapy. *Int J Nanomedicine* 6, 1747-1756, doi:10.2147/ijn.s23747 (2011).

35 Lai, W. Y. *et al.* Synergistic inhibition of lung cancer cell invasion, tumor growth and angiogenesis using aptamer-siRNA chimeras. *Biomaterials* 35, 2905-2914, doi:10.1016/j.biomaterials.2013.12.054 (2014).

36 Subramanian, N. *et al.* EpCAM aptamer-siRNA chimera targets and regress epithelial cancer. *PLoS One* 10, e0132407 (2015).

37 Dai, F. *et al.* The anti-chemoresistant effect and mechanism of MUC1 aptamer-miR-29b chimera in ovarian cancer. *Gynecol Oncol* 131, 451-459, doi:10.1016/j.ygyno.2013.07.112 (2013).

38 Rohde, J.-H., Weigand, J. E., Suess, B. & Dimmeler, S. A universal aptamer chimera for the delivery of functional microRNA-126. *Nucleic Acid Ther* 25, 141-151 (2015).

39 Yu, X. *et al.* Targeting EGFR/HER2/HER3 with a Three-in-One Aptamer-siRNA Chimera Confers Superior Activity against HER2+ Breast Cancer. *Mol Ther Nucleic Acids* 10, 317-330 (2018).

40 Zhu, Q., Shibata, T., Kabashima, T. & Kai, M. Inhibition of HIV-1 protease expression in T cells owing to DNA aptamer-mediated specific delivery of siRNA. *Eur J Med Chem* 56, 396-399 (2012).

41 Hu, P. P. Recent Advances in Aptamers Targeting Immune System. *Inflammation* 40, 295-302, doi:10.1007/s10753-016-0437-9 (2017).

42 Soldevilla, M. M., Villanueva, H. & Pastor, F. Aptamers: A Feasible Technology in Cancer Immunotherapy. *J Immunol Res* 2016, 1083738-1083738, doi:10.1155/2016/1083738 (2016).

43 Berezhnoy, A. *et al.* Aptamer-targeted inhibition of mTOR in T cells enhances antitumor immunity. *J Clin Invest* 124, 188-197, doi:10.1172/JCI69856 (2014).

44 McNamara, J. O. *et al.* Multivalent 4-1BB binding aptamers costimulate CD8+ T cells and inhibit tumor growth in mice. *J Clin Invest* 118, 376-386, doi:10.1172/JCI33365 (2008).

45 Song, P. *et al.* CD4 aptamer-RORγt shRNA chimera inhibits IL-17 synthesis by human CD4(+) T cells. *Biochem Biophys Res Commun* 452, 1040-1045, doi:10.1016/j.bbrc.2014.09.037 (2014).

46 Chow, A., Brown, B. D. & Merad, M. Studying the mononuclear phagocyte system in the molecular age. *Nat Rev Immunol* 11, 788 (2011).

47 Guilliams, M. *et al.* Dendritic cells, monocytes and macrophages: a unified nomenclature based on ontogeny. *Nat Rev Immunol* 14, 571 (2014).

48 Hume, D. A. Differentiation and heterogeneity in the mononuclear phagocyte system. *Mucosal Immunol* 1, 432-441, doi:10.1038/mi.2008.36 (2008).

49 Varol, C. *et al.* Monocytes give rise to mucosal, but not splenic, conventional dendritic cells. *J Exp Med* 204, 171-180 (2007).

50 Lee, J. *et al.* Restricted dendritic cell and monocyte progenitors in human cord blood and bone marrow. *J Exp Med* 212, 385-399 (2015).

51 Chiu, S. & Bharat, A. Role of monocytes and macrophages in regulating immune response following lung transplantation. *Curr Opin Organ Transplant* 21, 239-245, doi:10.1097/MOT.0000000000000313 (2016).

52 Boyette, L. B. *et al.* Phenotype, function, and differentiation potential of human monocyte subsets. *PLoS One* 12, e0176460 (2017).

53 Patel, A. A. *et al.* The fate and lifespan of human monocyte subsets in steady state and systemic inflammation. *J Exp Med* 214, 1913-1923 (2017).

55 Ziegler-Heitbrock, L. *et al.* Nomenclature of monocytes and dendritic cells in blood. *Blood* 116, e74-80 (2010).

56 Wong, K. L. *et al.* Gene expression profiling reveals the defining features of the classical, intermediate and nonclassical human monocyte subsets. *Blood* 118, e16-31 (2011).

57 Geissmann, F., Jung, S. & Littman, D. R. Blood monocytes consist of two principal subsets with distinct migratory properties. *Immunity* 19, 71-82 (2003).

58 Tacke, F. & Randolph, G. J. Migratory fate and differentiation of blood monocyte subsets. *Immunobiology* 211, 609-618, doi:10.1016/j.imbio.2006.05.025 (2006).

59 Ghattas, A. *et al.* Monocytes in coronary artery disease and atherosclerosis: where are we now? *J Am Coll Cardiol* 62, 1541-1551 (2013).

60 Carlin, L. M. *et al.* Nr4a1-dependent Ly6C(low) monocytes monitor endothelial cells and orchestrate their disposal. *Cell* 153, 362-375, doi:10.1016/j.cell.2013.03.010 (2013).

61 Auffray, C. *et al.* Monitoring of blood vessels and tissues by a population of monocytes with patrolling behavior. *Science* 317, 666-670, doi:10.1126/science.1142883 (2007).

62 Cros, J. *et al.* Human CD14dim monocytes patrol and sense nucleic acids and viruses via TLR7 and TLR8 receptors. *Immunity* 33, 375-386, doi:10.1016/j.immuni.2010.08.012 (2010).

63 Thomas, G., Tacke, R., Hedrick, C. C. & Hanna, R. N. Nonclassical patrolling monocyte function in the vasculature. *Arterioscler Thromb Vasc Biol* 35, 1306-1316, doi:10.1161/ATVBAHA.114.304650 (2015).

64 Lavoie, P. M. & Levy, O. Mononuclear phagocyte system. *Fetal and Neonatal Physiology (Fifth Edition): Elsevier* 2017, 1208-1216 (2017).

65 Steinman, R. M. & Cohn, Z. A. Identification of a novel cell type in peripheral lymphoid organs of mice: I. Morphology, quantitation, tissue distribution. *J Exp Med* 137, 1142-1162 (1973).

66 Banchereau, J. & Steinman, R. M. Dendritic cells and the control of immunity. *Nature* 392, 245-252 (1998).

67 Van Brussel, I., Berneman, Z. N. & Cools, N. Optimizing dendritic cell-based immunotherapy: tackling the complexity of different arms of the immune system. *Mediators Inflamm* 2012, doi: 10.1155/2012/690643 (2012).

68 Banchereau, J. *et al.* Immunobiology of dendritic cells. *Annu Rev Immunol* 18, 767-811 (2000).

69 Granucci, F., Zanoni, I. & Ricciardi-Castagnoli, P. Central role of dendritic cells in the regulation and deregulation of immune responses. *Cell Mol Life Sci* 65, 1683-1697 (2008).

70 Steinman, R. M. & Banchereau, J. Taking dendritic cells into medicine. *Nature* 449, 419-426 (2007).

71 Merad, M. *et al.* The dendritic cell lineage: ontogeny and function of dendritic cells and their subsets in the steady state and the inflamed setting. *Annu Rev Immunol* 31, 563-604, doi:10.1146/annurev-immunol-020711-074950 (2013).

72 Constantino, J. *et al.* Dendritic cell-based immunotherapy: a basic review and recent advances. *Immunol Res* 65, 798-810 (2017).

73 Palucka, K. & Banchereau, J. Cancer immunotherapy via dendritic cells. *Nat Rev Cancer* 12, 265-277 (2012).

74 Borghaei, H., Smith, M. R. & Campbell, K. S. Immunotherapy of cancer. *Eur J Pharmacol* 625, 41-54 (2009).

75 Boudreau, J. E., Bonehill, A., Thielemans, K. & Wan, Y. Engineering dendritic cells to enhance cancer immunotherapy. *Mol Ther* 19, 841-853 (2011).

76 Joffre, O. P., Segura, E., Savina, A. & Amigorena, S. Cross-presentation by dendritic cells. *Nat Rev Immunol* 12, 557-569 (2012).

77 Banchereau, J. & Steinman, R. M. Dendritic cells and the control of immunity. *Nature* 392, 245-252, doi:10.1038/32588 (1998).

78 Wu, L. & Dakic, A. Development of dendritic cell system. *Cell Mol Immunol* 1, 112-118 (2004).

79 Romani, N. *et al.* Proliferating dendritic cell progenitors in human blood. *J Exp Med* 180, 83-93 (1994).

80 Hinrichs, C. S. & Rosenberg, S. A. Exploiting the curative potential of adoptive T-cell therapy for cancer. *Immunol Rev* 257, 56-71, doi:10.1111/imr.12132 (2014).

81 Kazemi, T., Younesi, V., Jadidi-Niaragh, F. & Yousefi, M. Immunotherapeutic approaches for cancer therapy: An updated review. *Artif Cells Nanomed Biotechnol* 44, 769-779, doi:10.3109/21691401.2015.1019669 (2016).

82 Chen, P. *et al.* Dendritic cell targeted vaccines: Recent progresses and challenges. *Hum Vaccin Immunother* 12, 612-622, doi:10.1080/21645515.2015.1105415 (2015).

83 Palucka, K., Ueno, H., Fay, J. & Banchereau, J. Harnessing dendritic cells to generate cancer vaccines. *Ann N Y Acad Sci* 1174, 88-98, doi:10.1111/j.1749-6632.2009.05000.x (2009).

84 Palucka, K. & Banchereau, J. Cancer immunotherapy via dendritic cells. *Nat Rev Cancer* 12, 265-277, doi:10.1038/nrc3258 (2012).

85 Shang, N. *et al.* Dendritic cells based immunotherapy. *Am J Cancer Res* 7, 2091-2102 (2017).

86 Wesley, J. D., Whitmore, J., Trager, J. & Sheikh, N. An overview of sipuleucel-T: autologous cellular immunotherapy for prostate cancer. *Hum Vaccin Immunother* 8, 520-527, doi:10.4161/hv.18769 (2012).

87 Kantoff, P. W. *et al.* Sipuleucel-T immunotherapy for castration-resistant prostate cancer. *N Engl J Med* 363, 411-422, doi:10.1056/NEJMoa1001294 (2010).

88 Mulders, P. F., De Santis, M., Powles, T. & Fizazi, K. Targeted treatment of metastatic castration-resistant prostate cancer with sipuleucel-T immunotherapy. *Cancer Immunol Immunother* 64, 655-663, doi:10.1007/s00262-015-1707-3 (2015).

89 Pizzurro, G. A. & Barrio, M. M. Dendritic cell-based vaccine efficacy: aiming for hot spots. *Front Immunol* 6, 91, doi: 10.3389/fimmu.2015.00091, (2015).

90 Macri, C., Dumont, C., Johnston, A. P. & Mintern, J. D. Targeting dendritic cells: a promising strategy to improve vaccine effectiveness. *Clin Transl Immunology* 5, e66-e66, doi:10.1038/cti.2016.6 (2016).

91 Saluja, S. S. *et al.* Targeting human dendritic cells via DEC-205 using PLGA nanoparticles leads to enhanced cross-presentation of a melanoma-associated antigen.
Int J Nanomedicine 9, 5231-5246 (2014).

92 Thomann, J.-S. *et al.* Antitumor activity of liposomal ErbB2/HER2 epitope peptide-based vaccine constructs incorporating TLR agonists and mannose receptor targeting. *Biomaterials* 32, 4574-4583 (2011).

93 Flynn, B. J. *et al.* Immunization with HIV Gag targeted to dendritic cells followed by recombinant New York vaccinia virus induces robust T-cell immunity in nonhuman primates. *Proc Natl Acad Sci U S A* 108, 7131-7136, doi: 10.1073/pnas.1103869108 (2011).

94 Hartung, E. *et al.* Induction of potent CD8 T cell cytotoxicity by specific targeting of antigen to cross-presenting dendritic cells in vivo via murine or human XCR1. *J Immunol* 194, 1069-1079 (2015).

95 Rosalia, R. A. *et al.* Dendritic cells process synthetic long peptides better than whole protein, improving antigen presentation and T-cell activation. *Eur J Immunol* 43, 2554-2565 (2013).

96 Vingert, B. *et al.* The Shiga toxin B-subunit targets antigen in vivo to dendritic cells and elicits anti-tumor immunity. *Eur J Immunol* 36, 1124-1135 (2006).

97 Kreutz, M., Tacken, P. J. & Figdor, C. G. Targeting dendritic cells: why bother? *Blood* 121, 2836-2844 (2013).

98 Gangadhar, T. C. & Vonderheide, R. H. Mitigating the toxic effects of anticancer immunotherapy. *Nat Rev Clin Oncol* 11, 91-99 (2014).

99 Gilboa, E., McNamara, J. & Pastor, F. Use of oligonucleotide aptamer ligands to modulate the function of immune receptors. *Clin Cancer Res* 19, 1054-1062 (2013).

100 Nimjee, S. M., Rusconi, C. P. & Sullenger, B. A. Aptamers: an emerging class of therapeutics. *Annu Rev Med* 56, 555-583 (2005).

101 Lehmann, C. *et al.* Direct delivery of antigens to dendritic cells via antibodies specific for endocytic receptors as a promising strategy for future therapies. *Vaccines* 4, 8, doi: 10.3390/vaccines4020008 (2016).

102 Haßel, S. K. Aptamers for targeted activation of T cell-mediated immunity. *Universitäts-und Landesbibliothek Bonn* (2016).

103 Gordon, S. & Martinez, F. O. Alternative activation of macrophages: mechanism and functions. *Immunity* 32, 593-604 (2010).

104 Sica, A. & Mantovani, A. Macrophage plasticity and polarization: in vivo veritas. *J Clin Invest* 122, 787-795 (2012).

105 Fujiwara, N. & Kobayashi, K. Macrophages in inflammation. *Curr Drug Targets Inflamm Allergy* 4, 281-286 (2005).

106 Hirayama, D., Iida, T. & Nakase, H. The Phagocytic Function of Macrophage-Enforcing Innate Immunity and Tissue Homeostasis. *Int J Mol Sci* 19, E92, doi:10.3390/ijms19010092 (2017).

107 Gordon, S. & Martinez-Pomares, L. Physiological roles of macrophages. *Pflugers Arch* 469, 365-374, doi:10.1007/s00424-017-1945-7 (2017).

108 Mosser, D. M. & Edwards, J. P. Exploring the full spectrum of macrophage activation. *Nat Rev Immunol* 8, 958-969, doi:10.1038/nri2448 (2008).

109 Schultze, J. L., Freeman, T., Hume, D. A. & Latz, E., editors. A transcriptional perspective on human macrophage biology. *Semin Immunol* 27, 44-50 (2015).

110 Gregory, C. D. & Devitt, A. The macrophage and the apoptotic cell: an innate immune interaction viewed simplistically? *Immunology* 113, 1-14, doi:10.1111/j.1365-2567.2004.01959.x (2004).

111 Martinez, F. O. & Gordon, S. The M1 and M2 paradigm of macrophage activation: time for reassessment. *F1000prime Rep* 6, 13-13, doi:10.12703/P6-13 (2014).

112 Biswas, S. K. & Mantovani, A. Macrophage plasticity and interaction with lymphocyte subsets: cancer as a paradigm. *Nat Immunol* 11, 889-896 (2010).

113 Mosmann, T. R. *et al.* Two types of murine helper T cell clone. I. Definition according to profiles of lymphokine activities and secreted proteins. *J Immunol* 136, 2348-2357 (1986).

114 Perkel, J. M. Distinguishing Th1 and Th2 Cells. *The Scientist* 15, 22-22 (2001).

115 Xue, J. *et al.* Transcriptome-based network analysis reveals a spectrum model of human macrophage activation. *Immunity* 40, 274-288 (2014).

116 O'shea, J. J. & Murray, P. J. Cytokine signaling modules in inflammatory responses. *Immunity* 28, 477-487 (2008).

117 Gordon, S. & Taylor, P. R. Monocyte and macrophage heterogeneity. *Nat Rev Immunol* 5, 953-964 (2005).

118 Martinez, F. O., Sica, A., Mantovani, A. & Locati, M. Macrophage activation and polarization. *Front Biosci* 13, 453-461 (2008).

119 Kielian, T. L. & Blecha, F. CD14 and other recognition molecules for lipopolysaccharide: a review. *Immunopharmacology* 29, 187-205 (1995).

120 Weinstein, S. L., June, C. & DeFranco, A. Lipopolysaccharide-induced protein tyrosine phosphorylation in human macrophages is mediated by CD14. *J Immunol* 151, 3829-3838 (1993).

121 Meng, F. & Lowell, C. A. Lipopolysaccharide (LPS)-induced macrophage activation and signal transduction in the absence of Src-family kinases Hck, Fgr, and Lyn. *J Exp Med* 185, 1661-1670 (1997).

122 Shi, C. & Pamer, E. G. Monocyte recruitment during infection and inflammation. *Nat Rev Immunol* 11, 762-774 (2011).

123 Gratchev, A. *et al.* Alternatively activated macrophages differentially express fibronectin and its splice variants and the extracellular matrix protein βIG-H3. *Scand J Immunol* 53, 386-392 (2001).

124 Mosser, D. M. The many faces of macrophage activation. *J Leukoc Biol* 73, 209-212 (2003).

125 Chinetti-Gbaguidi, G. & Staels, B. Macrophage polarization in metabolic disorders: functions and regulation. *Curr Opin Lipidol* 22, 365-372, doi:10.1097/MOL.0b013e32834a77b4 (2011).

125 Ponzoni, M. *et al.* Targeting Macrophages as a Potential Therapeutic Intervention: Impact on Inflammatory Diseases and Cancer. *Int J Mol Sci* 19, E1953, doi:10.3390/ijms19071953 (2018).

126 Schultze, J. L., Schmieder, A. & Goerdt, S. Macrophage activation in human diseases. *Semin Immunol* 27, 249-256, (2015).

127 Wynn, T. A., Chawla, A. & Pollard, J. W. Macrophage biology in development, homeostasis and disease. *Nature* 496, 445-455 (2013).

128 Schultze, J. L. Reprogramming of macrophages—new opportunities for therapeutic targeting. *Curr Opin Pharmacol* 26, 10-15 (2016).

129 Mantovani, A., Vecchi, A. & Allavena, P. Pharmacological modulation of monocytes and macrophages. *Curr Opin Pharmacol* 17, 38-44 (2014).

130 Ries, C. H., Hoves, S., Cannarile, M. A. & Ruettinger, D. CSF-1/CSF-1R targeting agents in clinical development for cancer therapy. *Curr Opin Pharmacol* 23, 45-51 (2015).

131 Patel, S. K. & Janjic, J. M. Macrophage targeted theranostics as personalized nanomedicine strategies for inflammatory diseases. *Theranostics* 5, 150-172 (2015).

132 Suzuki, T. *et al.* Pulmonary macrophage transplantation therapy. *Nature* 514, 450-454 (2014).

133 Ries, C. H. *et al.* Targeting tumor-associated macrophages with anti-CSF-1R antibody reveals a strategy for cancer therapy. *Cancer Cell* 25, 846-859, doi:10.1016/j.ccr.2014.05.016 (2014).

134 Papadopoulos, K. P. *et al.* First-in-Human Study of AMG 820, a Monoclonal Anti-Colony-Stimulating Factor 1 Receptor Antibody, in Patients with Advanced Solid Tumors. *Clin Cancer Res* 23, 5703-5710, doi:10.1158/1078-0432.ccr-16-3261 (2017).

135 Purnama, C. *et al.* Transient ablation of alveolar macrophages leads to massive pathology of influenza infection without affecting cellular adaptive immunity. *Eur J Immunol* 44, 2003-2012 (2014).

136 Poh, A. R. & Ernst, M. Targeting Macrophages in Cancer: From Bench to Bedside. *Front Oncol* 8, 49-49, doi:10.3389/fonc.2018.00049 (2018).

137 Gutiérrez-González, A. *et al.* Evaluation of the potential therapeutic benefits of macrophage reprogramming in multiple myeloma. *Blood* 128, 2241-2252 (2016).

138 Mantovani, A. *et al.* Tumour-associated macrophages as treatment targets in oncology. *Nat Rev Clin Oncol* 14, 399-416 (2017).

139 Aras, S. & Zaidi, M. R. TAMeless traitors: macrophages in cancer progression and metastasis. *Br J Cancer* 117, 1583-1591 (2017).

140 Song, M. *et al.* Bioconjugated Manganese Dioxide Nanoparticles Enhance Chemotherapy Response by Priming Tumor-Associated Macrophages toward M1-like Phenotype and Attenuating Tumor Hypoxia. *ACS Nano* 10, 633-647, doi:10.1021/acsnano.5b06779 (2016).

141 Panni, R. Z., Linehan, D. C. & DeNardo, D. G. Targeting tumor-infiltrating macrophages to combat cancer. *Immunotherapy* 5, 1075-1087, doi:10.2217/imt.13.102 (2013).

142 Teng, K. Y. *et al.* Blocking the CCL2-CCR2 Axis Using CCL2-Neutralizing Antibody Is an Effective Therapy for Hepatocellular Cancer in a Mouse Model. *Mol Cancer Ther* 16, 312-322, doi:10.1158/1535-7163.mct-16-0124 (2017).

143 Arakaki, R. *et al.* CCL2 as a potential therapeutic target for clear cell renal cell carcinoma. *Cancer Med* 5, 2920-2933, doi:10.1002/cam4.886 (2016).

144 Bonapace, L. *et al.* Cessation of CCL2 inhibition accelerates breast cancer metastasis by promoting angiogenesis. *Nature* 515, 130-133, doi:10.1038/nature13862 (2014).

145 Wong, D., Kandagatla, P., Korz, W. & Chinni, S. R. Targeting CXCR4 with CTCE-9908 inhibits prostate tumor metastasis. *BMC Urol* 14, 12-12, doi:10.1186/1471-2490-14-12 (2014).

146 Huang, E. H. *et al.* A CXCR4 antagonist CTCE-9908 inhibits primary tumor growth and metastasis of breast cancer. *J Surg Res* 155, 231-236, doi:10.1016/j.jss.2008.06.044 (2009).

147 Xiang, Y. *et al.* MicroRNA-487b is a negative regulator of macrophage activation by targeting IL-33 production. *J Immunol* 196, 3421-3428 (2016).

148 Roy, S. miRNA in Macrophage Development and Function. *Antioxid Redox Signal* 25, 795-804, doi:10.1089/ars.2016.6728 (2016).

149 Nahid, M. A. *et al.* Regulation of TLR2-mediated tolerance and cross-tolerance through IRAK4 modulation by miR-132 and miR-212. *J Immunol* 190, 1250-1263 (2013).

150 Liu, G. *et al.* miR-147, a microRNA that is induced upon Toll-like receptor stimulation, regulates murine macrophage inflammatory responses. *Proc Natl Acad Sci U S A* 106, 15819-15824 (2009).

151 Wightman, B., Ha, I. & Ruvkun, G. Posttranscriptional regulation of the heterochronic gene lin-14 by lin-4 mediates temporal pattern formation in C. elegans. *Cell* 75, 855-862 (1993).

152 Lee, R. C., Feinbaum, R. L. & Ambros, V. The C. elegans heterochronic gene lin-4 encodes small RNAs with antisense complementarity to lin-14. *Cell* 75, 843-854 (1993).

153 Reinhart, B. J. *et al.* The 21-nucleotide let-7 RNA regulates developmental timing in Caenorhabditis elegans. *Nature* 403, 901-906, doi:10.1038/35002607 (2000).

154 Krol, J., Loedige, I. & Filipowicz, W. The widespread regulation of microRNA biogenesis, function and decay. *Nat Rev Genet* 11, 597-610, doi:10.1038/nrg2843 (2010).

155 Friedman, R. C., Farh, K. K.-H., Burge, C. B. & Bartel, D. P. Most mammalian mRNAs are conserved targets of microRNAs. *Genome Res* 19, 92-105, doi:10.1101/gr.082701.108 (2009).

156 Fu, G., Brkic, J., Hayder, H. & Peng, C. MicroRNAs in Human Placental Development and Pregnancy Complications. *Int J Mol Sci* 14, 5519-5544, doi:10.3390/ijms14035519 (2013).

157 Tufekci, K. U., Oner, M. G. & Meuwissen, R. L., Genc, S. The role of microRNAs in human diseases. *Methods Mol Biol* 1107, 33-50, doi:10.1007/978-1-62703-748-8_3 (2014).

158 Paul, P. *et al.* Interplay between miRNAs and human diseases. *J Cell Physiol* 233, 2007-2018, doi:10.1002/jcp.25854 (2018).

159 Li, Z. & Rana, T. M. Therapeutic targeting of microRNAs: current status and future challenges. *Nat Rev Drug Discov* 13, 622-638, (2014).

160 Catalanotto, C., Cogoni, C. & Zardo, G. MicroRNA in Control of Gene Expression: An Overview of Nuclear Functions. *In J Mol Sci* 17, 1712-1729, doi:10.3390/ijms17101712 (2016).

161 O'Brien, J., Hayder, H., Zayed, Y. & Peng, C. Overview of MicroRNA Biogenesis, Mechanisms of Actions, and Circulation. *Front Endocrinol (Lausanne)* 9, 402-402, doi:10.3389/fendo.2018.00402 (2018).

162 Lewis, B. P., Burge, C. B. & Bartel, D. P. Conserved seed pairing, often flanked by adenosines, indicates that thousands of human genes are microRNA targets. *Cell* 120, 15-20 (2005).

163 Eichhorn, S. W. *et al.* mRNA destabilization is the dominant effect of mammalian microRNAs by the time substantial repression ensues. *Mol Cell* 56, 104-115, doi:10.1016/j.molcel.2014.08.028 (2014).

164 Guo, H., Ingolia, N. T., Weissman, J. S. & Bartel, D. P. Mammalian microRNAs predominantly act to decrease target mRNA levels. *Nature* 466, 835-840, doi:10.1038/nature09267 (2010).

165 Pillai, R. S., Bhattacharyya, S. N. & Filipowicz, W. Repression of protein synthesis by miRNAs: how many mechanisms? *Trends Cell Biol* 17, 118-126, doi:10.1016/j.tcb.2006.12.007 (2007).

166 Stenvang, J. *et al.* Inhibition of microRNA function by antimiR oligonucleotides. *Silence* 3, 1-1, doi:10.1186/1758-907X-3-1 (2012).

167 Christopher, A. F. *et al.* MicroRNA therapeutics: Discovering novel targets and developing specific therapy. *Perspect Clin Res* 7, 68-74, doi:10.4103/2229-3485.179431 (2016).

168 Lu, J. *et al.* MicroRNA expression profiles classify human cancers. *Nature* 435, 834-838, doi:10.1038/nature03702 (2005).

169 van Rooij, E. & Kauppinen, S. Development of microRNA therapeutics is coming of age. *EMBO Mol Med* 6, 851-864, doi:10.15252/emmm.201100899 (2014).

170 Shin, J. *et al.* Restoration of miR-29b exerts anti-cancer effects on glioblastoma. *Cancer Cell Int* 17, 104, doi: 10.1186/s12935-017-0476-9 (2017).

171 Bader, A. G. miR-34 - a microRNA replacement therapy is headed to the clinic. *Front Genet* 3, 120-120, doi:10.3389/fgene.2012.00120 (2012).

172 Beg, M. S. *et al.* Phase I study of MRX34, a liposomal miR-34a mimic, administered twice weekly in patients with advanced solid tumors. *Invest New Drugs* 35, 180-188, doi:10.1007/s10637-016-0407-y (2017).

173 Stenvang, J. *et al.* Inhibition of microRNA function by antimiR oligonucleotides. *Silence* 3, 1, doi: 10.1186/1758-907X-3-1 (2012).

174 Chery, J. RNA therapeutics: RNAi and antisense mechanisms and clinical applications. *Postdoc J* 4, 35-50 (2016).

175 Stein, C. A. & Castanotto, D. FDA-approved oligonucleotide therapies in 2017. *Mol Ther* 25, 1069-1075 (2017).

176 Sharma, V. K., Sharma, R. K. & Singh, S. K. Antisense oligonucleotides: modifications and clinical trials. *MedChemComm* 5, 1454-1471 (2014).

177 Meister, G., Landthaler, M., Dorsett, Y. & Tuschl, T. Sequence-specific inhibition of microRNA- and siRNA-induced RNA silencing. *RNA* 10, 544-550, doi:10.1261/rna.5235104 (2004).

178 Lennox, K. A. & Behlke, M. A. A direct comparison of anti-microRNA oligonucleotide potency. *Pharm Res* 27, 1788-1799 (2010).

179 Lennox, K. A. *et al.* Improved performance of anti-miRNA oligonucleotides using a novel non-nucleotide modifier. *Mol Ther Nucleic Acids* 2, e117 (2013).

180 Lennox, K. & Behlke, M. Chemical modification and design of anti-miRNA oligonucleotides. *Gene Ther* 18, 1111-1120 (2011).

181 Obad, S. *et al.* Silencing of microRNA families by seed-targeting tiny LNAs. *Nat Genet* 43, 371-378 (2011).

182 Hettinger, J. *et al.* Origin of monocytes and macrophages in a committed progenitor. *Nat Immunol* 14, 821-830 (2013).

183 Sefah, K. *et al.* Development of DNA aptamers using Cell-SELEX. *Nat Protoc* 5, 1169-1185 (2010).

184 van Helden, S. F., van Leeuwen, F. N. & Figdor, C. G. Human and murine model cell lines for dendritic cell biology evaluated. *Immunol Lett* 117, 191-197 (2008).

185 Smith, M. P., Young, H., Hurlstone, A. & Wellbrock, C. Differentiation of THP1 Cells into Macrophages for Transwell Co-culture Assay with Melanoma Cells. *Bio Protoc* 5, e1638 (2015).

186 Sampath, P., Moideen, K., Ranganathan, U. D. & Bethunaickan, R. Monocyte subsets: Phenotypes and Function in tuberculosis infection. *Front Immunol* 9, 1726, doi: 10.3389/fimmu.2018.01726 (2018).

187 O'neill, L. A., Golenbock, D. & Bowie, A. G. The history of Toll-like receptors—redefining innate immunity. *Nat Rev Immunol* 13, 453-460 (2013).

188 Paludan, S. R. & Bowie, A. G. Immune sensing of DNA. *Immunity* 38, 870-880 (2013).

189 Park, B. S. & Lee, J.-O. Recognition of lipopolysaccharide pattern by TLR4 complexes. *Exp Mol Med* 45, e66 (2013).

190 Bode, C. *et al.* CpG DNA as a vaccine adjuvant. *Expert Rev Vaccines* 10, 499-511, doi:10.1586/erv.10.174 (2011).

191 Zuker, M. Mfold web server for nucleic acid folding and hybridization prediction. *Nucleic Acids Res* 31, 3406-3415 (2003).

192 O Tucker, W., T Shum, K. & A Tanner, J. G-quadruplex DNA aptamers and their ligands: structure, function and application. *Curr Pharm Des* 18, 2014-2026 (2012).

193 Opazo, F. *et al.* Modular assembly of cell-targeting devices based on an uncommon G-quadruplex aptamer. *Mol Ther Nucleic Acids* 4, e25 (2015).

194 You, J. *et al.* Effects of monovalent cations on folding kinetics of G-quadruplexes. *Biosci Rep* 37, doi:10.1042/bsr20170771 (2017).

195 Kloosterman, W. P., Wienholds, E., Ketting, R. F. & Plasterk, R. H. Substrate requirements for let-7 function in the developing zebrafish embryo. *Nucleic Acids Res* 32, 6284-6291, doi:10.1093/nar/gkh968 (2004).

196 Christopher, A. F. *et al.* MicroRNA therapeutics: Discovering novel targets and developing specific therapy. *Perspect Clin Res* 7, 68-74 (2016).

197 Chery, J. RNA therapeutics: RNAi and antisense mechanisms and clinical applications. *Postdoc J* 4, 35-50 (2016).

198 Lennox, K. A. *et al.* Improved Performance of Anti-miRNA Oligonucleotides Using a Novel Non-Nucleotide Modifier. *Mol Ther Nucleic Acids* 2, e117, doi:10.1038/mtna.2013.46 (2013).

199 McFarland, B. J., Sant, A. J., Lybrand, T. P. & Beeson, C. Ovalbumin (323−339) Peptide Binds to the Major Histocompatibility Complex Class II I-Ad Protein Using Two Functionally Distinct Registers. *Biochemistry* 38, 16663-16670 (1999).

200 Rötzschke, O. *et al.* Exact prediction of a natural T cell epitope. *Eur J Immunol* 21, 2891-2894 (1991).

201 Burgdorf, S., Lukacs-Kornek, V. & Kurts, C. The mannose receptor mediates uptake of soluble but not of cell-associated antigen for cross-presentation. *The Journal of Immunology* 176, 6770-6776 (2006).

202 Chatterjee, B. *et al.* Internalization and endosomal degradation of receptor-bound antigens regulate the efficiency of cross presentation by human dendritic cells. *Blood* 120, 2011-2020 (2012).

203 Hogquist, K. A. *et al.* T cell receptor antagonist peptides induce positive selection. *Cell* 76, 17-27 (1994).

204 Quah, B. J. C. & Parish, C. R. The use of carboxyfluorescein diacetate succinimidyl ester (CFSE) to monitor lymphocyte proliferation. *J Vis Exp 44,* 2259, doi:10.3791/2259 (2010).

205 Ganji, A., Varasteh, A. & Sankian, M. Aptamers: new arrows to target dendritic cells. *J Drug Target* 24, 1-12 (2016).

206 Thiviyanathan, V. & Gorenstein, D. G. Aptamers and the next generation of diagnostic reagents. *Proteomics Clin Appl* 6, 563-573, doi:10.1002/prca.201200042 (2012).

207 Civit, L. *et al.* Systematic evaluation of cell-SELEX enriched aptamers binding to breast cancer cells. *Biochimie* 145, 53-62, doi:10.1016/j.biochi.2017.10.007 (2018).

208 Lutz, M. B., Strobl, H., Schuler, G. & Romani, N. GM-CSF monocyte-derived cells and Langerhans cells as part of the dendritic cell family. *Front Immunol* 8, 1388, doi: 10.3389/fimmu.2017.01388 (2017).

209 Hui, Y., Shan, L., Lin-Fu, Z. & Jian-Hua, Z. Selection of DNA aptamers against DC-SIGN protein. *Mol Cell Biochem* 306, 71-77, doi:10.1007/s11010-007-9555-x (2007).

210 Berezovski, M. V. *et al.* Aptamer-facilitated biomarker discovery (AptaBiD). *J Am Chem Soc* 130, 9137-9143, doi:10.1021/ja801951p (2008).

211 Chanput, W., Mes, J. J. & Wichers, H. J. THP-1 cell line: an in vitro cell model for immune modulation approach. *Int Immunopharmacol* 23, 37-45, doi:10.1016/j.intimp.2014.08.002 (2014).

212 Dou, X.-Q. *et al.* Aptamer-drug conjugate: targeted delivery of doxorubicin in a HER3 aptamer-functionalized liposomal delivery system reduces cardiotoxicity. *Int J Nanomedicine* 13, 763-776, doi:10.2147/IJN.S149887 (2018).

213 Maeß, M. B., Buers, I., Robenek, H. & Lorkowski, S. Improved protocol for efficient nonviral transfection of premature THP-1 macrophages. *Cold Spring Harb Protoc* 2011, doi: 10.1101/pdb.prot5612 (2011).

214 Catuogno, S., Esposito, C. L. & de Franciscis, V. Aptamer-Mediated Targeted Delivery of Therapeutics: An Update. *Pharmaceuticals (Basel)* 9, E69, doi:10.3390/ph9040069 (2016).

215 Tawiah, K. D., Porciani, D. & Burke, D. H. Toward the Selection of Cell Targeting Aptamers with Extended Biological Functionalities to Facilitate Endosomal Escape of Cargoes. *Biomedicines* 5, E51, doi:10.3390/biomedicines5030051 (2017).

216 Wang, J. *et al.* Oligonucleotide-Based Drug Development: Considerations for Clinical Pharmacology and Immunogenicity. *Ther Innov Regul Sci* 49, 861-868 (2015).

217 FDA, U. Draft Guidance for Industry: Assay Development for Immunogenicity Testing of Therapeutic Proteins. US Department of Health and Human Services, US FDA, *Center for Drug* (2009).

218 Pisetsky, D. S. The origin and properties of extracellular DNA: from PAMP to DAMP. *Clin Immunol* 144, 32-40 (2012).

219 Blasius, A. L. & Beutler, B. Intracellular toll-like receptors. *Immunity* 32, 305-315 (2010).

220 Fülle, L. *et al.* RNA Aptamers Recognizing Murine CCL17 Inhibit T Cell Chemotaxis and Reduce Contact Hypersensitivity In Vivo. *Mol Ther* 26, 95-104 (2018).

221 Zhou, J. & Rossi, J. Aptamers as targeted therapeutics: current potential and challenges. *Nat Rev Drug Discov 16*, 181-202, doi:10.1038/nrd.2016.199 (2017).

222 Swayze, E. E. *et al.* Antisense oligonucleotides containing locked nucleic acid improve potency but cause significant hepatotoxicity in animals. *Nucleic Acids Res* 35, 687-700, doi:10.1093/nar/gkl1071 (2007).

223 Agrawal, S., Joshi, M. & Christoforidis, J. B. Vitreous inflammation associated with intravitreal anti-VEGF pharmacotherapy. *Mediators Inflamm* 2013, 943409-943415, doi:10.1155/2013/943409 (2013).

224 Boyer, D. S., Goldbaum, M., Leys, A. M. & Starita, C. Effect of pegaptanib sodium 0.3 mg intravitreal injections (Macugen) in intraocular pressure: posthoc analysis from V.I.S.I.O.N. study. *Br J Ophthalmol* 98, 1543-1546, doi:10.1136/bjophthalmol-2013-304075 (2014).

225 Falavarjani, K. G. & Nguyen, Q. D. Adverse events and complications associated with intravitreal injection of anti-VEGF agents: a review of literature. *Eye (Lond)* 27, 787-794, doi:10.1038/eye.2013.107 (2013).

226 Waring, M. J. Lipophilicity in drug discovery. *Expert Opin Drug Discov* 5, 235-248, doi:10.1517/17460441003605098 (2010).

227 Tan, W. *et al.* Molecular aptamers for drug delivery. *Trends Biotechnol* 29, 634-640, doi:10.1016/j.tibtech.2011.06.009 (2011).

228 Dyke, C. K. *et al.* First-in-human experience of an antidote-controlled anticoagulant using RNA aptamer technology: a phase 1a pharmacodynamic evaluation of a drug-antidote pair for the controlled regulation of factor IXa activity. *Circulation* 114, 2490-2497, doi:10.1161/circulationaha.106.668434 (2006).

229 Bing, T. *et al.* Triplex-quadruplex structural scaffold: a new binding structure of aptamer. *Sci Rep* 7, 15467 (2017).

230 Patel, D. J. Structural analysis of nucleic acid aptamers. *Curr Opin Chem Biol* 1, 32-46 (1997).

231 Thiel, K. W. *et al.* Delivery of chemo-sensitizing siRNAs to HER2+-breast cancer cells using RNA aptamers. *Nucleic Acids Res* 40, 6319-6337, doi:10.1093/nar/gks294 (2012).

232 Liu, H. Y. & Gao, X. A universal protein tag for delivery of SiRNA-aptamer chimeras. *Sci Rep* 3, 3129, doi: 10.1038/srep03129 (2013).

233 Diao, Y. *et al.* A specific aptamer-cell penetrating peptides complex delivered siRNA efficiently and suppressed prostate tumor growth in vivo. *Cancer Biol Ther* 17, 498-506, doi:10.1080/15384047.2016.1156266 (2016).

234 Taghavi, S. *et al.* Preparation and evaluation of polyethylenimine-functionalized carbon nanotubes tagged with 5TR1 aptamer for targeted delivery of Bcl-xL shRNA into breast cancer cells. *Colloids Surf B Biointerfaces* 140, 28-39 (2016).

235 Perepelyuk, M., Maher, C., Lakshmikuttyamma, A. & Shoyele, S. A. Aptamer-hybrid nanoparticle bioconjugate efficiently delivers miRNA-29b to non-small-cell lung cancer cells and inhibits growth by downregulating essential oncoproteins. *Int J Nanomedicine* 11, 3533-3544 (2016).

236 Porciani, D. *et al.* Modular cell-internalizing aptamer nanostructure enables targeted delivery of large functional RNAs in cancer cell lines. *Nat Commun* 9, 2283, doi: 10.1038/s41467-018-04691-x (2018).

237 Juliano, R. L. The delivery of therapeutic oligonucleotides. *Nucleic Acids Res* 44, 6518-6548, doi:10.1093/nar/gkw236 (2016).

238 Halenius, A., Gerke, C. & Hengel, H. Classical and non-classical MHC I molecule manipulation by human cytomegalovirus: so many targets—but how many arrows in the quiver? *Cell Mol Immunol* 12, 139-153, doi:10.1038/cmi.2014.105 (2015).

239 Embgenbroich, M. & Burgdorf, S. Current Concepts of Antigen Cross-Presentation. *Front Immunol* 9, 1643-1643, doi:10.3389/fimmu.2018.01643 (2018).

240 Wengerter, B. C. *et al.* Aptamer-targeted antigen delivery. *Mol Ther* 22, 1375-1387, doi:10.1038/mt.2014.51 (2014).

9 Supplementary data

9.1 Binding of DC 12.53 to BM-DCs

Table 9-1: % BM-DCs bound by ATTO 647N-labeled aptamers and MFI in flow cytometry binding assay

Aptamer	% Cells bound	MFI
Ctrl 2	11.5±1.56	1.0±0.01
DC 12	63.6±0.21	9.1±4.08
DC 12.53	57.7±4.95	11.8±3.7
DC 12.53sc1	9.54±0.02	1.0±0.04

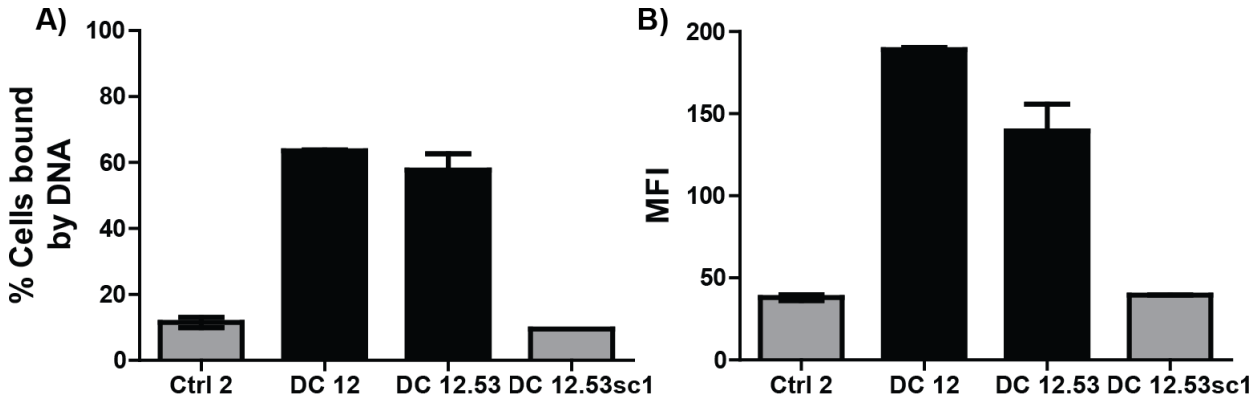

Figure S 9.1.1: ATTO 647N-labeled aptamers binds to BM-DCs in flow cytometry binding assay4×10^5 BM-DCs were incubated with 250nM of 5'-ATTO 647N-labeled aptamers at 37°C for 10 minutes. The percentage cells bound with aptamers were measured by flow cytometry.(n=1, mean ± SD).

9.2 Binding of DC 12ext to THP-1 cells

Table 9-2: % THP-1 cells bound by ATTO 647N-labeled aptamers and relative MFI in flow cytometry compeition binding assay

Aptamer		% Cells bound	Relative MFI (aptamer/control)
Ctrl 2*		6.12±0.47	1.00±0.02
DC 12**+**	No competition	80.6±6.85	2.40±0.32
	1:2 DC 12ext	61.6±14.7	2.13±0.43
	1:4 DC 12ext	43.5±3.41	1.77±0.18
	1:8 DC 12ext	26.3±7.30	1.74±0.25
	1:8 Ctrl 2 ext	68.4±14.6	2.51±0.21

*control

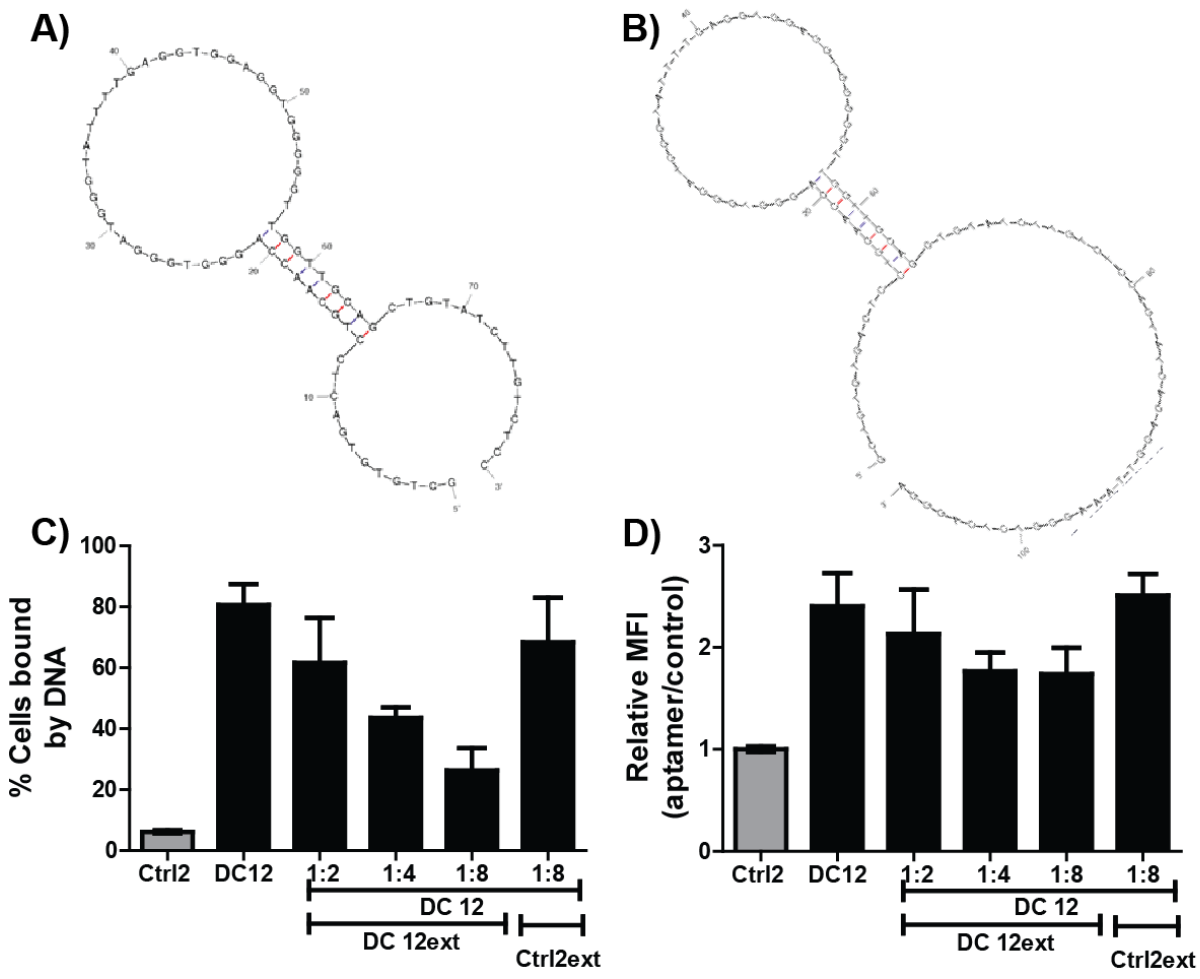

Figure S 9.2.1: Competition binding assay for 28 nucleotide extended DC 12
(A) Mfold predicted secondary structure of DC 12 and **(B)** 28 nucleotide extended DC 12 (DC 12ext). **(C)** 250 nM ATTO-647 N labeled DC 12 was co-incubated with an increasing concentration of DC 12ext with THP-1 cells and binding was analyzed by flow cytometry (n=2, mean ± SD).

9.3 Aptamer-targeted delivery of OT-I peptide for CD8 T cells activation

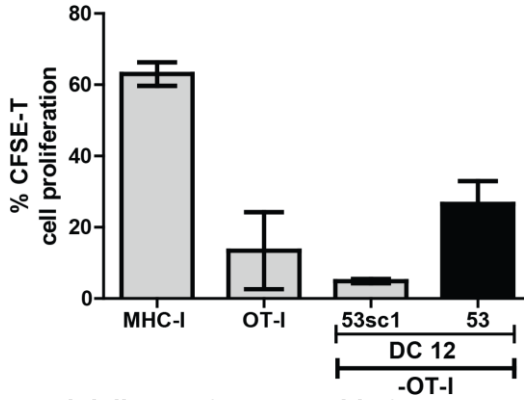

Figure S 9.3.1: Aptamer-targeted delivery of OT-I peptide for CD8 T cells activation
1×10^5 OVA-CD8 specific T cells were stained with fluorescent staining dye (CFSE) and incubated with 5×10^4 BM-DCs treated with 100 nM of aptamer-conjugates, OT-I peptide and 1 nM of MHC I peptide. The ranged gate percentage of CFSE T cell proliferation of triplicates (mean ± SD) was plotted (n=1 in triplicates).The assay was performed by Dr.SilvanaHaβel.

10 Abbreviations

2’-O-Me	2’-O-Methyl
2’-O-MOE	2’-O-methoxyethyl
AGO	Argonaute
ASO	antisense oligonucleotides
APCs	Antigen presenting cells
APS	Ammoniumperoxodisulfate
BM-DC	Bone marrow-derived dendritic cell
BSA	Bovine serum albumin
CD	Cluster of differentiation
cDCs	conventional/classical DCs
CDP	Common DC precursor
CFSE	Carboxyfluoresceine succinimidyl ester
CLEC-1	C-type lectin receptor-1
CMV	cytomegalovirus
CTLs	Cytotoxic T-lymphocyte
CTLA-4	CTL-associated protein 4
CLRs	C-type lectin-like receptors
Ctrl 2	Control DNA sequence 2
DAMP	Damage-associated molecular pattern
DAPI	4’,6-diamidino-2-phenylindole
DC	Dendritic cell
DCIR	DC immunoreceptor
DC-SIGN	DC-specific ICAM-3 grabbing non-integrin
DEC-205	Dendritic and epithelial cells, 205 kDa
Dectin	DC-associated C-type lectin
DLEC	DC lectin
DNA	Deoxyribonucleic acid
DTT	1,4-Dithiothreitol
EDTA	Ethylendiamintetraacetic acid
EEA1	Early endosome antigen 1
EGFP	Enhanced green fluorescent protein
ELISA	Enzyme-linked immunosorbent assay
FACS	fluorescence-activated cell sorter
FDA	Food and drug administration (USA)
GM-CSF	Granulocyte macrophage colony-stimulating factor
H	Human
HFIP	1,1,1,3,3,3-hexafluoro-2-propanol
HPLC	High-performance liquid chromatography
IFN Type I	Interferons
IFN-ɤ	Interferon-gamma
IL	Interleukin
LAMP-1	Lysosome-associated membrane glycoprotein 1
LC-MS	Liquid chromatography-mass spectrometry
LNA	Locked nucleic acid
LPS	Lipopolysaccharide
M1	Classically activated macrophages
M2	Alternatively activated macrophages
M-CSF	Macrophage colony-stimulating factor
MDP	Monocyte-dendritic cell precursor

MFI	Mean fluorescence intensity
MHC	Major histocompatibility complex
miRISC	miRNA-mediated silencing complex
miRNA	MicroRNA
MPS	Mononuclear phagocyte system
mRNA	Messenger RNA
MR	Mannose receptor
NGS	Next generation sequencing
NOD-like	Nucleotide-binding oligomerization domain-like receptors
Nt	nucleotides
ODN	Oligonucleotide
OVA	Ovalbumin
PAGE	Polyacrylamide gel electrophoresis
PAMP	Pathogen-associated molecular pattern
PBMC	Peripheral blood mononuclear cells
PCR	Polymerase chain reaction
pDCs	Plasmacytoid DCs
PEG	Polyethylene glycol
PNK	Polynucleotide kinase
pre-miRNA	Precursor miRNA
pri-miRNA	Primary RNA
PRR	Pattern recognition receptor
PSMA	Prostate-specific membrane antigen
RISC	RNA-induced silencing complex
RNA	Ribonucleic acid
PKR	Protein kinase R
PS	Phosphorothioate
SD	Standard deviation
SDS	Sodium dodecylsulfate
SELEX	Systematic evolution of ligands by exponential enrichment
siRNA	Small interfering RNA
ssDNA	Single stranded DNA
STAT4	Signal Transducer And Activator Of Transcription 4
TAMs	Tumor associated macrophages
TCR	T cell receptor
TEA	Triethylamine
TEAA	Triethylammonium acetat
TEMED	N,N,N',N'-tetramethylethylendiamide
Th	T helper cell
TLR	Toll-like receptor
TNF-α	Tumor necrosis factor α
TPP	Tumor necrosis factor, prostaglandin E2 and TLR2-ligand(Pam3CK)
TRBP	trans-activation response RNA-binding protein
UTR	Untranslated region
WGA	Wheat germ agglutinin

11 Acknowledgement

First of all, I would like to express my heartfelt gratitude to my supervisor Prof. Dr. Günter Mayer for giving me the opportunity to do my Ph.D. in his lab at the University of Bonn, Germany. He has supported me throughout the hard times of my thesis and his advice, support, guidance, and encouragement are highly appreciated. I am very grateful to him for accepting me as a Ph.D. student in his group. I am also grateful to Dr. Silvana Haβel for giving me the opportunity to work on her follow-up study and provide me with continuous guidance, support, and motivation. I am indebted to her for her help, constructive criticism and suggestions during the whole span of my project.

I am very grateful to Prof. Dr. Gerd Bendas, Pharmacy Institute, University of Bonn for his interest in my work and for being kindly accepted as my second supervisor in the doctoral thesis. Moreover, I am also highly thankful to PD. Dr. Anton Schmitz and Prof. Dr. Michael Frei for their willingness to review my thesis and to be part of the examination committee.

I am also grateful to Prof. Dr. Joachim L. Schultze and Dr. Anna Aschenbrenner for their technical support and guidance regarding TPP macrophage protocol. Additionally, I would like to thank Dr. Katarzyna Placek and Brita Wilhelm for the demonstration of isolation of PBMC from buffy coats. I am thankful to Prof. Dr. Sven Burgdorf and Dr. Maria Embgenbroich for providing BM-DCs. I would like to acknowledge the assistance of the Flow Cytometry Core Facility at the Institute of Experimental Immunology, Medical Faculty of the University of Bonn.

Furthermore, I would also like to thank all the people who are directly or indirectly involved in this journey. I am grateful to Dr. Zeeshan Danish for his help and encouragement during my placement at University of Bonn, Germany. I am grateful to all my past and present colleagues from Famulok, Mayer and kath-Schorr group. I am very grateful to Dr. Ankana, Laura.E., Tjaša, Olga, Laura.L., Julia, Dr. Franziska,

Dr. Laia, Dr. Daniel, Dr. Anna S., Anna W., Anna J., Moujab, Jörg, Ignazio, Georg, Sebastian, Christian, Dr. Amir and Malte for their support and friendly working environment in the lab. I am also very grateful to Sandra Ulrich, Sarah Hensel, Stefan Künne, Dr. Sven Jan Freudenthal, Nicole Krämer and Justina Stark. I sincerely thank my dear friend Dr. Basharat Ali and Mohsin for their precious time during my stay in Bonn.

I am very grateful to Dr. Silvana Haβel, Dr. Ankana, Tjaša, Paras Ahmad, Mohsin Aziz, Rahamath Bivi M Shahul Hameed and Rana Shoaib for proofreading and valuable suggestions. I am very grateful to my colleague Georg Pietruschka for the translation into German of the English abstract of this thesis. I am very grateful to my colleague Tjaša Legen for helping with and submitting my thesis at the Dean's office. Moreover, I would also like to acknowledge my funding agency, The Higher Education Commission of Pakistan (HEC), for providing me with financial support. I would like to express my heartfelt gratitude to my whole family, especially to my father Prof. Dr. Muhammad Akhtar and my lovely mother, they are always there for me and they are supporting me during tough times. They supported me in all aspects of my life and provided me endless support, encouragement, and love. Thank you both from the core of my heart for giving me the strength to reach my goal. I am so grateful to my brothers Ali Akhtar and Farooq Akhtar, and to my lovely fiance for your support during my stay in Germany.